NOTICE

The quality of this microform is heavily dependent upon the quality of the original thesis submitted for microfilming. Every effort has been made to ensure the highest quality of reproduction possible.

If pages are missing, contact the university which granted the degree.

Some pages may have indistinct print especially if the original pages were typed with a poor typewriter ribbon or if the university sent us an inferior photocopy.

Previously copyrighted materials (journal articles, published tests, etc.) are not filmed.

Reproduction in full or in part of this microform is governed by the Canadian Copyright Act, R.S.C. 1970, c. C-30.

AVIS

La qualité de cette microforme dépend grandement de la qualité de la thèse soumise au microfilmage. Nous avons tout fait pour assurer une qualité supérieure de reproduction.

S'il manque des pages, veuillez communiquer avec l'université qui a conféré le grade.

La qualité d'impression de certaines pages peut laisser à désirer, surtout si les pages originales ont été dactylographiées à l'aide d'un ruban usé ou si l'université nous a fait parvenir une photocopie de qualité inférieure.

Les documents qui font déjà l'objet d'un droit d'auteur (articles de revue, tests publiés, etc.) ne sont pas microfilmés.

La reproduction, même partielle, de cette microforme est soumise à la Loi canadienne sur le droit d'auteur, SRC 1970, c. C-30.

Canada

An analysis of the gas phase $[C_7H_7]^+$ ion populations generated from simple aromatic molecules.

Jeffrey J. Ridal

A thesis submitted to the
School of Graduate Studies
of the University of Ottawa
in partial fulfilment of the
requirements for the degree
of
Masters' of Science.
May 15, 1987.

ISBN 0-315-46847-5

UNIVERSITÉ D'OTTAWA
UNIVERSITY OF OTTAWA

Acknowledgements

I would like to thank my supervisor, Professor John Holmes, for his interest, patience, and creative input during the course of this work. These are things that will be well-remembered.

I am grateful to Dr. John Buschek, who has contributed a great deal, through his experience and resourcefulness, to this project. Contributions especially worth noting are the syntheses of tropylium tetrafluoroborate and cycloheptatriene, both of which have proved to be key compounds for this research.

I am also grateful to Drs. Sander Mommers and John Krause, who have provided advice and assistance on many occasions in the past three years.

I would like to thank Dr. Fred Lossing for providing appearance energy measurements, and Dr. Clem Kazakoff and Mr. Raj Capoor for prompt analyses of a number of compounds.

I express my gratitude to my friends and colleagues, Marcia Blanchette, Jozsef Bordas-Nagy and Marcel Hop. Each was always willing to help out whenever possible—their support and friendship have made my stay in Ottawa a very positive experience.

I am thankful to Chris Carruthers for tuning me into LaTeX and for helping me out with formatting problems.

A special thanks is given to the secretaries of the Chemistry office, especially to Noëla Simard and Cass Guthridge, for keeping the administrative

I stand at a crossroad
And only the wind
Dares whisper
The direction
I may take.

But I am buoyed
By what I have learned,
The people I have met,
And the Friendships
I have made.

Contents

List of Figures

List of Tables

Abstract

Collisional activation (CA) mass spectrometry of the $[C_7H_7]^+$ ions generated from various tropylium salts has resulted in a new value for the structure specific m/z 77/74 peak intensity ratio used to characterize pure tropylium ions. A re-examination of the isomer contents of $[C_7H_7]^+$ ions produced by 70 eV ionisation of a variety of precursor molecules resulted in ion populations which are in general agreement with previous CA mass spectrometry determinations, but which agree poorly with ion cyclotron resonance (ICR) results.

Analysis of $[C_7H_7]^+$ ion populations generated with low ionising electron energies show general agreement with the results of similar previous CA mass spectrometry and ICR studies. Notable exceptions are the results for ion populations from toluene and cycloheptatriene, both of which give greater benzyl ion contents than those found in the previous studies. This resulted in extensive CA mass spectrometry experiments which probed the spectra of $[C_7H_7]^+$ ions generated with threshold ionising electron energies from toluene and cycloheptatriene precursor molecules. It was found that artefact peaks distort the m/z 77/74 peak intensity ratios for source-generated ions from toluene; less well-resolved CA mass spectra may have

led to a previous conclusion that the structure of threshold $[C_7H_7]^+$ ions from toluene is tropylium.

The $[C_7H_7]^+$ ion populations have been studied as a function of the ion lifetime. A clear trend was observed toward greater tropylium ion contents with longer ion lifetimes for all precursor molecules examined. It was therefore concluded that the equilibration between benzyl and tropylium ions is not complete on the microsecond time-scale.

The m/z 74/91 peak intensity ratio for $[C_7H_7]^+$ ions derived from nitro and halotoluene precursor molecules has been found in many cases to be significantly greater than that for pure fluxes of benzyl and tropylium ions. The difference must be due to an appreciable amount of another $[C_7H_7]^+$ isomer—presumably with the tolyl ion structure. Analysis of the tolyl, benzyl and tropylium ion contents for $[C_7H_7]^+$ ions generated from the nitro and halotoluenes is generally in poor agreement with previous CA determinations.

The fluxes of metastably-generated $[C_7H_7]^+$ ions from ionised iodotoluenes were found to contain different amounts of the three isomers.

Scope of this thesis

Gas phase ions are elusive; not readily obtained from a bottle. To a chemist accustomed to holding the species of interest in his hands, seeing its colour, smelling its odour, and subjecting it to the battery of analytical tests available, the characterisation of gas phase ions may seem an impossible task. Indeed, gas phase ion research might be thought of as one of the remaining frontiers of physical organic chemistry. Instrumentation with which to study organic gas phase ions has developed rather slowly[1,2]. Fortunately, mass spectrometry has evolved from an important analytical technique with which to infer the structures of neutral organic compounds into also a very powerful method with which information about the structures of gas phase ions can be gained.

The mass spectrometer is essentially an all-in-one laboratory for the study of isolated gaseous ions. In it, ions are *synthesized* by electron impact on a neutral precursor, *purified* by momentum selection through a magnetic field, and their decomposition products *analysed* with a translational energy analyser (the electric sector). The information gained can be used in concert with theoretical and other experimental data to infer the structure(s) of an ion—an important stage toward comprehending the chemical behaviour of

gaseous ions. In turn, understanding the chemistry of gaseous organic ions has great significance for those researchers concerned with ionospheric[3] and interstellar[4] species. Furthermore, knowledge of the behaviour of gaseous ions aids the interpretation of mass spectra.

This thesis is concerned with mass spectrometric studies that have probed the structures of the gas phase ion $[C_7H_7]^+$. Numerous hydrocarbon compounds generate $[C_7H_7]^+$ as the most intense fragment ion in their mass spectra, and in most cases, the $[C_7H_7]^+$ ion population generated is a mixture of isomers. It has been the aim of the work detailed in this thesis to analyse qualitatively and quantitatively the isomer content of the $[C_7H_7]^+$ ion population.

Chapter 1 of this thesis provides an introduction of the mass spectrometer used for the bulk of the experimental work, and a description of the experimental applications of this instrument that have proved most useful in the course of the work. Emphasis has been placed on describing how information gained by experiment can be applied to the characterisation of gas phase ion structures.

The wealth of scientific literature that is concerned with the gas phase $[C_7H_7]^+$ ions is reviewed in Chapter 2. Each Section of this Chapter ends with a discussion of a number of points regarding the $[C_7H_7]^+$ ions that remain unclear or unanswered prior to the present work.

Chapters 3 and 4 contain the experimental results and present interpretation(s) of these results with respect to the chemistry of the gas phase $[C_7H_7]^+$ ion.

Chapter 1

Introduction

1.1 The mass spectrometer

Although there are many different types of mass spectrometers, the basic principles governing their use are similar. Discussion in this thesis will refer to the VG-Analytical ZAB-2F[5] shown in Figure 1.1. As mentioned above, this mass spectrometer may be thought of as a complete laboratory for the study of isolated gas phase ions. In it, ions are synthesized, purified, analysed, detected and finally the results are compiled. Each of these processes corresponds to a different region of the instrument.

1.1.1 Synthesis: the ionisation chamber

The ionisation or source chamber of the ZAB is equipped with four inlet systems that allow entry of the sample. The sample must be volatilized; hence, choice of inlet system depends somewhat on the ambient state of the sample.

The septum inlet system is designed for easy injection of liquid samples by means of a micro-syringe. The septum temperature can be varied so that

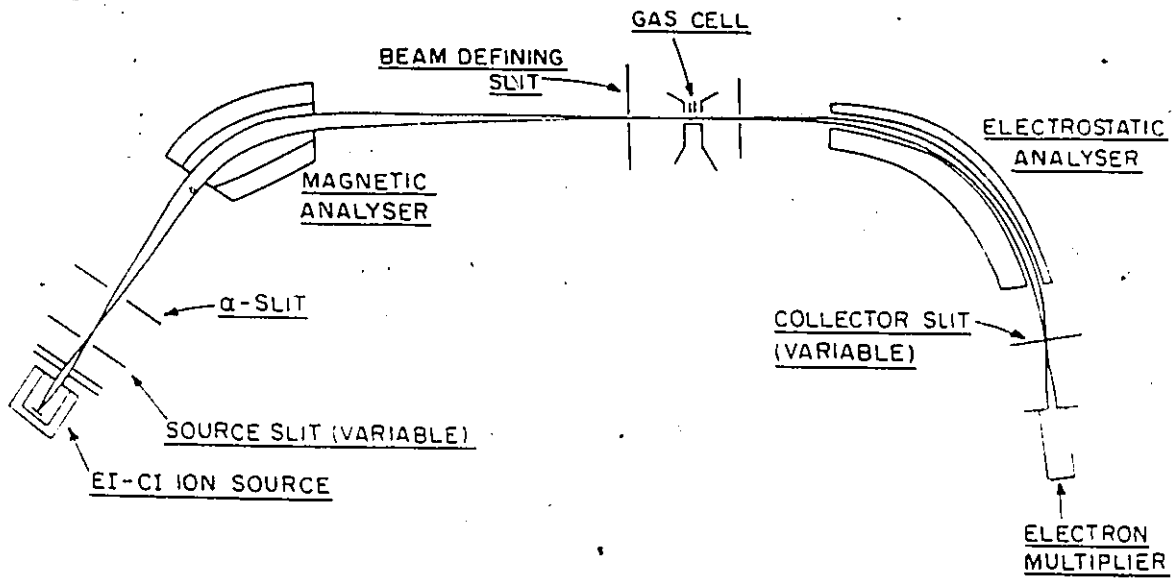

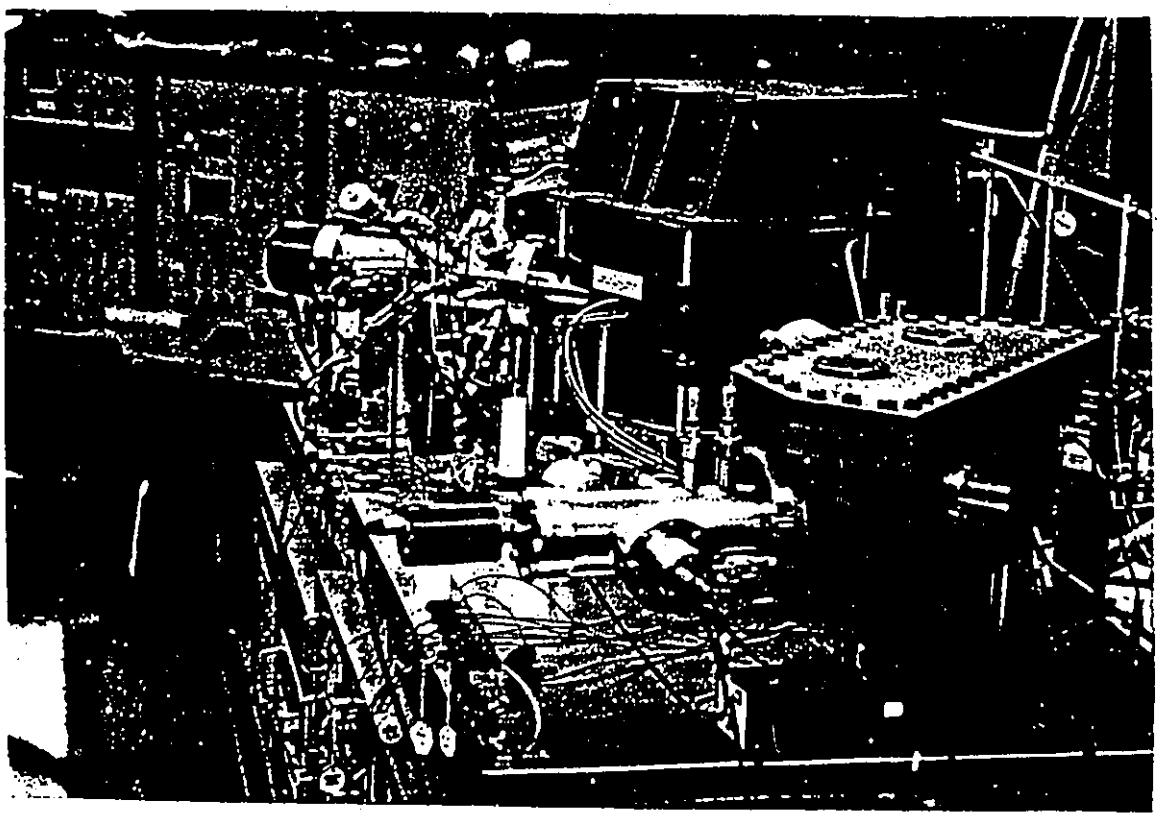

Figure 1.1: The Vacuum Generators ZAB-2F mass spectrometer at the University of Ottawa. (From reference [37]).

a satisfactory source pressure can be obtained for liquids of various boiling points. Source pressure can also be controlled by varying the amount of sample injected or by gently pumping away excess sample until an acceptable level is obtained. Once volatilized, the neutral gas molecules diffuse *via* a capillary to the ionisation chamber due to the pressure gradient effected by maintaining the chamber under a high vacuum when free of sample (*ca.* 10^{-8} torr as measured by the ionisation gauge). For most compounds, a constant rate of sample entry is maintained at a source pressure of *ca.* 10^{-6} torr. Disadvantages with using the septum are inadequate source pressures for some poorly volatile compounds and the continuous sample depletion, which after a time results in a steadily falling ion source pressure. Care should be taken that the compound does not undergo decomposition or thermal rearrangement at the septum temperature being used[6].

The Granville-Phillips inlet system allows entry of gases, liquids or volatile solids. This all-glass inlet system is the most versatile of the inlet systems and maintains a constant source pressure for long periods of time—excellent for experiments that require time-consuming signal averaging or very slow scans. The Granville-Phillips is the inlet of choice for compounds that have a chance of decomposing at the higher temperatures used with the septum inlet system. A disadvantage of the Granville-Phillips is the amount of time required for the sample to pump out of the source entry line. Changing samples can be a slow process.

The direct probe is used for relatively involatile solids. Sample pressures can be hard to control but heating or cooling the probe, plus manipulating

the physical proximity of the probe tip to the source chamber, does have some effect.

There is a gas line fitted to the source chamber that allows direct entry of gases from a high-pressure cylinder into the source. The gas pressure is controlled by a needle valve located between the gas cylinder and the source chamber. This line is most useful when chemical ionisation (CI) mass spectrometry is desired *(vide infra)*.

Once the sample has been admitted to the source chamber, the neutral molecules may be ionised by electron impact. Electrons are produced from an incandescent tungsten filament and are accelerated by a potential gradient into the ionisation chamber. Once in the chamber the electrons have a constant velocity. A magnetic field along the direction of the electron beam helps maintain a collimated beam and imposes a tight helical motion on the electrons. This allows each electron to sweep out a greater area, thereby increasing the probability of an encounter with a neutral molecule.

Ionisation occurs by interaction of these fast moving (typically 70 eV) electrons with the outer shell electrons of the sample molecule. An electron is ejected from the sample molecule and a *positive* ion is generated. The interaction time is of the order of 10^{-16} seconds corresponding to a vertical process of Franck-Condon nature[7]. Following their production, the positive ions are repelled from the ion source by an electrode positively charged with respect to the chamber and situated opposite the exit slit as shown in Figure 1.2. Collisions between ions and neutrals do not occur, because the mean free path is about 40 metres[7] with the source pressures commonly

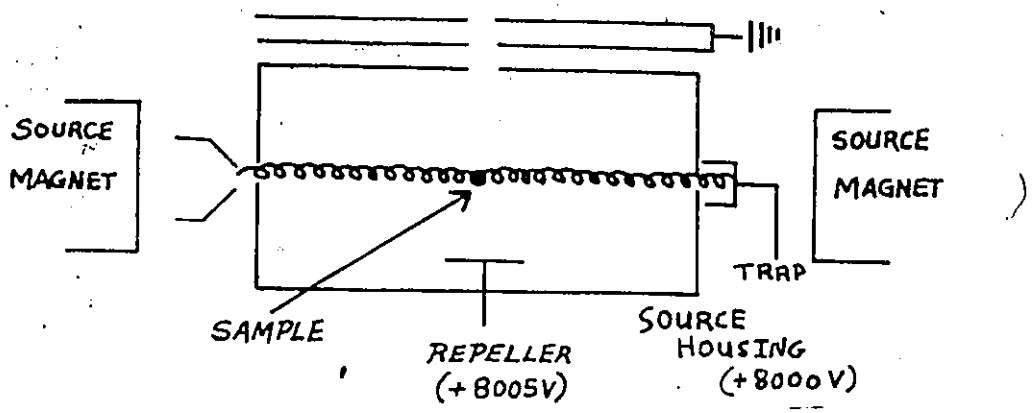

Figure 1.2: The ionisation chamber.

used (1×10^{-6} torr).

It is only in chemical ionisation (CI) conditions that ion/molecule collisions are desired in the source. In this instance, the source pressure is raised to *ca.* 0.1 torr by admitting to the ionisation chamber, *via* the CI inlet line, a reagent gas in about 1000 fold excess, such as CH_4 or H_2, along with the sample. The reagent gas is preferentially ionised whereupon ion/molecule reactions occur in the following way:

$$\begin{aligned} CH_4 + e &\longrightarrow CH_4^{+\cdot} + 2e \\ CH_4^{+\cdot} + CH_4 &\longrightarrow CH_5^+ + CH_3^{\cdot} \\ CH_5^+ + M &\longrightarrow [M+H]^+ + CH_4 \end{aligned} \tag{1.1}$$

Donation of a proton to the neutral sample molecule produces an ion which has a mass-to-charge ratio of M + 1, where M is the mass of the neutral sample. Also under CI conditions, using the proper reagent gas can produce a considerable amount of negative ions; however, negative ions will not not be discussed further in this thesis.

1.1.2 Ion acceleration

As ions exit the source chamber they come under the influence of a strong potential gradient, the accelerating voltage, V_{acc}, which is typically 8 keV. The kinetic energy of an ion falling through this potential gradient depends on its charge, z, and the magnitude of V_{acc}:

$$\frac{1}{2}mv^2 = zV_{acc} \tag{1.2}$$

where m is the mass and v is the terminal velocity of the ion. The source chamber is designed to minimize penetration of the electric field into the chamber which would disperse the ion kinetic energies; furthermore, the ion beam is collimated by slits to achieve a monoenergetic beam of ions. Ions produced have a small spread of thermal energies which is negligible compared to the kinetic energy of the ions after acceleration; therefore, all ions have the same kinetic energy regardless of their masses.

1.1.3 Purification: the magnetic sector (momentum separation)

Ions emitted from the source chamber after acceleration have the same kinetic energies but are a mélange of masses. The ions are passed through a magnetic field perpendicular to their motion in order to select the desired ion from this mixture. The magnetic field, B, causes a particle of charge z, to follow a curved path of radius r, according to its momentum mv, so that,

$$mv = Bzr \tag{1.3}$$

thus, a fixed radius, R, can be described by ions of momentum, mv, by changing the magnetic field, B.

We know that

$$\frac{1}{2}mv^2 = zV_{acc}$$

thus,

$$mv = (2mzV_{acc})^{\frac{1}{2}} \tag{1.4}$$

whereupon equations 1.3 and 1.4 give,

$$\frac{m}{z} = \frac{B^2R^2}{2V_{acc}} \tag{1.5}$$

which describes how ions of a given mass-to-charge ratio are directed along a fixed radius, R, according to the parameters, B and V_{acc}. Only ions of the desired mass-to-charge ratio (m/z) proceed further down the instrument. The ion beam selected by the magnet is known as the *main beam.*

The magnet also serves to focus the ion beam. Low resolution mass spectra can be obtained by scanning the magnet and using the first electron multiplier to detect the ions. Under these conditions, the instrument is operating in the single focussing mode.

1.1.4 Field-free regions

There are drift regions before and after the magnetic sector called the first and second field-free regions respectively. Both of these regions can be exploited for experimental purposes, as will become evident in Section 1.2 where the fragmentation behaviour of ions formed in the mass spectrometer is discussed.

1.1.5 Analysis: the electric sector analyser (energy separation)

A second analysing sector follows the second field-free region and consists of an electric field, E, generated by applying a voltage to two concentrically curved plates with a mean radius, R_e. Ions are transmitted through the electric sector analyser (ESA) if their centripetal force due to their kinetic energy is balanced by the electrostatic force acting on the ions:

$$\frac{mv^2}{r_e} = zE \tag{1.6}$$

Note that the radius described by an ion depends on the ion's kinetic energy, therefore scanning the electric sector analyses the kinetic energy distribution among the mass-selected ions.

We know for source-generated ions that

$$mv^2 = 2zV_{acc}$$

thus,

$$r_e = \frac{2V_{acc}}{E} \tag{1.7}$$

From equation 1.7, it can be seen that source-generated ions will describe a radius, R_e, through the electric sector *regardless of their mass*. High resolution mass spectra can be obtained with the ZAB-2F by setting E in appropriate proportion to V_{acc} and scanning the magnet. This is known as the double-focussing mode, which has enhanced mass resolution compared to the single-focussing mode. Increased mass resolution is derived from focussing the small spread of kinetic energies still possessed by the ions forming the ion beam after selection by the magnet.

1.1.6 Detectors

Ions that succeed in making their way through the instrument are detected by off-axis electron multipliers. Ions are deflected onto a negatively charged dynode. Upon ion impact electrons are ejected from the dynode and are accelerated onto the electron multiplier. Each impinging electron causes a cascade of electrons in the electron multiplier resulting in the production of as many as 10^6 electrons per incoming positive ion. The current flow from the terminal electrode is amplified electronically to produce a signal on the appropriate recorder.

Summary

To review, the mass spectrometer is comprised of a number of sectors which together serve as a complete laboratory for the gas phase ion chemist. Precursor compounds are admitted to the *ion source* through the appropriate inlet system. Positive ions generated by electron impact ionisation are directed out of the source by a repeller electrode and upon exiting the source fall through a large potential difference—the *accelerating voltage*. These fast-moving ions are separated according to their momenta in the *magnetic sector* which allows ions of a desired mass-to-charge ratio to pass into a drift region leading to the *electric sector analyser (ESA)*. Ions possessing a specific translational energy can be focussed by the ESA to the *detector* which transmits a signal to the experimenter's oscilliscope.

1.2 Ions

This section will introduce the fragmentation behaviour of positive ions formed in a mass spectrometer and will discuss how their detection can lead to useful information for the gas phase ion chemist.

Ionisation of a molecule in the source chamber by a 70 eV electron occurs in a time of the order of 10^{-16} second. This is essentially a vertical event according to the Franck-Condon principle since molecular vibrations are in the time range 10^{-14}–10^{-12} seconds. Ions formed by this ionisation are in various excited electronic states, but due to relaxation this electronic energy is transferred into electronic ground state vibrational energy as predicted by the quasi-equilibrium theory (QET)[8]. Ions formed initially by electron impact will have a wide range of internal energies (0–10 eV)[9]. As discussed below, the unimolecular decomposition behaviour of an ion depends on its internal energy content, however detection of the resulting fragments is limited by the instrumental time-scale—which for the ZAB-2F mass spectrometer is illustrated in Figure 1.3. Various types of unimolecular reactions can take place within this time-frame to result in detectable ions.

1.2.1 Molecular ions

If the ionisation process left the nascent ion with only a small amount of internal energy and if the ion is energetically stable, i. e. exists in a deep well on the potential energy surface, it can traverse the instrument without fragmenting. This species is known as the *molecular ion* and will

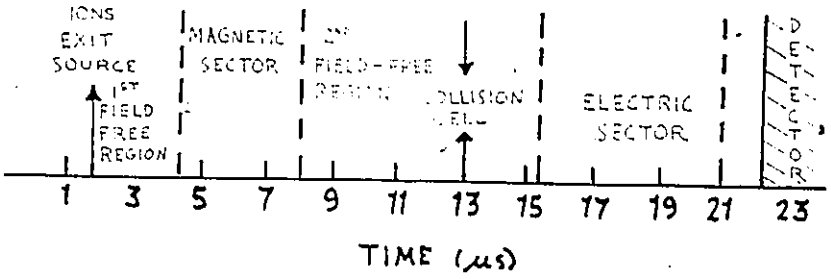

Figure 1.3: **Instrumental time-scale of the ZAB-2F.** (V_{acc} = 8kV and ion m/z = 100). Changing V_{acc} from 8 to 1 keV changes the time-scale, t, by $2\sqrt{2} \times t$.

be detected at the m/z equal to the molecular mass of the neutral sample and at a kinetic energy equal to V_{acc}.

1.2.2 Fragment Ions

Excess internal energy imparted by ionisation causes the molecular ion, m_1^+, to fragment with rate, k, producing the fragment ion, m_2^+, and the neutral, m_3. Fragment ions are also known as *daughter ions*, because they are derived unimolecularly from the *parent* molecular ion.

$$m_1^+ \xrightarrow{k} m_2^+ + m_3$$

The rate constant for this unimolecular reaction is a function of this excess energy, $\epsilon^\ddagger$, above the minimum energy, ϵ_0, required for the reaction to occur, and the frequency factor, ν, for the reaction. This can be summarised by a simplified QET expression[10]:

$$k = \nu \left(\frac{\epsilon^\ddagger - \epsilon_0}{\epsilon^\ddagger} \right)^{s-1} \tag{1.8}$$

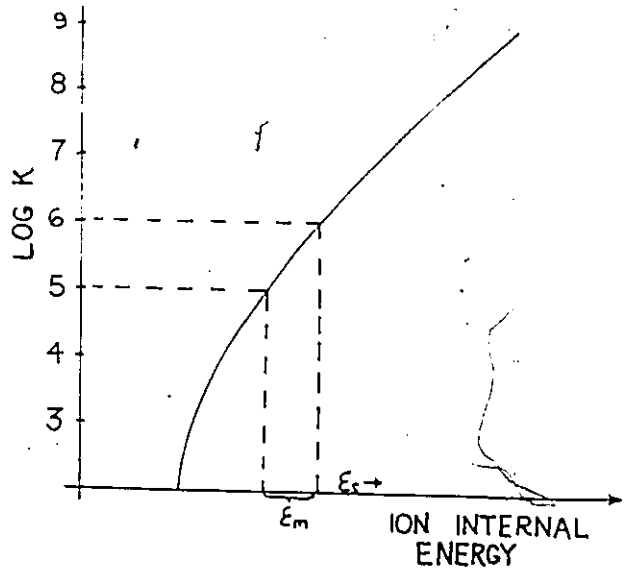

Figure 1.4: **Log k vs. ϵ plot.** Source-generated daughter ions must have a rate constant of formation corresponding to a time of $\leq 10^{-6}$ s and excess internal energy ϵ_s. Metastably-generated daughter ions have rate constants corresponding to $10^{-5} - 10^{-6}$ seconds and internal energy ϵ_m.

where, S, is the number of effective oscillators in the reacting ion. The quasi-exponential relationship between the rate constant and $\epsilon^{\ddagger}$ is depicted in Figure 1.4. It can be seen that the rate constant must be defined for a particular value of $\epsilon^{\ddagger}$. An ion may decompose *via* a number of different routes and each reaction is associated with a particular rate constant. A mass spectrum might, therefore, be viewed as a network of competing and consecutive unimolecular reactions observed within a limited time-scale.

Source-generated daughter ions

Ions with sufficient excess internal energy may fragment rapidly ($\leq 10^{-6}$ seconds) in the source chamber. Fragment ions come under the influence

of the repeller electrode, exit the source chamber, and fall through the potential gradient, V_{acc}. These ions are detected according to the m/z of the fragment ion formed.

Metastable ions

When the frequency factor for a fragmentation is low and/or the rise of the log k vs. ϵ curve is slow, fragmentation may take place in flight as the ion traverses the instrument. Ions with sufficient internal energies to fragment unimolecularly but which do so after exiting the source chamber are called *metastable ions*. Metastable ions define a particular internal energy channel (< 2 eV wide)[11] since these ions must have lifetimes between 10^{-6}–10^{-5} seconds (see Figure 1.4). If fragmentation occurs in the first or second field-free regions, the resulting metastably-generated daughter ion can be detected. Metastable ions that fragment in the magnetic sector or in the ESA are lost to the walls of the instrument.[1] Metastable peaks can be important observations in mass spectrometry and may provide valuable information when deciding upon possible isomeric structures of the ion[11].

To detect ions generated metastably in the *first* field-free region the magnet is tuned to select the ion of interest at its apparent mass, m^*,

$$m^* = \frac{(m_2)^2}{m_1} \tag{1.9}$$

for the first field-free region reaction,

$$m_1^+ \rightarrow m_2^+ + m_3 \tag{1.10}$$

[1]There are rare cases when fragmentation in a non-field-free region can still result in detectable ions;[12] one such case, which is particularly significant to the work of this thesis, is described in Chapter 3.

These ions traverse the magnet and are transmitted through the electric sector at a kinetic energy corresponding to $\left(\frac{m_2}{m_1} \times V_{acc}\right)$, where m_1 is the ion undergoing metastable decomposition to produce m_2, the ion of interest.

Metastable daughter ions arising from fragmentation in the *second* field-free region can also be detected. For reverse-geometry mass spectrometers such as the ZAB-2F, a single m/z is selected by the magnet. The metastable daughter ions arising from this parent ion by fragmentation in the second field-free region are then analysed by the electric sector. If the parent ion undergoes the fragmentation depicted in equation 1.10, its kinetic energy, zV_{acc}, will be distributed among the products.

$$1/2m_2v_2^2 = m_2/m_1 \times zV_{acc} \qquad (1.11)$$
$$1/2m_3v_3^2 = m_3/m_1 \times zV_{acc}$$

Thus, one can calculate the mass of a product ion by the knowledge of its kinetic energy measured by the electric sector, using equation 1.11. This technique is known as mass analysed ion kinetic energy (MIKE) spectrometry. A MIKE spectrum thus shows the second field-free region unimolecular decompositions of a particular molecular or fragment ion. An important aspect of a MIKE spectrum is that it clearly defines parent–daughter relationships, which is not usually evident from a normal mass spectrum. MIKE spectra can be used to distinguish between isomeric forms of an ion by revealing different unimolecular decomposition routes for the ion generated from different precursor molecules[13].

When a metastable ion, m^*, fragments, the excess internal energy is partitioned among all the degrees of freedom of the fragments—some of it

is released into translational degrees of freedom. This results in a signal broader than source-generated ion signals. The kinetic energy release, T, is usually estimated from the metastable peak width at one half height, $\omega_{0.5}$, when measured under conditions of good energy resolution (main beam width *ca.* 2 volts). In such a case, $T_{0.5}$ is easily calculated,

$$T_{0.5} = \frac{m_1^2\,\omega_{0.5}^2}{16\,m_2\,m_3\,V_{acc}} \tag{1.12}$$

where m_1 is the mass of the metastable ion that undergoes fragmentation, m_2 and m_3 are the departing fragments, and $\omega_{0.5}$ is the width of the metastable peak at one half its height and measured in volts. In the simplest cases, $T_{0.5}$ can be used to characterize the structure of metastably fragmenting ions. Such *was* the case for the ions with empirical formula $[C_2H_4O]^{+\cdot}$[14]. Ions identified as $[CH_3CHO]^{+\cdot}$, $[\overbrace{CH_2CH_2O}]^{+\cdot}$, and $[CH_2CHOH]^{+\cdot}$ each showed different metastable peak shapes and $T_{0.5}$ values for H atom loss. However, further studies[15] have revealed that the picture is more involved than originally thought, when it was found that the isomer, $[CH_3COH]^{+\cdot}$, exists and indeed is responsible for the metastable peak previously associated with $[CH_2CHOH]^{+\cdot}$.

Summary

Loss of an electron from the precursor molecule upon electron impact in the ion source results in a *molecular ion.* Molecular ions generated with sufficient internal energies may decompose unimolecularly in the ion source to produce *fragment ions*, also known as *source-generated daughter ions.*

Fragment and molecular ions may also decompose in a field-free region resulting in *metastable daughter ions*. The shape of the peak and the *kinetic energy release* associated with the production of metastable daughter ions can provide information concerning the structure(s) of both the parent and daughter ions.

1.3 The determination of ion structure

Strategies for assigning structures to organic gas phase positive ions will be discussed below with emphasis on those techniques most frequently referred to in the course of this thesis. It should be first noted that 'structure' at this stage in gas phase ion chemistry refers only to which atoms are bound together in the ion rather than implying such things as bond lengths and bond angles.

When faced with the puzzle of assigning a structure to an ion, the mass spectrometrist may first determine the ion's thermochemistry. This establishes the ion's *heat of formation*, $\Delta H_f^o(ion)$, which can then be compared with the known heats of formation of its isomers. In this way, the number of energetically feasible structures which may be assigned to the ion can be reduced to a minimum. The heat of formation also gives the gas phase ion chemist some idea of the ion's thermodynamic stability with respect to other ions of known structure and heat of formation. This enables general trends in heats of formation, such as those found for ions belonging to a homologous series[17], to be established.

Next, the ion's dissociation characteristics as a function of its inter-

nal energy may be probed from the observation of metastable or collision-induced decompositions. Isotopically labeled compounds may be used to enhance the information gained from the ion's dissociations by discovering which atoms are involved at the reaction centre of the fragmentation[18].

1.3.1 Ionisation, appearance energies and heats of formation

Figure 1.5 outlines the energy levels established by measurements of *ionisation energies (IE)* and *appearance energies (AE)*. These measurements are best performed (±50 meV)with specialized instruments such as photoionisation mass spectrometers[19], or energy-selected electron impact mass spectrometers[20].

A molecular ion's heat of formation, $\Delta H_f^o([M]^{+\cdot})$, is obtained from the IE (process(i) in Figure 1.5) and the knowledge of the standard heat of formation of the neutral molecule[21],

$$\Delta H_f^o([M]^{+\cdot}) = IE(M) + \Delta H_f^o(M) \qquad (1.13)$$

If the ion of interest, $[M]^{+\cdot}$, is a daughter ion formed by dissociative ionisation of the precursor molecule, MB, (process(ii) in Figure 1.5), the following equation applies,

$$\Delta H_f^o([M]^{+\cdot}) = \Delta H_f^o(MB) + AE([M]^{+\cdot}) - \Delta H_f^o(B) \qquad (1.14)$$

The ion enthalpy derived from equation 1.14 will be the same as that obtained from equation 1.13, provided the structures of $[M]^{+\cdot}$ are indeed the same, and there is no energy barrier for the reverse reaction, $B + [M]^{+\cdot} \rightarrow [MB]^{+\cdot}$.

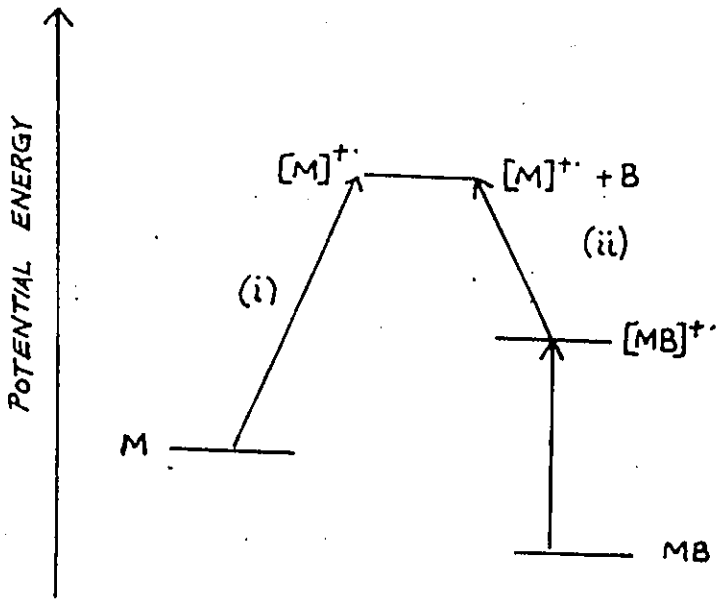

Figure 1.5: **Energy diagram for the formation of $[M]^{+\cdot}$.**

Apart from the possible presence of a barrier for the reverse reaction, there are three reasons why the heat of formation obtained in these ways represents an upper limit. First of all, it is important to remember that the most probable ionisation event for photoionisation and electron impact measurements is the vertical process.[2] Vertical ionisation may not form ions in their vibrational ground states (see Figure 1.6). The difference between IE_v and IE_a can be as large as 0.7 eV[22].

Another factor influencing energetic measurements is the limited time-scale of the experiment. Ion source residence times of instruments used for such measurements are about 10^{-3} seconds[20]; hence, fragment ions formed in the ion source must arise from a reaction having a rate constant

[2]Both of these methods approach the adiabatic threshold by detecting the (often) small amount of signal corresponding to the lower probability adiabatic transition.

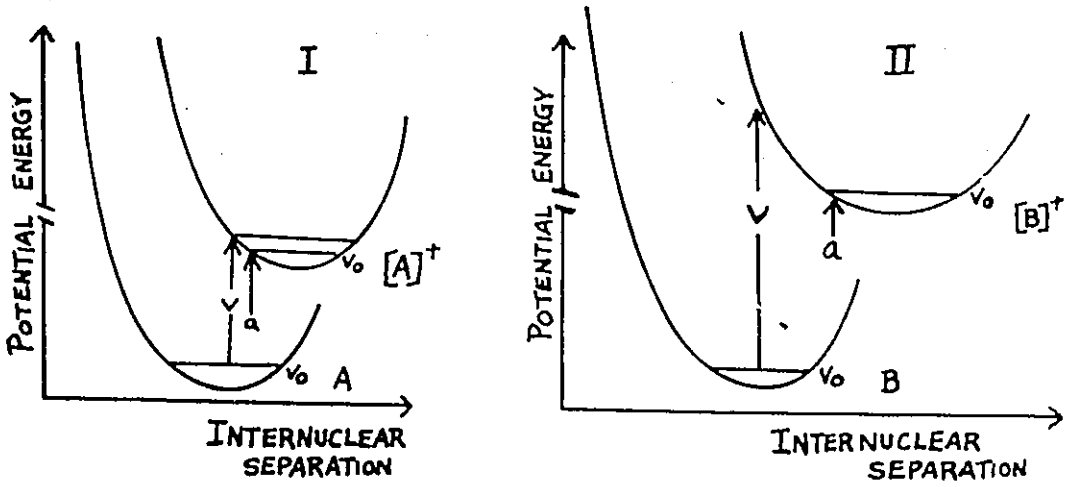

Figure 1.6: **Electronic transition curves.** Vertical (v) and adiabatic (a) ionisations for case I where ionised state and neutral state geometries are similar, and for case II where geometries are significantly different.

corresponding to less than this period of time. The internal energy required to attain this rate of fragmentation may not very closely correspond to the thermochemical threshold. The excess energy, $\epsilon^{\ddagger}$, required to achieve this fragmentation rate is known as the *kinetic shift*. Its magnitude depends on the shape of the log k vs. $\epsilon^{\ddagger}$ curve for the ion in this time period. Kinetic shift can contribute as much as 1 eV to appearance energy measurements in extreme cases[23].

Thirdly, AE measurements can be subject to what has been termed *competitive shift*. This arises when competing reactions also occur at energies close to the threshold of the reaction under study, causing the number of fragment ions to rise slowly with increasing ionising energy. Competitive shift can add up to 2 eV to AE measurements[24].

An example of the use of heats of formation for structure assignment,

and also how the above mentioned limitations can influence the situation, are the isomeric ions, $[C_2H_6O]^{+\cdot}$. Initial experimental work[25] with a variety of precursor molecules revealed three different ions with heats of formation of 774 ± 1 kJ/mole, 778 ± 2 kJ/mole, and 757 ± 8 kJ/mole. The three ions were thought to have the structures, $[CH_3CH_2OH]^{+\cdot}$, $[CH_3OCH_3]^{+\cdot}$, and $[CH_2CH_2OH_2]^{+\cdot}$, respectively. A fourth heat of formation, 732 ± 5 kJ/mole, for the $[C_2H_6O]^{+\cdot}$ ion generated from 2-methoxyethanol was also found, and being significantly different from the other values was believed to correspond to a new isomer. This isomer was proposed to have the structure $[CH_2{=}CH\cdots H\cdots OH_2]^{+\cdot}$. High level theoretical calculations[26,27] confirmed that these four species were stable ions, however they pointed out that the isomer, $[CH_2{=}CH\cdots H\cdots OH_2]^{+\cdot}$, has a heat of formation 7 kJ/mole above that of ionised ethanol, 774 kJ/mole. This structure, therefore, could not correspond to the experimentally measured heat of formation, 732 ± 5 kJ/mole.

It was also calculated that the isomer, $[CH_2CH_2OH_2]^{+\cdot}$, has a heat of formation of 43 kJ/mole below that of ionised ethanol. Obviously, the experimental value lying only 17 kJ/mole below that of ionised ethanol was in error. New experiments showed that the experimental value was indeed an upper limit and extended measurements[27] were able to lower the heat of formation to 740 kJ/mole for the isomer $[CH_2CH_2OH_2]^{+\cdot}$. This was now in good agreement with the theoretical calculations. The new experimental evidence[27] and the heat of formation, 732 ± 5 kJ/mole, confirmed that the isomer generated from 2-methoxyethanol must correspond to threshold

generated $[CH_2CH_2OH_2]^{+\cdot}$ ions.

A second important use of energy measurements is the assignment of a probable range of internal energies to an ion population. For example, an ion, $[M_1]^+$, is formed at threshold with an ionisation energy of 10.8 eV and its thermodynamically most favourable fragmentation produces an ion, $[M_2]^+$, which has an appearance energy of 12.5 eV. Barring significant kinetic energy shifts or reverse activation barriers one can set an upper bound of about 1.7 eV internal energy to those ions, $[M_1]^+$, that do not fragment before detection. This information can be helpful when considering whether the ion, $[M_1]^+$, could possibly rearrange to another structure before fragmenting.

1.3.2 Ion dissociation characteristics

The information gained by measuring an ion's heat of formation can be complemented by additional evidence found from observing metastable and/or collision-induced fragmentations. Structure characteristic dissociations of an ion can be investigated as a function of its internal energy by the exploitation of these two types of fragmentations.

Metastable dissociations

Metastable ions have been previously introduced. A MIKE spectrum will show the second field-free metastable decompositions for a particular ion which has been mass-selected by the magnet. The shape of the resulting metastable peak corresponds to the ionic transition state(s) before fragmentation[28]. Isotopic labeling studies may be used to determine how

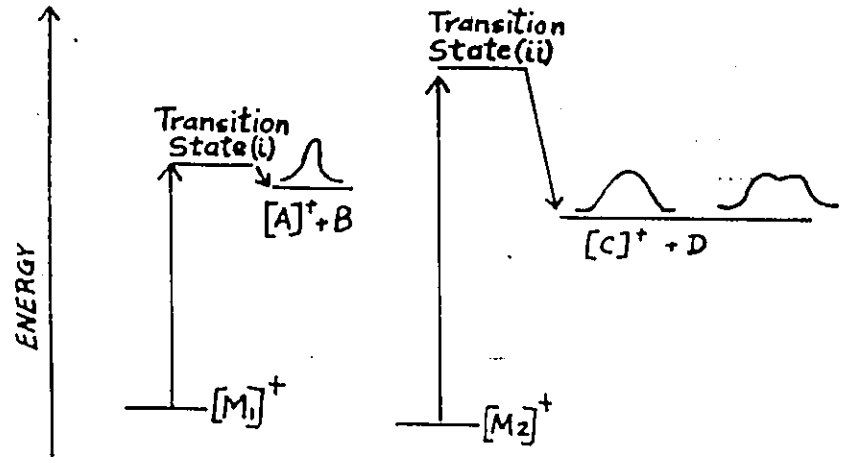

Figure 1.7: **The shapes of metastable peaks.** Reactions having transition states (i) near or equal to the thermochemical threshold give narrow Gaussian-shaped peaks. Reactions having transition states (ii) significantly greater than the thermochemical threshold give wide Gaussian-shaped peaks or dished-shaped peaks. The dished shape is due to z-axial discrimination effects of the instrument for processes that undergo large kinetic energy releases.

the stable configuration of the ion which leads directly to the transition state relates to the ground state ion structure. The average kinetic energy release, $< T >$, is a function of the excess energy in the transition state and can be correlated with the shape of the resulting metastable peak as shown in Figure 1.7. Calculating $< T >$, however, can be difficult[28] so the more easily obtainable $T_{0.5}$ is used as a relative measure of the excess energy released upon metastable decomposition.

If the observed metastable peak clearly consists of a combination of two or more components (i. e. it possesses a non-Gaussian shape), then daughter ions are being generated *via* different transition states. This may reflect different parent isomers, different reacting configurations, and/or

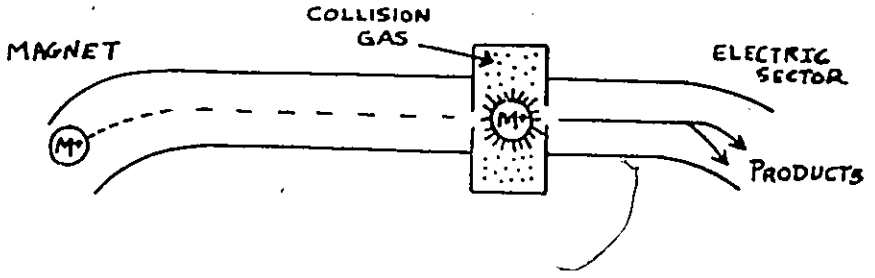

Figure 1.8: **Arrangement of the collision gas chamber for CA mass spectrometry with the ZAB-2F.**

isomeric product ions. Such an observation may give new significance to an AE measurement since only the lowest thermochemical threshold will be identified when measuring the appearance energy[16]. Thus, metastable peaks are often a valuable complement to energetic values and a useful characteristic of ion structure.

Collision-induced dissociations

Studies by Jennings[29], McLafferty[30,31], and Beynon[32] have shown that collision-induced processes caused by the interaction of the ion beam with a neutral target gas can result in fragmentations that provide a wealth of information about the structure of organic gas phase ions. Most reverse-geometry double-focussing mass spectrometers used for research now have at least one differentially pumped collision gas chamber for collision-induced decomposition (CID) mass spectrometry, also known as collisional activation (CA) mass spectrometry (see Figure 1.8).

When the translational energy of the ion beam is high (> 1 keV) and the target gas is small (e. g. He), the main process that results from an inelastic ion-atom collision is electronic excitation of the impinging ion[33].

The encounter occurs in a time of the order of 10^{-15} seconds and corresponds to a vertical excitation, i. e. which is Franck-Condon in nature[28]. A relatively small amount of the translational energy is converted into internal energy in the ion. This excess internal energy degenerates rapidly from electronic excitation to ground state vibrational excitation of the ion, and within several picoseconds is statistically distributed among the degrees of freedom of the ground state ion. The internal energy acquired by collision may be sufficient to cause decomposition of the ion into fragments. When the ion beam has translational energy 8–10 keV, CA mass spectra often display relative ion intensities similar to 70 eV mass spectra of the source-generated ion; this is shown for acetic acid in Table 1.1. This similarity is not surprising since the range of ion internal energies (0–12 eV)[3] and the time-scale on which ions are sampled (10^{-6} s) are similar[30]. Differences between EI and CA mass spectra are often attributable to the different lifetimes of the parent ion. Since collisional activation does not take place until after the parent ion has proceeded through two-thirds of the instrument, rearrangement of the ion to another structure may occur in flight prior to collisional activation. The similarity of the two spectra listed in Table 1.1 indicates that $[CH_3COOH]^{+\cdot}$ ions do not undergo significant rearrangement before collisional activation.

CA mass spectrometry can be used, therefore, to produce a 'secondary mass spectrum' of fragment ions found in the normal electron impact mass

[3]A small part of the ion internal energy distribution produced by CA does actually exceed this range, which accounts for the observation of doubly charged ions—a process requiring about 20 eV internal energies.

m/z	EI mass spectrum	CA mass spectrum
60	(74)	-
45	90	66
44	3	4
43	100	100
42	13	7
41	3	3
40	1	1
31	2	2
30	0.5	0.4
29	10	7
28	3	2
26	0.3	0.4
25	0.3	0.4
24	0.1	0.2
18	1	-
17	0.5	0.5
16	3	2
15	26	6
14	6	3
13	2	1
12	0.5	0.5

Table 1.1: **EI vs CA mass spectra of acetic acid.** Since the intensity of the molecular ion, m/z 60, in CA mass spectra depends on the collision efficiency, the molecular ion intensities are not directly comparable. (From reference [34]).

spectrum of a compound. Since these spectra may serve as characteristic fingerprints of a particular molecule, CA mass spectrometry is a powerful tool for the analytical chemist as well as the gas phase ion researcher.

A CA mass spectrum obtained with the ZAB-2F is usually obtained by scanning the electric sector. The ion of interest is selected by the magnet and drifts into the second field-free region where it encounters the collision gas. Collisional activation occurs and the ion may fragment in a number of ways producing different daughter ions with different kinetic energies. The electric sector scans the possible range of kinetic energies and the daughter ions are detected. Their m/z ratios may be calculated by using equation 1.11—as for second field-free region metastable ions.

After collisional activation, part of the excess energy (including the kinetic shift and the reverse activation energy, if they exist) is released as translational energy of the fragments, resulting in signal broadening greater than, but analogous to, that found with metastable peaks. Signal broadening is greater for ions produced by CA than for those ions produced by metastable decompositions, because the internal energy range of the collisionally activated ions is greater than the range of energies associated with their metastable counterparts. Signal broadening can be a disadvantage for CA spectra obtained with the electric sector scan method when fragment ions have similar masses and therefore similar translational energies. Peaks corresponding to adjacent masses will overlap slightly. The problem is most serious for ions with $m/z > 200$ or when a small peak is next to a much larger one. Peaks can be deconvoluted by assuming Gaussian profiles.

Because of the orientation of collector slits in the mass spectrometer, only those ions which undergo little or no scattering after collision with the target gas will be collected. One can assume that the observed ions do not impart appreciable amounts of translational energy to the target gas; consequently, the excess energy of the ion will be of the same magnitude as their translational energy loss[33]. The decrease of translational energy, Q, can be measured, permitting a direct determination of the excitation energy.

Factors affecting CA mass spectra

Ion translational energy. Changing the ion translational energy changes both the time-of-flight and the amount of excess energy deposited in the ion by collision with the neutral gas. Since the ion's lifetime changes by only a small amount (Figure 1.3), differences between CA spectra at different ion translational energies is mainly due to the changing excess energy gained by the ion upon collision. The amount of excess energy, E, deposited in the ion will depend on the 'closeness' of the encounter,and the velocity and molecular weight of the impinging ions for each collision, according to the Massey adiabatic criterion:

$$E = \frac{h}{a}\left(\frac{2eU}{m}\right)^{\frac{1}{2}} \tag{1.15}$$

where h is Planck's constant, a is the interaction distance, eU is the ion's translational energy and m is the mass of the ion. From equation 1.15, Durup[35] has derived that the cross-section for vertical excitation of inci-

dent ions reaches a maximum at ion velocity v_0 when,

$$v_0 \approx \frac{aE^*}{h} \qquad (1.16)$$

where E^* is the excitation energy. Kim and McLafferty[36] used this approximation to estimate that an ion of m/z 40 will receive 0.9, 1.3, and 2.0 eV as the most probable internal energy upon collision with helium at 2, 4, and 8 keV translational energy, respectively. In a different study[38], Beynon and co-workers determined that the most probable internal energy received by an ion of m/z 134 upon 8 keV collision with helium was 3.2 eV. Obviously, the translational energy of the incident ions can affect CA mass spectra appreciably. A good example of this is found with the study of the allyl and 2-propenyl structures for the ion $[C_3H_5]^+$, as shown in Figure 1.9.

Collision gas. Another parameter influencing CA mass spectra is the nature of the collision gas. The intensity ratios of fragment ions can change when, for example, the collision gas is changed from He to N_2 or O_2; e. g. in the CA mass spectrum of m/z 91 ions from toluene, the structure specific peak intensity ratio m/z 77:74 changes by a factor of 4 when the collision gas is changed from He to N_2.

Figure 1.10 shows the relative CID efficiencies for different collision gases as measured on the ZAB-2F mass spectrometer[39]. Because of its superior efficiency in producing detectable ions, He has become the standard collision gas for CA experiments.

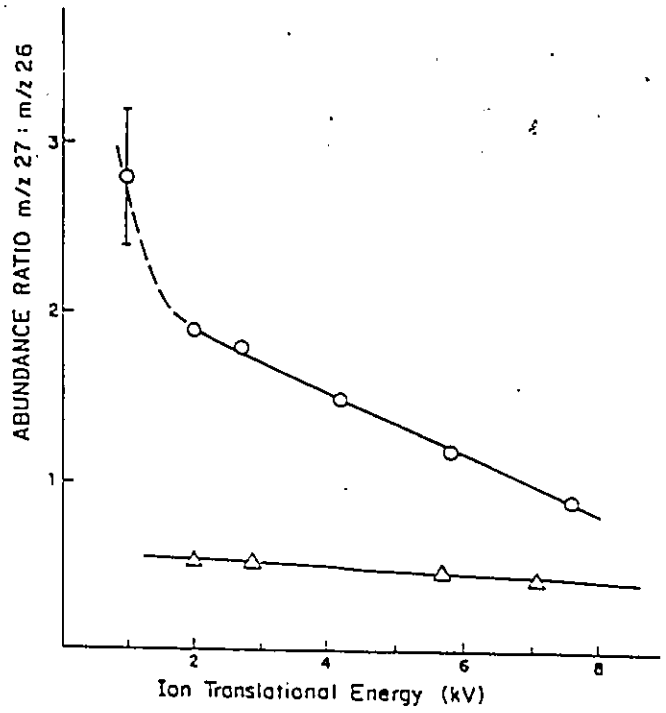

Figure 1.9: **The effect of ion translational energy on the structure specific m/z 27/26 peak intensity ratios in the CA mass spectra of $[C_3H_5]^+$ ions.** Discerning between allyl and 2-propenyl ions by examining the structure characteristic m/z 27 : 26 ratios. ($\triangle[CH_3C=CH_2]^+$ ions, $\bigcirc[CH_2CHCH_2]^+$ ions), from reference [37].

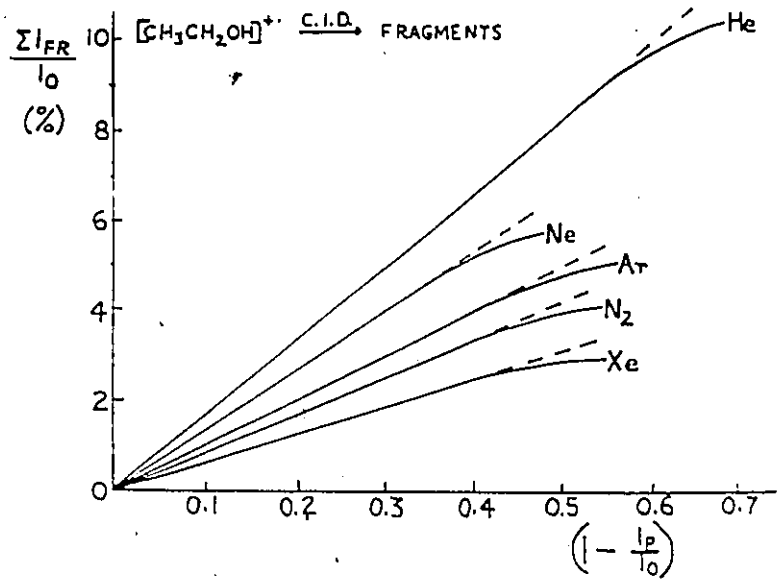

Figure 1.10: **Relative CID efficiencies for different collision gases.** $\sum I_{FR}/I_0$ represents the sum of the observed fragments, I_{FR}, with respect to the main beam intensity, I_0. $(1 - I_p/I_0)$ indicates main beam reduction. Experimental conditions: 8 keV accelerating voltage, 70 eV ionising electron energy. Adapted from reference [39].

Collision gas pressure. The pressure of the collision gas is usually controlled so that only one collision on average will occur (about 10% beam reduction as shown in Figure 1.11), otherwise multiple collisions will increase the internal energy content of the ion population beyond the range of internal energies normally associated with single collision CA mass spectra. Without control of the average number of collisions, comparisons between CA mass spectra are not possible. Multiple collisions may also suppress structure characteristic information in the CA spectrum as in the case documented by Figure 1.12. Furthermore, using collision gas pressures sufficient to reduce the main beam by only 10% minimizes leakage of the gas from the collision cell, helping to define a more precise collision region in the mass spectrometer.

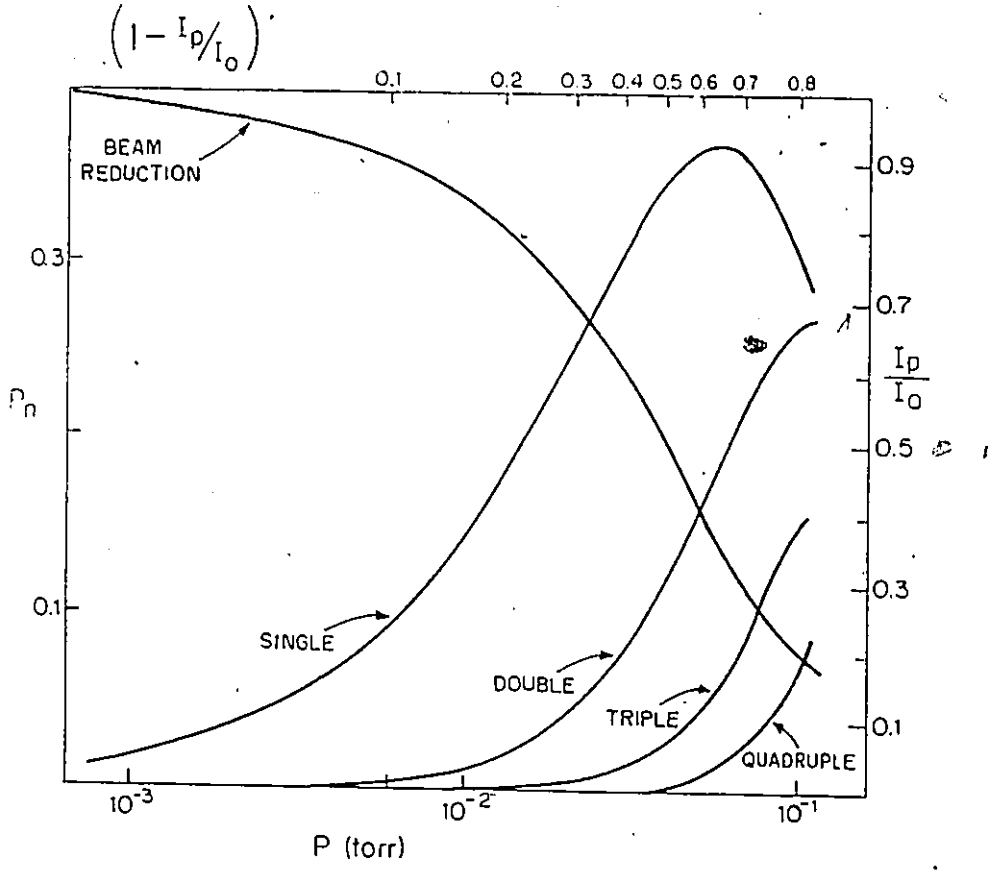

Figure 1.11: **Total collision probability (P_n) and beam reduction (I_p/I_0) as a function of collision gas pressure (P).** The upper scale shows $(1 - I_p/I_0)$ as an alternative pressure indicator. (Ion collision cross-section $= 5 \times 10^{-16}\, cm^2$, collision path 1 cm. From reference [28]).

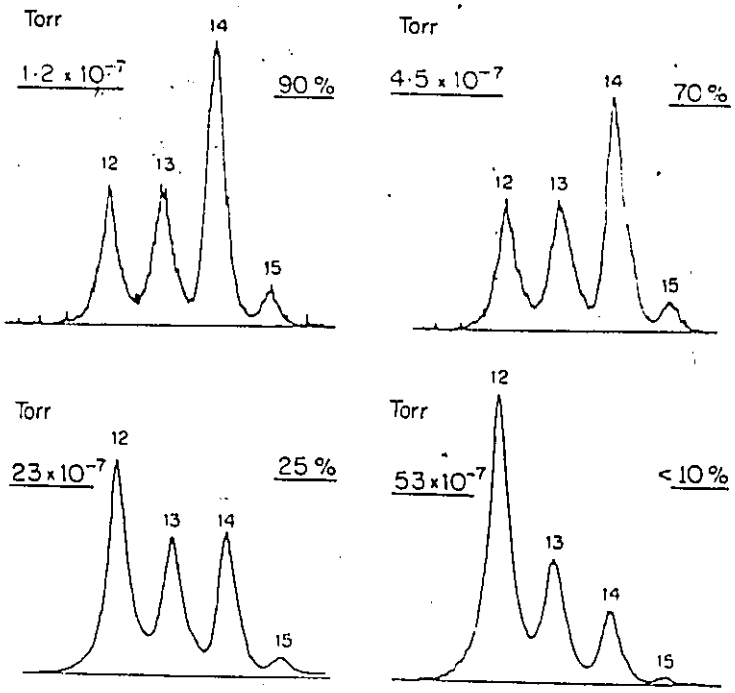

Figure 1.12: **The effect of multiple collisions on the CA mass spectra of [allene]$^+$ ions, m/z 12–15.** The main beam transmission is given as a percentage, and the He collision gas pressure is as indicated. (From reference [28]).

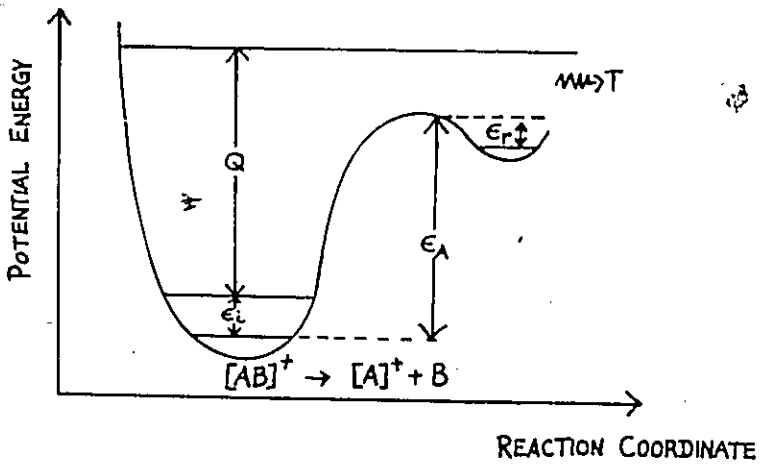

Figure 1.13: **Energy transfer in collision-induced decomposition for the reaction:** $[AB]^+ \rightarrow [A]^+ + B$. The average internal energy, ϵ_i, of $[AB]^+$ sampled by CA mass spectrometry is less than ϵ_A since these are ions that have not yet fragmented. Upon inelastic collision an amount of translational energy, Q, is converted into internal energy. Note that if $Q \gg \epsilon_i$, $Q + \epsilon_i \approx Q$ (true for high energy processes), and ϵ_i will have small effect on the intensity of the fragment ion $[A]^+$.

Inferring ion structure by CA mass spectrometry

A major advantage of the CA technique in terms of structure determination is that the internal energy content of the precursor ion prior to collision only *slightly* influences the internal energy distribution after collision, as illustrated by Figure 1.13. This is unlike metastable peaks, the intensity of which can be significantly influenced by precursor ion internal energy[40].

Since the internal energy of the precursor ion can influence the intensity of the peaks which correspond to low energy processes, it is important to establish the *energy-independent* CA mass spectrum of the ion under study. This can be established by correlating the low energy processes with

low appearance energies or to observable metastable peaks. Once the low energy signals have been discarded, the CA mass spectrum will be invarient for a single isomer ion population. Changes in the relative peak heights or the observation of new peaks indicate a changing mixture of isomers or the emergence of new isomers in the ion population. This is because intensity ratios of fragment ions depend on the rate constants for fragmentation, which in turn are functions of the vibrational and rotational frequencies. Different isomers will have observable differences in CA mass spectra as vibrational and rotational frequencies will not be the same for each isomer. Thus, differences between CA mass spectra of ions with the same empirical formula (but generated from different precursor molecules) reflect changes in the ion structure or the mixture of structures, and are not due to the method of preparation.[4]

However, since the structure or mixture of structures of the ion population may depend on the internal energy content *before* collisional activation, it may be useful to now consider the relative internal energies of ions sampled by CA mass spectrometry with respect to the entire ion population. As shown in Figure 1.14, source-generated ions, $[M_b]^+$, selected to undergo collisional activation possess a range of internal energies, which can be loosely bracketed as *greater* than those ions, $[M_a]^+$, generated metastably by low energy processes, but *less* than those ions, $[M_c]^+$, which decompose unimolecularly, either in the ion source or in the field-free regions of the mass spectrometer. If the ions which undergo collisional activation are assumed

[4]Again, this does not apply to those processes in the CA mass spectrum that give rise to metastable peaks, which may change in intensity with changes in ion internal energy.

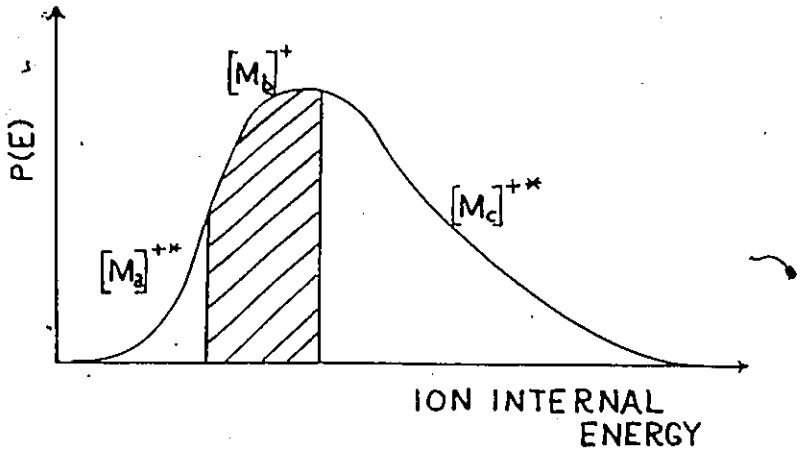

Figure 1.14: **The distribution of internal energies for ions, $[M]^+$, sampled by CA mass spectrometry.** Ions produced metastably, $[M_a]^{+\bullet}$, have the lowest internal energies. Source-generated $[M_b]^+$ ions that do not normally decompose before detection are collisionally activated in the second field-free region of the mass spectrometer. Before collision, these ions have a range of internal energies extending from metastably-generated ions to those ions with high enough internal energies to decompose in flight $[M_c]^{+\bullet}$.

to retain their structure within this range of (shaded) internal energies, then the CA mass spectrum can tentatively taken as characteristic of ions of that structure.

To substantiate the assumption that the ions retain a unique stucture within the ion population sampled by CA mass spectrometry, one may inspect parent ions with low internal energies[28]. This can be done by lowering the ionising electron energy to a level that gives the minimum acceptable signal (main beam $\div$1000 is usually obtainable). This will give the CA mass spectrum of low energy source-generated ions.

Alternatively, collisionally deenergizing the ions by admitting a large amount of an inert gas, such as helium, to the ion source also produces

low energy source-generated ions. A drawback of this method, however, is that some of the inert gas may diffuse into the first field-free region causing an increased amount of collisional energization and decomposition of ions before the magnet.

A third method transmits ions resulting from first field-free region metastable (unimolecular) decompositions. These metastably-generated ions are selected by the magnet (see Equation 1.9) and are collisionally activated in the second field-free region. It is important to remember that the translational energy of the ion produced by this means will be a fraction of V_{acc} corresponding to $\left(\frac{m_2}{m_1} \times V_{acc}\right)$, where m_1 is the ion undergoing metastable decomposition to produce m_2, the ion of interest.

If the CA spectra do not change across these internal energy ranges, it may be concluded that there is probably only one structure present[28]. One may now use this CA spectrum as a reference spectrum for the ion of the inferred structure. Comparisons can then be made between this spectrum and the CA spectra for the ion derived from other precursors. By generating the ion from a wide variety of precursor molecules, it is usually possible to identify different isomeric forms.

However, if the intensities of fragment ions are found to be dependent on the electron ionising energy, it can be concluded that a mixture of structures is present—each isomer being formed simultaneously from the parent ion(s) by competing mechanisms with different energy barriers[9].

1.3.3 Summary

At present, *collisional activation* mass spectrometry forms the backbone of the techniques used by mass spectrometrists to probe the chemistry of gas phase ions. CA mass spectrometry can lead to reliable structural assignments for gas phase ions when used in conjunction with energetic measurements and metastable peak observations. Energetic measurements, such as the *ionisation energy* or *appearance energy*, can lead to an assignment of an ion's *heat of formation*. Metastable peak observations give the *kinetic energy release* associated with a particular unimolecular fragmentation. The number of participating isomers in the metastable reaction may be assessed by examination of the shape of the observed metastable peak.

Chapter 2

Isomeric forms of the gaseous ion $[C_7H_7]^+$

2.1 The benzyl and tropylium ions

The normal mass spectra of many aromatic organic compounds and long-chain, unsaturated hydrocarbons contain a large peak corresponding to an ion of m/z 91. This ion, $[C_7H_7]^+$, was initially assumed to have the benzyl (1) structure when derived from alkylbenzenes and benzyl halides. However, in 1957 Meyerson and co-workers[41] offered the provocative suggestion that the $[C_7H_7]^+$ ion formed from toluene was not the familiar benzyl ion, but rather the symmetrical tropylium ion (2). This conclusion was

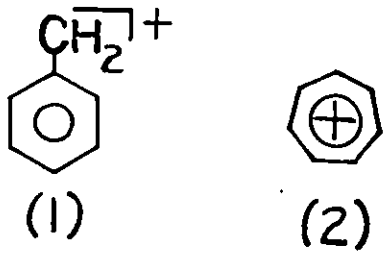

Figure 2.1: Benzyl (1) and tropylium (2) ions.

based on experimental evidence which showed that α-d_3-labeled toluene produced $[C_7(H,D)_7]^+$ ions by equivalent loss of D or H atoms. The labels had 'scrambled'; i.e. positional identity of the H, D atoms had been lost.[1] The observation of eight indistinguishable hydrogens suggested a symmetrical ion, and thus the gas phase tropylium ion was proposed as the daughter ion. No doubt the isolation of stable, high-melting tropylium salts[108] a few years earlier helped gain the acceptance of the tropylium ion as a viable gas phase species. It was originally thought[41] that tropylium was 9-15 kcal more stable than benzyl (see Table 2.4 at the end of this chapter for the $[C_7H_7]^+$ ion thermochemistry). This added stability for the $[C_7H_7]^+$ ion helped explain conflicting energetic measurements of what was thought to be the benzyl bond strength, $D[C_6H_5CH_2\text{–}H]$[43,44].

The existence of the $[C_7H_7]^+$ ion as tropylium received additional support when it was shown[45,46] that complete scrambling of hydrogen *and* carbon atoms occurs in the formation of $[C_5H_5]^+$ from both toluene and cycloheptatriene precursors. Furthermore, evidence was found[47] that suggested a large number of ionised C_7H_8 compounds fragment *via* the same intermediate(s), since the following fragmentation sequence is generally observed.

$$[C_7H_8]^{+\cdot} \xrightarrow{-H} [C_7H_7]^+ \xrightarrow{-C_2H_2} [C_5H_5]^+$$

Norbornadiene and quadricyclene, which lose C_2H_2 directly from the molec-

[1]The weakest C–H bond of toluene is the $C_6H_5CH_2$–H bond. Ignoring isotope effects, loss of deuterium is expected to occur with the most probability for α-d_3-labeled toluene precursors. Observation of relative H or D loss with statistical probability, however, is in accordance with migration of H and D atoms in the $[C_7(H,D)_8]^{+\cdot}$ ion to the extent that no memory of relative positions in the precursor molecule is retained.

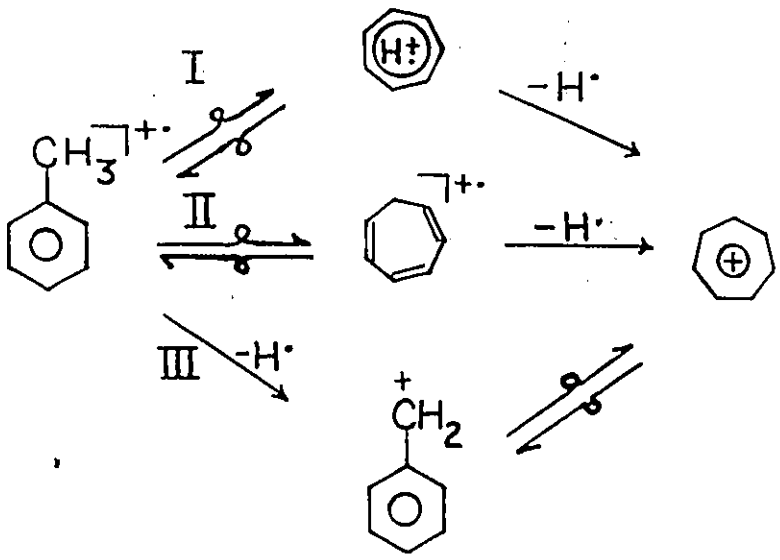

Figure 2.2: Mechanisms of tropylium ion formation.

ular ion *via* a *retro* Diels-Alder mechanism[47] are noteworthy exceptions. From these and other studies[45], the $[C_7H_7]^+$ ion became generally accepted as having the tropylium ion structure when formed from aromatic hydrocarbons, cycloheptatriene, and the benzyl halides[48].

Gas phase ion chemists were intrigued by the mechanism(s) by which formation of the tropylium ion might occur. It was known that loss of H from $[C_7H_8]^{+\cdot}$ precursors results in $[C_7H_7]^+$ ions in which all the hydrogens are scrambled. Moreover, further ^{13}C labeling experiments[49,50,51] confirmed that carbon atoms lose all positional identity prior to (or during) formation of the $[C_5H_5]^+$ ion by 70 eV electron impact on toluene, cycloheptatriene, and various other precursors. As shown in Figure 2.2, three possibile schemes were suggested to account for this observed behaviour[48]:

1. As originally suggested by Meyerson,[41] $[C_7H_8]^{+\cdot}$ ions may rearrange to a symmetrical intermediate which loses hydrogens randomly and makes carbons equivalent (Scheme I in Figure 2.2). Carbon scrambling is accounted for by reversible random insertion of the α-carbon between any carbon-carbon bond in the benzene ring.
2. $[C_7H_8]^{+\cdot}$ ions might undergo a series of rearrangements between the toluene and cycloheptatriene forms of the molecular ion (Scheme II). Again, hydrogen transfer from the methyl group to an adjacent carbon followed by random insertion of the methylene group into the ring accounts for the hydrogen and carbon scrambling *via* this mechanism.
3. The $[C_7H_8]^{+\cdot}$ molecular ion structure remains intact, but upon loss of hydrogen, rearrangement to tropylium from benzyl might rapidly occur (Scheme III). Carbon scrambling is accounted for by rapid equilibration between benzyl and tropylium forms of the $[C_7H_7]^+$ ion.

Scheme (I) demands complete hydrogen scrambling for all fragment ions proceeding *via* a symmetrical intermediate, while Schemes (II) and (III) involve stepwise randomization processes. Each of these processes could in principle result in completely scrambled C and H atoms in the $[C_7H_7]^+$ ion.[2] A distinction between these three routes was made possible, however, from

[2]Although carbon scrambling is believed to take place in the $[C_7H_7]^+$ ion, it cannot be determined experimentally that carbon scrambling precedes H atom loss from the molecular ion.

analysis of the relative losses of H and D from deuterium labeled toluenes with varying internal energies[52,53]. It was found that the extent of hydrogen scrambling decreases with *increasing* internal energy. This indicated that some (if not all) decomposing molecular ions do not proceed through a symmetrical intermediate. However, randomization must proceed rapidly in $[C_7H_7]^+$ ions with sufficient internal energies to decompose to $[C_5H_5]^+$ ions in the ion source, since complete hydrogen scrambling occurs in the formation of this ion[45].

Additional information came from ion cyclotron resonance (ICR) experiments[54], which showed that *non-decomposing* toluene molecular ions retain their structural integrity, and no rearrangement to cycloheptatriene molecular ions takes place on the time-scale of the ICR experiments (10^{-3} s). These results suggest that rearrangement of the toluene molecular ion takes place slowly unless highly excited (i. e. to energies sufficient for H atom loss); rearrangement may also occur during or after fragmentation to $[C_7H_7]^+$.

Hoffman[55] presented the mechanism shown in Figure 2.3 to explain carbon and hydrogen scrambling in $[C_7H_8]^{+\cdot}$ and $[C_7H_7]^+$ ions in a manner consistent with the available information. A $[C_7H_8]^{+\cdot}$ intermediate with the norcaradiene structure was postulated to occur *en route* to $[C_7H_7]^+$ generation.[3] The norcaradiene radical cations undergo a series of 1,5 sigmatropic shifts to scramble the carbon atoms. Loss of hydrogen simultaneous with concerted ring opening to tropylium was suggested as the rate-determining step in the production of $[C_7H_7]^+$ ions.

[3]This intermediate is analogous to the intermediate found in the thermal interconversion of cycloheptatriene molecules to toluene.[56]

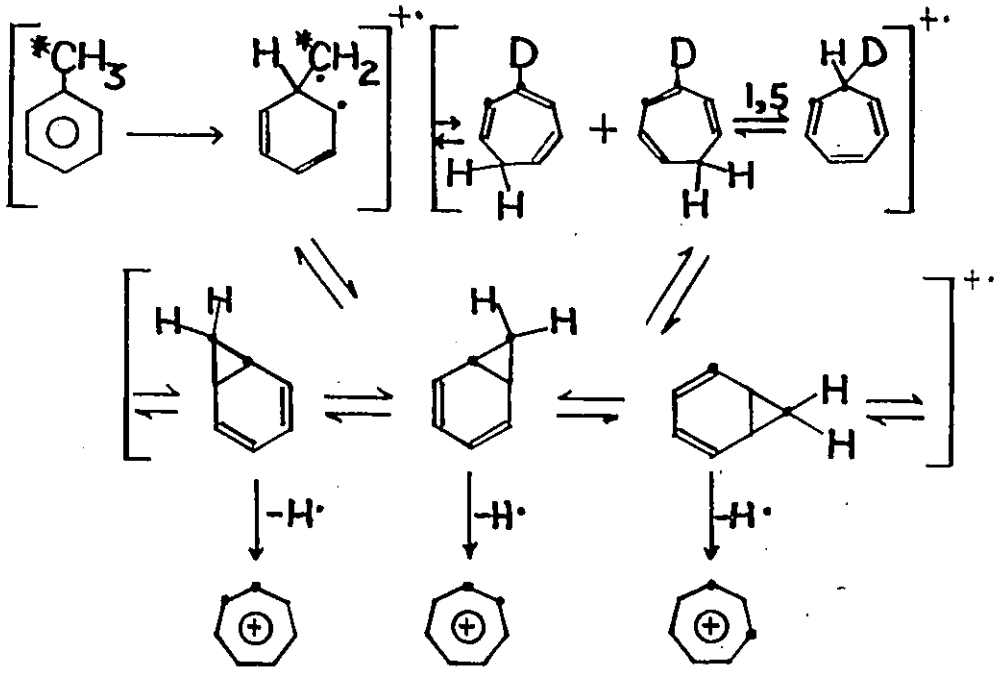

Figure 2.3: Formation of completely scrambled (C and H) tropylium ions. Scrambling of hydrogens from cycloheptatriene occurs *via* a series of hydrogen shifts in cycloheptatriene molecular ions. Carbon scrambling from toluene and cycloheptatriene occurs by rearrangement of the molecular ion to norcaradiene ion intermediates which undergo 1,5 sigmatropic shifts. 'Leakage' from norcaradienes to cycloheptatriene molecular ion accounts for hydrogen scrambling in *decomposing* toluene molecular ions. Adapted from reference [53].

Another possible intermediate, the methylenecyclohexadiene radical cation, shown in Figure 2.4, was introduced in a scheme by McLafferty and coworkers[57] for the formation of $[C_7H_8]^{+\cdot}$ from n-butylbenzene. They suggested that the methylenecyclohexadiene ion might also be a participant in a rearrangement between cycloheptatriene and toluene molecular ions.

Theoretical calculations[58] at the MNDO/3 level[4] provided evidence that rearrangement between toluene and cycloheptatriene molecular ions could indeed occur at the internal energies of ions sampled in the mass spectrometer. Both of the species mentioned above were calculated to be possible intermediates in a toluene-cycloheptatriene radical cation rearrangement by the Schemes shown in Figure 2.4. Since rearrangement *via* either intermediate involves an activation energy of about 40 kcal/mole, it was therefore concluded that both Schemes contribute to the rearrangement of $[C_7H_8]^{+\cdot}$ ions[58]. The calculated values for the overall activation energies agree well with a recent photoionisation matrix measurement[59] of 35 kcal/mole for the molecular ion rearrangement. Recently, the methylenecyclohexadiene radical cation has been observed experimentally[60,61].

A final study[62] by Baldwin, McLafferty and Jerina on the scrambling of $[C_7H_8]^{+\cdot}$ ions used high resolution mass spectrometry to resolve isobaric ions derived from deuterium and carbon-13 labeled toluene and cycloheptatriene precursors. The results of this study were consistent with four different and internal energy-dependent scrambling pathways of the $[C_7H_8]^{+\cdot}$ molecular ion:

[4] Although the accuracy of these calculations is somewhat modest, they are useful in comparing *relative* energies of reaction pathways.

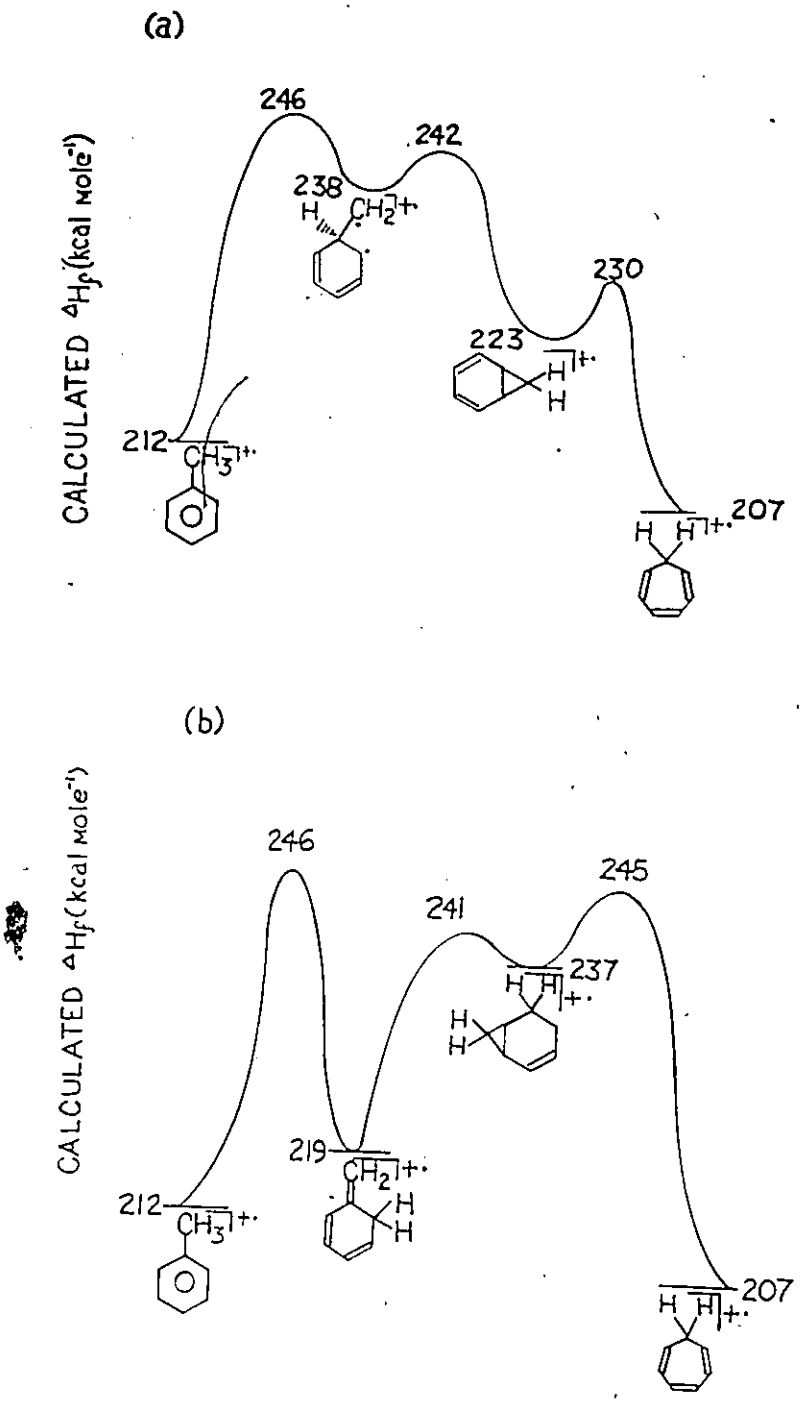

Figure 2.4: **Calculated minimum energy reaction paths for toluene/cycloheptatriene radical cation interconversion.** Path (a) rearrangement *via* norcaradiene radical cation intermediate. Path (b) rearrangement *via* methylenecyclohexadiene radical cation. Adapted from reference [56].

1. At the lowest ion internal energies, scrambling of the ring H atoms of the toluene molecular ion can occur.
2. At energies near the threshold for H atom loss, the interconversion of toluene and cycloheptatriene molecular ions occurs through norcaradiene ion intermediates, as suggested by Hoffman[55].
3. At higher internal energies, exchange between ring and α-hydrogens can occur via the methylenecyclohexadiene ion intermediate. At these energies, the participation of the norcaradiene ion intermediates is minimal.
4. At the highest internal energies (energies sufficient for decomposition to $[C_5H_5]^+$ ions), complete carbon and hydrogen scrambling can occur by the opening of the aromatic ring to linear $[C_7H_8]^{+\cdot}$ species.

These findings therefore give support for the involvement of the previously suggested intermediates, while also proposing another possible intermediate to account for the scrambling of isotopic labels in the $[C_7H_8]^{+\cdot}$ ion. This study additionally suggests that the participation of each intermediate is strongly energy-dependent, as the lower ion internal energies favour rearrangement *via* the intermediates with low activation energies and 'tight' activated complexes (such as the norcaradiene ions), while higher ion internal energies favour 'loose' complex, higher activation energy reactions (such as those involving the methylenecyclohexadiene ions).

2.1.1 A gas phase benzyl ion from toluene?

The ubiquity of the tropylium ion was challenged when McLafferty and Howe reported that further study of the production of $[C_7H_7]^+$ ions as a function of internal energy showed that significant retention of the α-deuterium labels from d_3-toluene precursors occurs from $[C_7H_8]^{+\cdot}$ ions with the highest internal energies, and is evidence for the formation of $[C_7H_7]^+$ as benzyl. [53,63]

The suggestion that benzyl is formed concomitantly with tropylium was supported by a mass spectrometric[64] study of those $[C_7H_7]^+$ ions with sufficient internal energy to fragment metastably (i. e. fragmentation in a field-free region) to $[C_5H_5]^+$ ions. Differing amounts of kinetic energy release for fragmenting $[C_7H_7]^+$ ions derived from various precursors was interpreted as being due to a mixture of metastably decomposing benzyl and tropylium isomers.

The strongest evidence for benzyl content in the $[C_7H_7]^+$ ion population came from high pressure mass spectrometry[65] and gas phase radiolysis[66] studies which showed a portion of the $[C_7H_7]^+$ ion population displays a reactivity typical of substituted aromatics. The radiolysis studies were initially interpreted[48] as misleading, due to the high internal energies generated in the $[C_7H_7]^+$ ions by this method; however, an ion cyclotron resonance (ICR) photodissociation study[67] confirmed that some low internal energy $[C_7H_7]^+$ ions also undergo reaction with neutral toluene. The ICR study found that the $[C_7H_7]^+$ ion population can be separated into two categories: 'reactive' and 'unreactive' to neutral toluene. It was as-

sumed that the unreactive component should be the stable tropylium ion, while the reactive species could only be attributed to a benzyl structure. It was suggested[67,68] and later confirmed[69] by labeling studies that the reaction of benzyl ions with toluene takes place by the methylene transfer mechanism shown below.

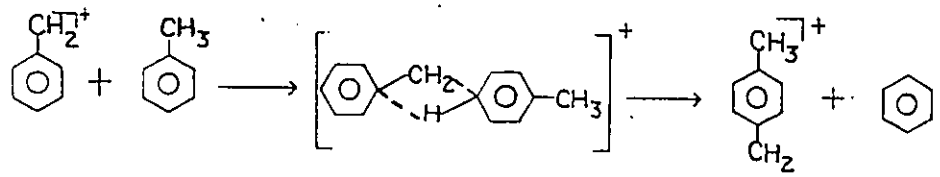

Collisional activation mass spectrometry studies

The advent of collisional activation (CA) mass spectrometry gave mass spectrometrists a powerful new tool with which to tackle the intriguing $[C_7H_7]^+$ system. In an initial study[71], McLafferty and Winkler used CA mass spectrometry to show that cycloheptatriene, toluene and more than 50 of their analogs give varying amounts of benzyl and tropylium in the $[C_7H_7]^+$ ion population. Quantitative analysis of the $[C_7H_7]^+$ isomer population was assigned by measuring the abundance of the peak (m/z 77), corresponding to a structure characteristic fragmentation (loss of methylene—assumed to occur most readily from ions with the benzyl structure). The m/z 77 peak intensities for (nearly) pure benzyl and (nearly) pure tropylium ions were set as limits, and percent mixtures of the two isomers for precursors that gave both benzyl and tropylium were assigned by assuming

'linear superposition'[40] of the pure ion spectra. That is, a 50% benzyl–50% tropylium ion precursor results in a m/z 77 abundance equal to that of 50% pure benzyl plus 50% pure tropylium. By this method, McLafferty and Winkler concluded that 70 eV electron impact on toluene results in a $[C_7H_7]^+$ ion population that was 25% benzyl. The CA results also showed that in the (broad) range of ion internal energies sampled, not only does interconversion between the cycloheptatriene and toluene molecular ions take place prior to H atom loss, but so does rearrangement among the benzyl and tropylium structures of the $[C_7H_7]^+$ ion itself. Both routes apparently favour the formation of tropylium—the most stable isomer. These CA measurements were repeated[72,40] with improved instrumentation and a new value was reported for the relative intensity of m/z 77 for 'pure' tropylium. Based on the observed reactivity of benzyl ions with neutral toluene, pure tropylium ions were allegedly generated by operating the ion source at chemical ionisation (CI) pressures (0.1 torr) with toluene. It was believed that benzyl ions formed from ionised toluene would quickly react with the excess neutral toluene in the ion source. The only $[C_7H_7]^+$ ions exiting the ion source would thus be ions with the tropylium structure.[5] This method gave a new value for the (small) amount of m/z 77 derived from tropylium ions and resulted in a slightly different analysis of the $[C_7H_7]^+$ ion isomer content (refer to Table 2.1).

Another new observation in the CA study was that decreasing the ionising electron energy from 70 to 16 eV resulted in an increased benzyl

[5] As shown in Chapter 3, rate constants published[67,80,81] for this reaction belie the assumption that total scavanging of benzyl ions can occur under these conditions.

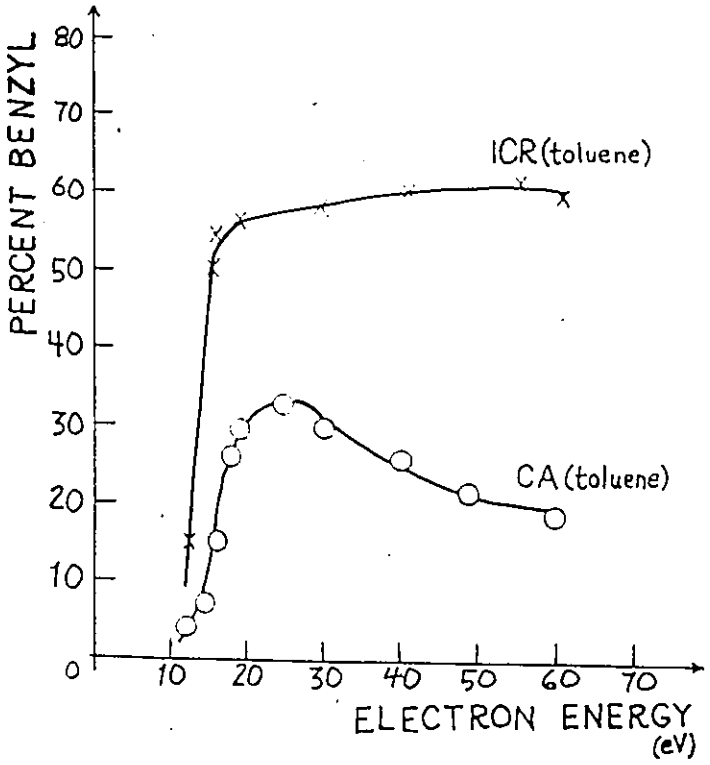

Figure 2.5: **Benzyl production at different ionising electron energies from CA[72] and ICR[82] studies.** CA results corrected as suggested in reference [40].

population. At the lowest ionising electron energies, the benzyl ion content was found to decrease sharply to zero at threshold production for $[C_7H_7]^+$ ions. These results were similar for both toluene and cycloheptatriene precursors and are shown in Figure 2.5. These observations agree with the relative thermochemistry of benzyl and tropylium formation as shown in Table 2.4. Tropylium should be formed at threshold energies since its heat of formation is lower than that of benzyl. At higher ionising energies, benzyl production can occur and will increase with increasing energy, as direct bond cleavage becomes kinetically favoured over predissociative rearrange-

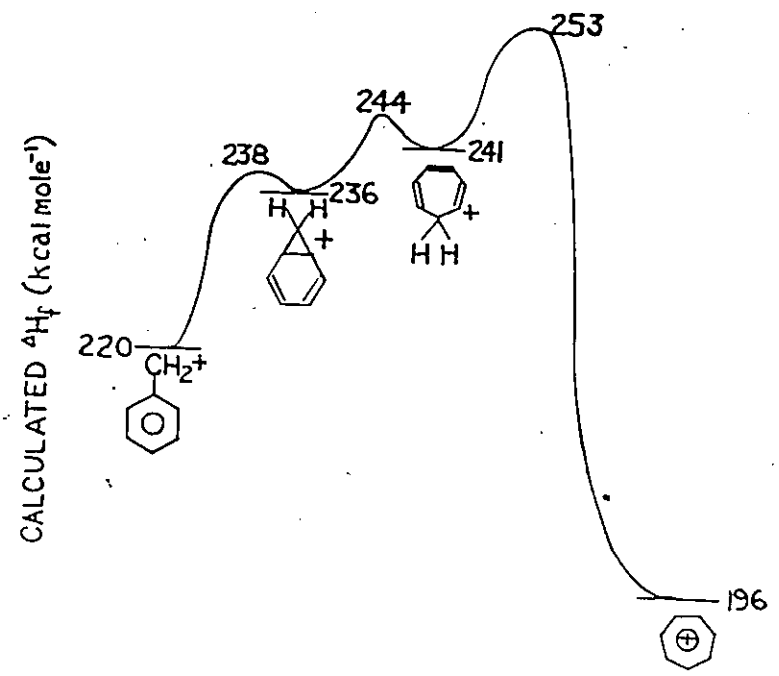

Figure 2.6: **Calculated minimum energy reaction path for the interconversion of benzyl and tropylium ions.** Adapted from reference [74].

ment. Finally, benzyl ions with sufficient internal energy to rearrange to tropylium are generated at the highest ionising energies, resulting in a decrease in the benzyl ion population. Since $[C_7H_7]^+$ ions must have $\geq$ 95 kcal/mole of internal energy to fragment to $[C_5H_5]^+$[73], benzyl ions can have sufficient internal energies to surmount a sizeable barrier in order to rearrange to tropylium.

A MNDO/3 study[74] calculated an activation energy of 33 kcal/mole for the benzyl $\rightarrow$ tropylium rearrangement *via* the norcaradienium and cycloheptatrienium ion intermediates shown in Figure 2.6. This is in agreement with recent experimental work that showed benzyl and tropylium ions interconvert upon photolysis in an argon matrix[75] at energies comparable

to low internal energy gas phase ions. It was suggested[76] that the overall activation energy was high enough to account for the failure to observe such rearrangements of benzyl ions in solution[77], where collisions rapidly quench excess internal energy.

Ion cyclotron resonance results

Ion cyclotron resonance (ICR)[78] is a technique in which ions are generated by electron impact on a neutral precursor and are accelerated into an ion trap, which keeps the ions whirling in helical motions down the length of the ion trap cell. Ion lifetimes can be as long as tens of seconds. Cell pressures are kept low (10^{-6}–10^{-5} torr), but due to the long lifetimes photodissociation[79] of these ions may also be effected.

As previously mentioned, photodissociation ICR work by Dunbar[67] first established the presence of 'reactive' and 'unreactive' species in the $[C_7H_7]^+$ ion population. Further studies by Ausloos and co-workers[80] confirmed the reaction mechanism of benzyl with toluene and also the rate constant of this reaction. High pressure mass spectrometry[81] was also used to observe this reaction of benzyl with a variety of neutral molecules.

Quantitative analysis of the two species comprising the $[C_7H_7]^+$ ion population from toluene was initially done with the ICR method for ions with internal energies near threshold[67], and later extended[80,82] to ions with higher internal energies and from different precursors. As shown in Table 2.1, these results[80,82] agree poorly with the CA mass spectrometry values—a much higher benzyl ion content is found in the ICR studies. Al-

Precursor	ICR		CA	
	Benzyl	Tropylium	Benzyl	Tropylium
Toluene	62	38	20	80
Benzyl bromide	94	6	43	57
Benzyl chloride	91	9	40	60

Table 2.1: **Relative abundances of $[C_7H_7]^+$ isomers from some aromatic compounds.** Ion cyclotron resonance (ICR) values from reference [80]. CA mass spectrometry values from reference [72] with corrections as suggested in reference [40]. All values with 70 eV ionising electron energy, CA mass spectrometry data with 8 keV accelerating voltage.

though longer observation times (250-200 ms) were used in the ICR experiments, it was rationalized[80] that longer ion lifetimes should favour rearrangement of $[C_7H_7]^+$ ions to the more stable tropylium form, thus decreasing (if anything) the amount of benzyl observed. A photoelectron-photoion coincidence study[84] also confirmed that longer ion lifetimes should increase the amount of tropylium observable at low ion internal energies.

As shown in Figure 2.5, the ICR results also do not agree with those of the CA study[72] describing the $[C_7H_7]^+$ benzyl ion content as a function of the ionising electron energy. The falloff of benzyl content at high energies found in the CA study was not repeated in the ICR results, rather benzyl ion content rose to a maximum value and remained the same as the ionising electron energy was increased. It was countered[72] that the benzyl $\rightleftharpoons$ tropylium rearrangement biased the ICR results in favour of benzyl, as the preferential removal of the benzyl ion by chemical reaction causes a shift in the 'equilibrium', resulting in the observation of greater amounts of benzyl than that found in the CA studies.

A recent study by Ausloos[83] indicated that the equilibrium between

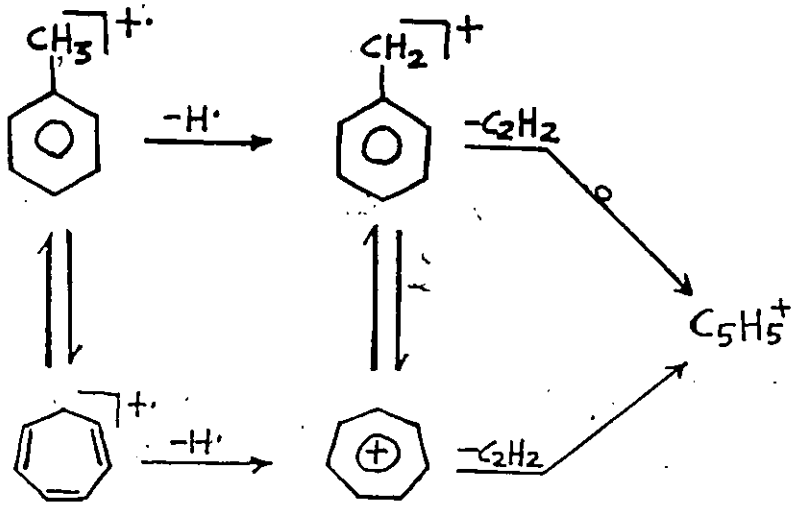

Figure 2.7: Scheme for the reactions of $[C_7H_8]^{+\cdot}$ ions.

benzyl and tropylium is not rapid at ion energies less than 100 kcal/mole, and therefore the ICR results at lower ion internal energies should not be affected. This did not reduce the level of disagreement in the quantitative assignment of benzyl ion content of the $[C_7H_7]^+$ ion population, since the ion internal energies sampled in the CA study were estimated to be no greater than 65 kcal/mole. Neither McLafferty nor Ausloos could explain the apparent disagreement between the CA and the ICR results[40].

2.1.2 Summary

To summarise, the scheme shown in Figure 2.7 for the reactions of $[C_7H_8]^{+\cdot}$ ions is generally accepted along with the following points:

1. The heat of formation of the toluene molecular ion is less than that of the cycloheptatriene molecular ion (by about 20 kcal/mole).

2. Rearrangement between toluene and cycloheptatriene molecular ions can occur before H atom loss, probably *via* norcaradiene or methylenecyclohexadiene radical cation intermediates (activation energy *ca.* 35 kcal/mole).

3. At threshold energies for $[C_7H_7]^+$ ion formation, tropylium is formed first since H loss occurs most easily from the cycloheptatriene molecular ion, and the heat of formation of tropylium is lower than that of benzyl (by about 8 kcal/mole, see Table 2.4).

4. At higher ion internal energies, benzyl is formed by simple bond cleavage from the toluene molecular ion.

5. Those $[C_7H_7]^+$ ions with internal energies $\geq$ 33 kcal/mole undergo rapid equilibration between benzyl and tropylium.

6. At higher $[C_7H_7]^+$ ion internal energies ($\geq$ 95 kcal/mole), fragmentation by loss of C_2H_2 to produce $[C_5H_5]^+$ can occur.

A number of points of disagreement remain. The amount of benzyl ion produced in the 70 eV ionisation of toluene and other precursors is the most obvious point of contention. There is also disagreement over the form of the curve describing benzyl (or tropylium) ion content with increasing $[C_7H_7]^+$ ion internal energy. Less obvious inconsistencies are still of concern. CA mass spectra were published with different ion translational energies[40,71,72,85], and revealed different relative abundances for the structure characteristic m/z 77 peak at different ion translational energies. Does this reflect a changing benzyl/tropylium mixture? Finally,

as will be shown in Chapter 3, rate constants published[67,80,81] for the reaction of benzyl with neutral toluene call into question whether complete scavenging of benzyl ions could take place within the time spent (typically 1-2 μs) in the ion source of the mass spectrometer. The validity of the CA mass spectrometry value for pure tropylium is therefore in question.

2.2 Tolyl ions

Other possible isomers of the $[C_7H_7]^+$ ion derived from toluene and cycloheptatriene precursors have not been given a great deal of consideration, since arguably a third isomer would have to have a heat of formation comparable to that of benzyl or tropylium to be present in significant amounts in the $[C_7H_7]^+$ ion populations[72,86]. To this date no such isomer has been found, despite a great amount of research that has probed the structures and chemistry of $[C_7H_7]^+$ ions generated from toluene, cycloheptatriene, and many analogous precursors.

On the other hand, those $[C_7H_7]^+$ ions formed from single ring-substituted toluenes, such as the halotoluenes, could *initially* have the tolyl structures shown in Figure 2.8, provided that their formation is not precluded by ring expansion in the molecular ion. Although these high internal energy (see Table 2.4) $[C_7H_7]^+$ ions should rearrange to the greatly more stable tropylium and/or benzyl isomers, the rate constants for their rearrangement could be low enough to allow detection of tolyl ions in the mass spectrometer.

Studies on mono-substituted toluenes, most notably the halotoluenes,

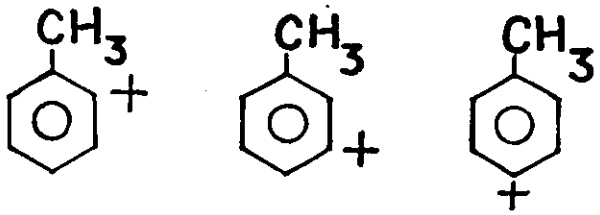

Figure 2.8: The o, m, and p-tolyl ions.

can be separated into two categories: (i) studies which probed the structure(s) of the decomposing $[CH_3C_6H_4X]^{+\cdot}$ ion (where X is the substituent), and (ii) studies which probed the structure of the resulting $[C_7H_7]^+$ ion by loss of X. Obviously, the first studies are of great significance to the tolyl problem, for if the molecular ions were found to undergo major structural rearrangement in all cases, the existence of tolyl ions would not be probable.

2.2.1 The structure of halotoluene molecular ions

Threshold energy studies.

ICR photodissociation studies[79,87] investigated halotoluene molecular ions formed by electron impact with threshold ionising electron energies. Comparison was made[79] between the photodissociation spectra for halogen loss and the corresponding photoelectron spectra of para-substituted fluoro, chloro, bromo, and iodotoluenes. Excellent agreement between the two types of spectra was found for these precursors which was taken as evidence that structural integrity is retained in the molecular ions at threshold ionisation energies.

A further study[87] using the ICR photodissociation technique compared the spectra of isomeric halotoluene and benzyl halide cations. Loss of halogen is favoured upon photolysis for the chloro, bromo and iodo isomers, whereas fluorotoluenes and benzyl fluoride lose an H atom preferentially. The benzyl halide photodissociation spectra were found to be very different from the corresponding halotoluene spectra; rearrangement of the parent ions to a common structure at threshold energies for halogen loss was not evident.

Metastable halotoluene molecular ion studies

A variety of mass spectrometric studies have investigated the structure(s) of halotoluene molecular ions with sufficient internal energies to fragment metastably. Initial studies[88] using metastable ion abundance observations concluded that the loss of H from m, p-chloro and bromotoluenes originates from parent molecular ions with unrearranged and distinct structures. However, a later study[89] by the same researcher on the loss of Cl from m, p-chlorotoluenes led to the suggestion that the reaction takes place from a common structure for the parent molecular ions. These sets of results appear to be contradictory. Since the internal energy required for H loss is greater than that required for Cl loss from the chlorotoluene molecular ions[79], the same reaction channels to rearrangement found for the molecular ions losing chlorine atoms should be operative during H atom loss. The validity of these early results is, therefore, questionable; but they foreshadow the delicate nature of the halotoluene molecular ion system.

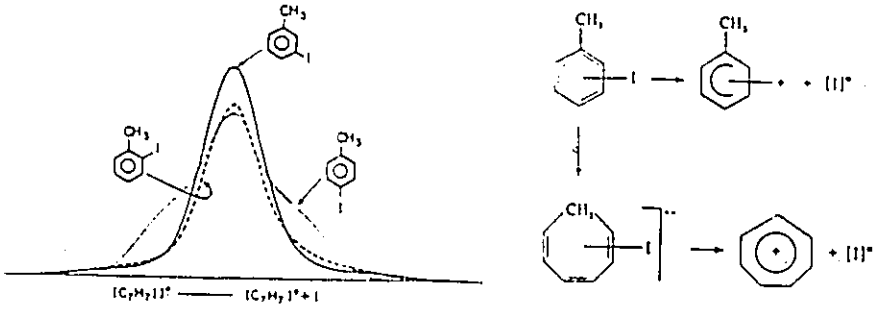

Figure 2.9: Metastable peak shapes for I atom loss and suggested scheme for unimolecularly reacting iodotoluenes. From reference [90].

A more recent mass spectrometry study[90] observed the metastable peak shapes for $[C_7H_7]^+$ ions formed by loss of I from the three iodotoluenes. As shown in Figure 2.9, these metastable peaks exhibit distinctly different, composite peaks. The formation of these composite peaks must be due to fragmentation occurring from isomeric parent ions and/or to the production of isomeric daughter ions. Rearrangement in the parent ions was considered the more likely occurrence, and thus the composite nature of the metastable peaks was proposed to be due to fragmentation from the two reacting configurations shown in Figure 2.9.

This general scheme was supported by a study[91] which compared the kinetic energy release accompanying halogen loss from fragmenting metastable p-halotoluenes with that of the corresponding halogenbenzenes and benzyl halides. The relatively large kinetic energy releases found for the halotoluene precursors was seen as evidence for rearrangement of these

molecular ions to another structure (postulated as halocycloheptatriene) prior to fragmentation.

Halotoluene fragment ions.

In 1970, Yeo and Williams[92] compared the normal mass spectra of the halotoluenes with those of corresponding halobenzenes and benzyl halides. It was assumed that loss of a halogen from an unrearranged halotoluene would involve a similar type of bond cleavage as loss of halogen from a halobenzene. If this was indeed the case, similar mass spectral intensities for halogen loss would be observed. In the same way, loss of a halogen from a rearranged halotoluene might involve a similar bond cleavage as that for a benzyl halide. A third possible case, rearrangement to a halocycloheptatriene, was probed with the help of appearance energy measurements. Using these techniques, it was concluded that the molecular ions of fluoro and chlorotoluenes undergo ring-expansion rearrangement prior to fragmentation in the ion source; whereas the bromo and iodotoluenes fragment from unrearranged structures in the ion source of the mass spectrometer.

Additionally, measured differences between the ionisation energies of the molecular ions and the appearance energies of $[C_7H_7]^+$ ions, used as a crude measure of the activation energies for halogen loss, indicated that rearrangement in the molecular ion is a sensitive function of the required energy for bond cleavage. As shown in Table 2.2, the required internal energy for rearrangement suggested from this study was in the range 2.6-2.8 eV.

Substituent	AE-IE (eV)	Ring expansion
F	3.1	Yes
Cl	2.8	Yes
Br	2.5	No
I	2.4	No

Table 2.2: **Relative activation energies (AE - IE) for loss of halogen from halotoluene molecular ions.** Adapted from references [48,92].

In summary, studies on the structures of fragmenting halotoluene molecular ions have shown that the structure of the reacting configuration for halogen loss depends on the available internal energy of the molecular ion. At threshold ionisation energies, the molecular ions appear to retain their neutral structures. At 70 eV ionisation energies, low internal energy, relatively long-lived molecular ions appear to undergo *some* rearrangement to a halocycloheptatriene structure. Finally, higher internal energy molecular ions appear to undergo ring expansion in the fluoro and chlorotoluenes in which the carbon-halogen bond strengths are high, but not for bromo and iodotoluenes in which the bond strengths are relatively low. It appears from these studies that rearrangement in halotoluene molecular ions is thermochemically favoured and kinetically feasible for all halotoluene precursors on a relatively long time-scale (metastable ions), but not kinetically favourable in bromo and iodotoluenes for the shorter time-scale ion source processes.

2.2.2 The structure(s) of $[C_7H_7]^+$ ions from nitro and halotoluene precursors

An early deuterium labeling study[45] on p-chlorotoluene led researchers to suggest that the 'nominal' structure of the $[C_7H_7]^+$ ion generated is tolyl,

presumably the para isomer. However, this distinction is lost for $[C_7H_7]^+$ ions which fragment to $[C_5H_5]^+$. In view of the fact that deuterium labels scramble in reacting $[C_7H_7]^+$ ions from p-chlorotoluene as precursor, it was originally concluded that rearangement occurs rapidly to tropylium at high ion internal energies in the mass spectrometer[45].

This view was supported by a study[93] based on the relative abundances of $[C_7H_7]^+$ ions that decompose metastably to $[C_5H_5]^+$, when formed from o, m, p-xylene; m, p-chlorotoluene and p-nitrotoluene precursors. This investigation concluded that only those $[C_7H_7]^+$ ions formed from p-nitrotoluene did not fit the data expected for a tropylium $[C_7H_7]^+$ structure. The structure of $[C_7H_7]^+$ ions from p-nitrotoluene was presumably tolyl.

It was with the use of CA mass spectrometry that *direct* evidence was found for the existence of tolyl cations as stable $[C_7H_7]^+$ isomers with lifetimes extending to 10^{-5} seconds. An exploratory study[71] into the structures of $[C_7H_7]^+$ ions from a variety of precursors was able to distinguish between the CA mass spectra of benzyl and tropylium structures, and the spectra of those ions generated from nitro and iodotoluene precursors. The structure characteristic region (m/z 74, 75, 76, and 77) was found to be also characteristic of tolyl ions. While the relative intensity of the m/z 77 ion decreased dramatically for the tolyl precursors compared to that found for benzyl and tropylium, the higher energy process, m/z 74, increased in relative intensity. No significant increase in m/z 76 was noted, although one might have expected an increased tendency for m/z 15 loss from m/z

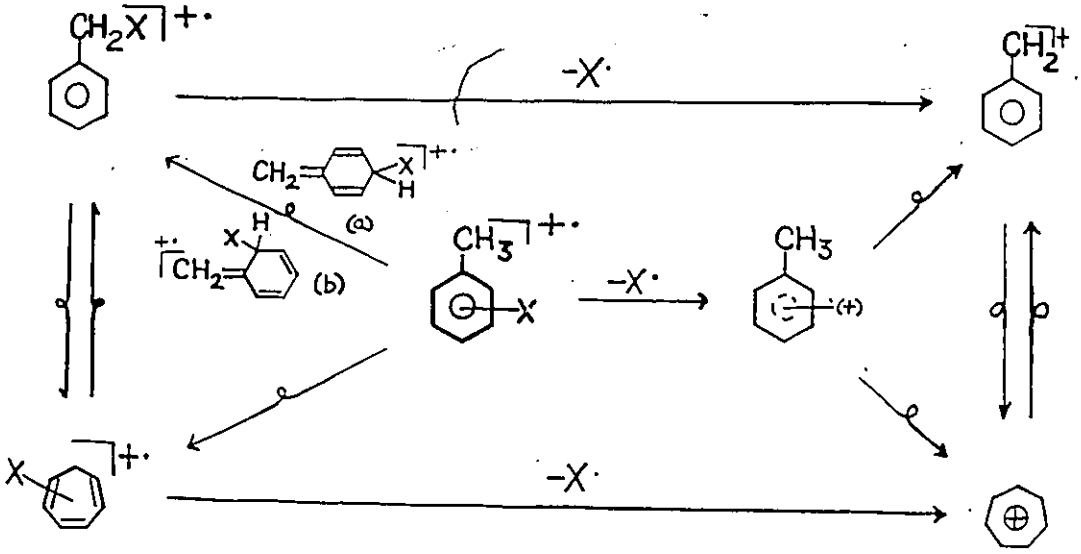

Figure 2.10: Scheme for the production and rearrangement of tolyl ions. Adapted from references [71,94].

91 ions with tolyl structures.[6]

Using the above criterion for tolyl ions, a further distinction between m, p-tolyl ions and o-tolyl ions was made, as ortho-tolyl had apparently a lower m/z 74 relative abundance than those found for the meta and para isomers. The CA data for chloro and bromotoluenes did not support the formation of $[C_7H_7]^+$ ions as stable (lifetimes $\geq 10^{-5}$ s) tolyl isomers. The scheme shown in Figure 2.10 was presented to account for the production and rearrangement of tolyl ions. It was suggested that low rate constants for rearrangement enabled observation of these high internal energy (see Table 2.4) $[C_7H_7]^+$ ions.

Further support for tolyl ions as stable structures came from theoret-

[6]Reference [71] notes that even after extensive signal averaging, the m/z 76 peak was poorly resolved due to overlap with adjacent peaks. An increase in the relative abundance of m/z 76 may have gone unnoticed.

ical MNDO/3 calculations[58]. The three isomers were calculated to be stable gaseous ions and to have similar heats of formations (about 240 kcal/mole). The activation energy for rearrangement of o-tolyl cation to benzyl was calculated as 25 kcal/mole, while the calculated activation energy for interconversion for m-tolyl to o-tolyl was 38.9 kcal/mole. It was suggested[58] that the rearrangements tolyls → benzyl should occur quite easily in the mass spectrometer, precluding interconversion among the tolyl isomers themselves.

A more detailed CA mass spectrometry study[94] on gaseous tolyl ions made use of the observation[95] that high purity tolyl ions could be prepared in the mass spectrometer under CI conditions with methane as the reactant gas. Protonation and subsequent loss of HF from fluorotoluene produces $[C_7H_7]^+$ ions with the tolyl structures[95]. Using the CA mass spectra from these precursors as references for m/z 74 and 77 relative abundances[94] for tolyl ions (in comparison to those for benzyl and tropylium), McLafferty and Bockhoff assigned varying amounts of tolyl ion content to $[C_7H_7]^+$ ions formed from m-bromotoluene, and o, m, p-nitro and iodotoluenes. An abbreviated version of these results is given in Table 2.3. The assignment was simplified by assuming that only benzyl and tolyl ions were formed from these precursors, although appreciable amounts of tropylium were thought to be present in particular cases[94]. It was suggested that severe steric restrictions inhibited molecular ion rearrangement, especially the isomerisation to halocycloheptatrienes, thus limiting the amount of tropylium ions produced directly by loss of halogen.

Precursor	% Tolyl
o-Iodotoluene	80
m-Iodotoluene	95
m-Bromotoluene	50
p-Iodotoluene	75

Table 2.3: **Tolyl ion content of $[C_7H_7]^+$ ions from some halotoluene precursor molecules as analysed by CA mass spectrometry[94].** Electron ionising energy 70 eV, accelerating voltage 8 keV.

Finally, ICR experiments[80] reveal that tolyl ions lead a tenuous existence. Investigations into the structures of $[C_7H_7]^+$ ions from halotoluene precursors by the reactivity method discussed in Section 2.1.1 found that no change in the reaction rate occurred relative to known benzyl precursors. Since tolyl ions were expected to be highly reactive if present, it was concluded that tolyl ions rearrange on the time-scale of the ICR experiments (10^{-3}–10^{-1} s).

2.2.3 Conclusions and comments

There is ample evidence to say that $[C_7H_7]^+$ ions with tolyl structures can be formed from mono-substituted toluenes, especially from iodo and nitrotoluenes in the mass spectrometer. While apparently stable for as long as 10^{-5} seconds, tolyl ions undergo rearrangement to benzyl and possibly tropylium on longer time-scales (10^{-3} s).

A number of points are open to comment. As in the studies on benzyl and tropylium isomer mixtures, CA studies on tolyls were done at different accelerating voltages (4 and 8 keV)[94,94] and the spectra appear to have very different relative intensities. Do these differences reflect a changing

tolyl isomer content? Furthermore, the latter tolyl study was based on the relative abundances of structure characteristic peaks (m/z 74 and 77) for benzyl and tropylium determined from a previous study[72]. However, these values were later found to be in error[40]. How are the published tolyl isomer contents affected by these errors? Finally, the CA studies only examined source-generated $[C_7H_7]^+$ ions, but many studies suggest that tolyl ions can be metastably-generated from halotoluene precursors. Is it possible to examine the $[C_7H_7]^+$ isomer content of these metastably-generated ions? These questions have been motivation for the work detailed in this thesis.

Ion	Precursor	IE or AE (eV)	ΔH^0_{298}(g) (kcal/mole)	Ref.
$[C_7H_8]^{+\cdot}$, $[Tol]^{+\cdot}$	toluene	8.82±0.01	215±1	[19]
$[C_7H_8]^{+\cdot}$, $[CHT]^{+\cdot}$	cycloheptatriene	8.29±0.01	235±1	[19]
$[C_7H_7]^+$, $[Bz]^+$	benzyl radical	7.20±0.02	214 ± 2	[96]
$[C_7H_7]^+$, $[Tr]^+$	cycloheptatrienyl radical	6.24±0.01	206 ± 2	[96]
$[C_7H_7]^+$, $[o-Tolyl]^+$	o-iodotoluene	11.3[a]	267 ± 10	[92]
$[C_7H_7]^+$, $[m-Tolyl]^+$	m-iodotoluene	11.3[a]	267 ± 10	[92]
$[C_7H_7]^+$, $[p-Tolyl]^+$	p-iodotoluene	11.3[a]	264 ± 10	[92]

Table 2.4: **Selected thermochemical data.** Calculated using heats of formation of neutrals from reference [21]. [a]Only published values; values of high uncertainty. 1 eV/molecule = 23.06 kcal/mole = 96.487 kJ/mole.

Chapter 3

Analysis of benzyl and tropylium ions

Introduction

The quantitative analysis of a mixture of two isomeric ions using collisional activation mass spectrometry is based on the CA mass spectra generated by the pure flux of each isomer. Once these reference spectra have been obtained, analysis of a mixed CA mass spectrum can be carried out by assuming a linear superposition of the two reference spectra[40].

For $[C_7H_7]^+$ ions, the CA mass spectra are remarkably similar for a wide range of precursor molecules, as can be seen from Figure 3.1 which compares the CA mass spectra of m/z 91 generated from toluene, cycloheptatriene, and benzyl bromide precursors. Indeed, the only observable differences between the spectra of $[C_7H_7]^+$ ions occur in the region of daughter ions with m/z 74, 75, 76, and 77. This mass region offers the sole means by which the isomer content of the $[C_7H_7]^+$ ions may be quantitatively analysed by CA mass spectrometry. The peak corresponding to m/z 77 is believed[71]

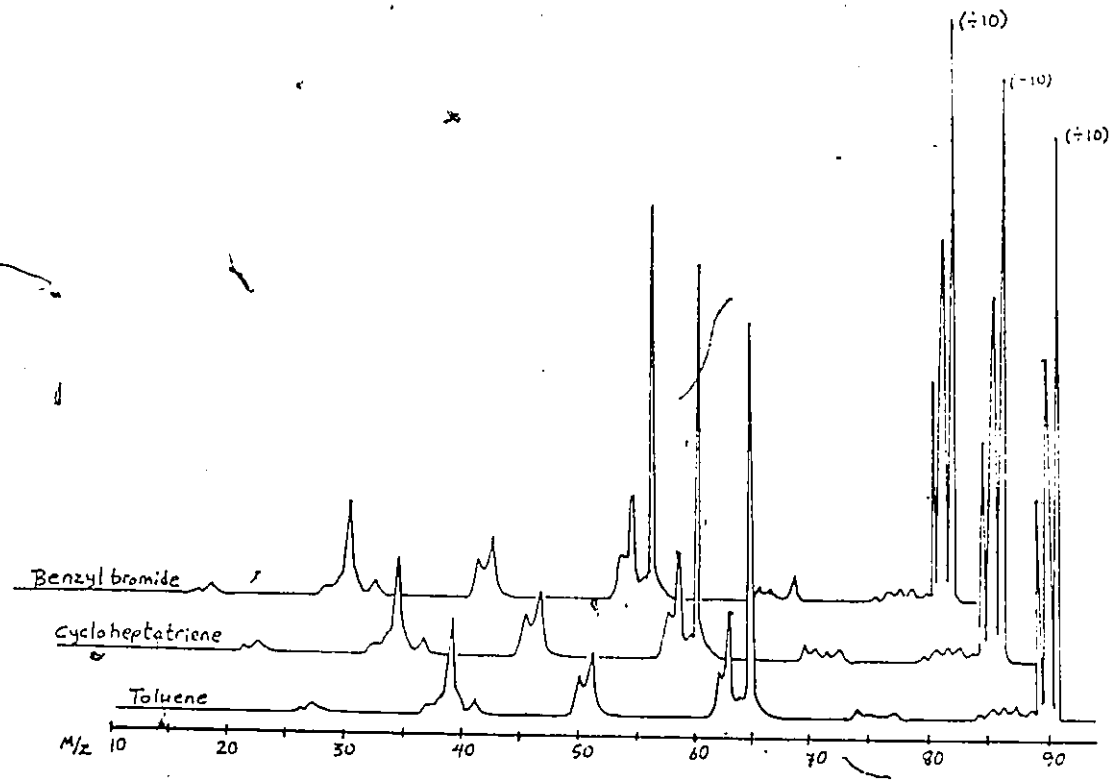

Figure 3.1: Collisional activation mass spectra of m/z 91 ions derived from different precursor molecules. Operating conditions: 70 eV electron ionising energy, 8 keV accelerating energy, helium collision gas pressure corresponding to 10% main beam reduction.

to be generated most favourably from the benzyl ion—a not unreasonable assumption since α-bond cleavage of the methylene group from the benzyl ion generates $[C_6H_5]^+$, m/z 77, directly; whereas a more difficult route must be envisaged to produce this ion from the tropylium structure.

An initial CA mass spectrometry analysis[71] of the $[C_7H_7]^+$ ion isomer population related the intensity of this fragment ion, m/z 77, to the sum of the intensities of the daughter ions produced by collisional activation, with appropriate corrections for those ions generated unimolecularly. Precursor molecules thought most likely to give benzyl ions upon ionisation were found to yield relatively high amounts of m/z 77, while precursor molecules expected to give tropylium ions gave low yields of m/z 77. The extreme values were proposed to correspond to the pure isomers and analysis of precursor molecules that gave $[C_7H_7]^+$ ion isomer mixtures was then established by assuming superposition of different amounts of the m/z 77 ion found in the spectra of the two 'pure' ions.

A second analysis[72] of $[C_7H_7]^+$ ions used the ratio of the peak heights of m/z 77/74 as a means of avoiding the long task of detailed fragment ion intensity measurements. The rationale of this approach was based on the invariant yield of the m/z 74 ion (relative to the sum of the daughter ion abundances) with the nature of the precursor ion.[1] It was established in this study that the m/z 74 ion abundance is indeed a constant percentage of the total daughter ion abundance within experimental error. A measurement

[1]The appearance energy of the m/z 74 ion is about 7 eV greater than that of the m/z 77 ion[85], therefore the m/z 74 ion signal intensity is unaffected by the relatively small changes in the internal energy of $[C_7H_7]^+$ ions caused by generating the ions from different precursor molecules.

of the peak heights m/z 77/74 thus enabled experimenters to establish the relative yields of the structure characteristic m/z 77 ion generated in the CA mass spectra of $[C_7H_7]^+$ ions from different precursor molecules.

Recently, it has been shown[40] that the intensity of the m/z 74 ion is a constant proportion of the m/z 91 ion flux generated from toluene and bibenzyl precursor molecules. Similar measurements have been repeated in the present study, and they confirm that the yield of m/z 74 is the same percentage of the main beam flux for the precursor molecules used to generate benzyl and tropylium ions in this work.[2] Since the m/z 77/74 peak height ratio is a reliable means by which the relative amount of m/z 77 ion can be measured, the isomer content can be easily determined for $[C_7H_7]^+$ ions derived from different precursor molecules using CA mass spectrometry.

3.1 Pure benzyl and tropylium ions

3.1.1 Pure benzyl ions

It is necessary to establish the m/z 77/74 ratio for pure benzyl ions. Measurements on benzyl bromide and bibenzyl at low ionising electron electron energy[3] results in a ratio of 3.15±0.2, in good agreement with the 7.8 keV ion translational energy result of 3.1±0.3 recorded by McLafferty and Bockhoff[72].

[2]This is not the case, however, for precursor molecules that give an appreciable amount of tolyl ion, as will be shown in Chapter 4.

[3]Ionising electron energy lowered so as to reduce the m/z 91 signal by a factor of at least 10,000 from that at 70 eV ionising electron energy.

3.1.2 Pure tropylium ions.

The previous CA studies[94,72] of $[C_7H_7]^+$ ions used a m/z 77/74 ratio of 0.52±0.02 for pure tropylium ions. This value was obtained by operating the ion source at high pressures of toluene, under which conditions the large excess of neutral toluene was believed to scavenge *all benzyl* ions formed, while tropylium ions remained unreacted[72]. This method did not produce a low m/z 77/74 ratio with the Ottawa mass spectrometer, even when ion source pressures of up to about .5 torr were used. Although the ion source of the Ottawa instrument is not specifically designed for such high pressure ion-molecule reactions, it is still disconcerting that no trend toward the lower m/z 77/74 ratio was seen. A calculation[4] based on a published rate constant[67] for this reaction shows that under very generous ion source conditions complete scavenging of benzyl ions by neutral toluene would not be complete. Indeed, as many as 12.5% of the benzyl ion population could remain unreacted.

It seemed more likely that high purity tropylium ions could be generated from the tropylium salts: tropylium bromide, tropylium iodide, and tropylium tetrafluoroborate. The normal electron impact mass spectra of these compounds have been reported[97,98,99] and show m/z 91 as base peak. A curious feature of these published spectra are the m/z 92 ion peak intensities which exceed the normal ^{13}C isotopic abundance of 7.7% of the m/z 91 ion intensities. The same anomaly was found with the tropylium salts used in this study. Tropylium salts giving different m/z 92/91 ratios

[4] See Appendix.

were found to correlate with different m/z 77/74 CA ratios. This is not surprising, since any m/z 92 abundance greater that the isotopic contribution of 7.7% must be derived from unidentified $[C_7H_8]^{+\cdot}$ species which, in turn, can contribute a mixture of benzyl and tropylium ions to the $[C_7H_7]^+$ ion population. In Figure 3.2, the m/z 92/91 ratios from different batches of tropylium salts have been plotted against the 77/74 ratios obtained upon CA mass spectrometric analysis of their m/z 91 ion. The resulting graph extrapolates to a m/z 77/74 ratio of 0.35 ± .03 at a 92/91 value of 7.7%. It is proposed that this m/z 77/74 ratio reflects an accurate value for pure tropylium ions at 70 eV ionising electron energy and 8 keV ion translational energy.[5]

Figure 3.3 compares the m/z 74-77 region of the CA spectra generated by pure benzyl ions with that CA spectrum found for pure tropylium ions generated from a high purity tropylium salt.

3.2 $[C_7H_7]^+$ ion mixture analysis

Table 3.1 lists the benzyl and tropylium populations found in this study for $[C_7H_7]^+$ ions produced by 70 eV ionisation of a variety of neutral precursors.[6]

The results indicate that the benzyl ion is produced most favorably by precursor molecules containing a relatively weakly bonded substituent, X,

[5] Although this value is even lower than that measured by McLafferty and Bockhoff[94], however the effect on the isomer mixture analysis is small (see Figure 3.4).

[6] See the Appendix at the end of this Chapter for a sample calculation of the isomer content.

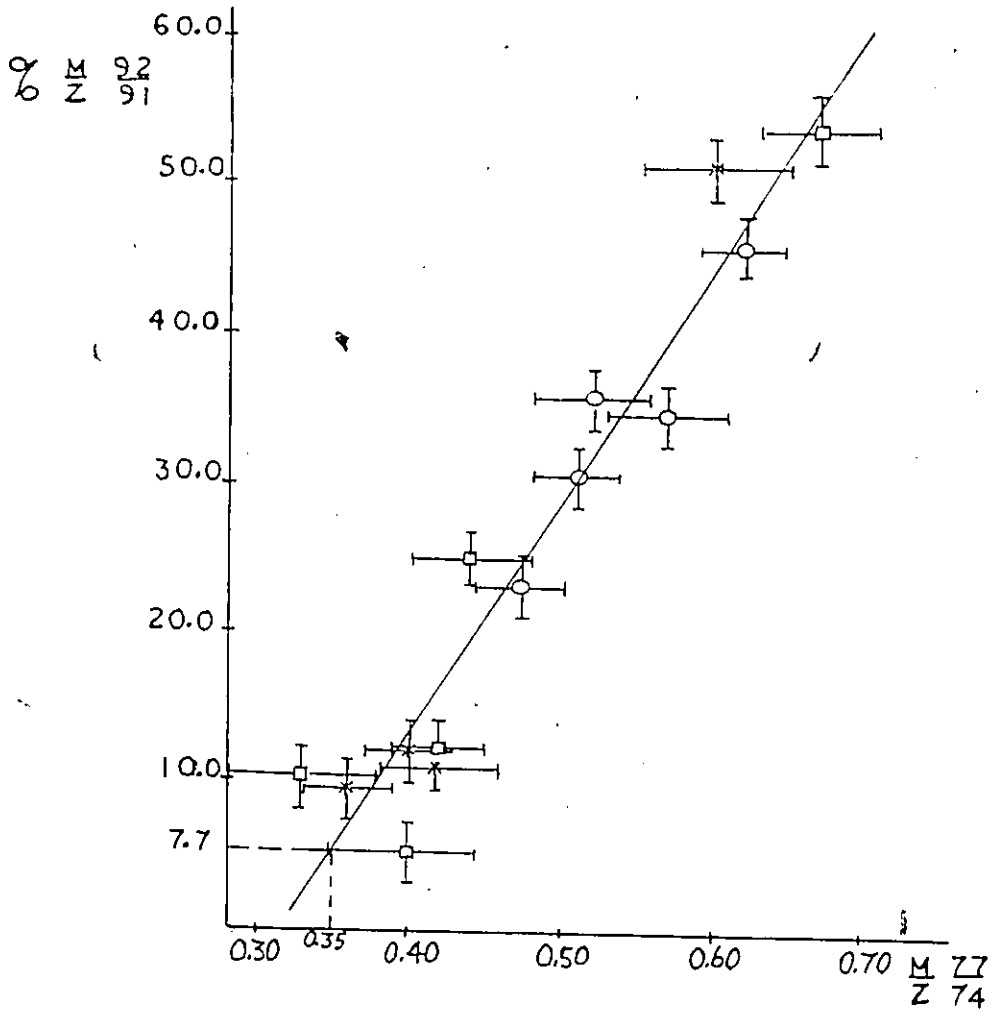

Figure 3.2: A graph of m/z 92/91 versus m/z 77/74 peak intensity ratios for the tropylium salts. The peak intensities are measured from the normal EI mass spectra and the CA mass spectra, respectively, of different batches of the tropylium salts synthesized for this study. Mass spectrometer operating conditions: 70 eV ionising electron energy, 8 keV ion translational energy. o tropylium tetrafluoroborate, □ tropylium bromide, * tropylium iodide.

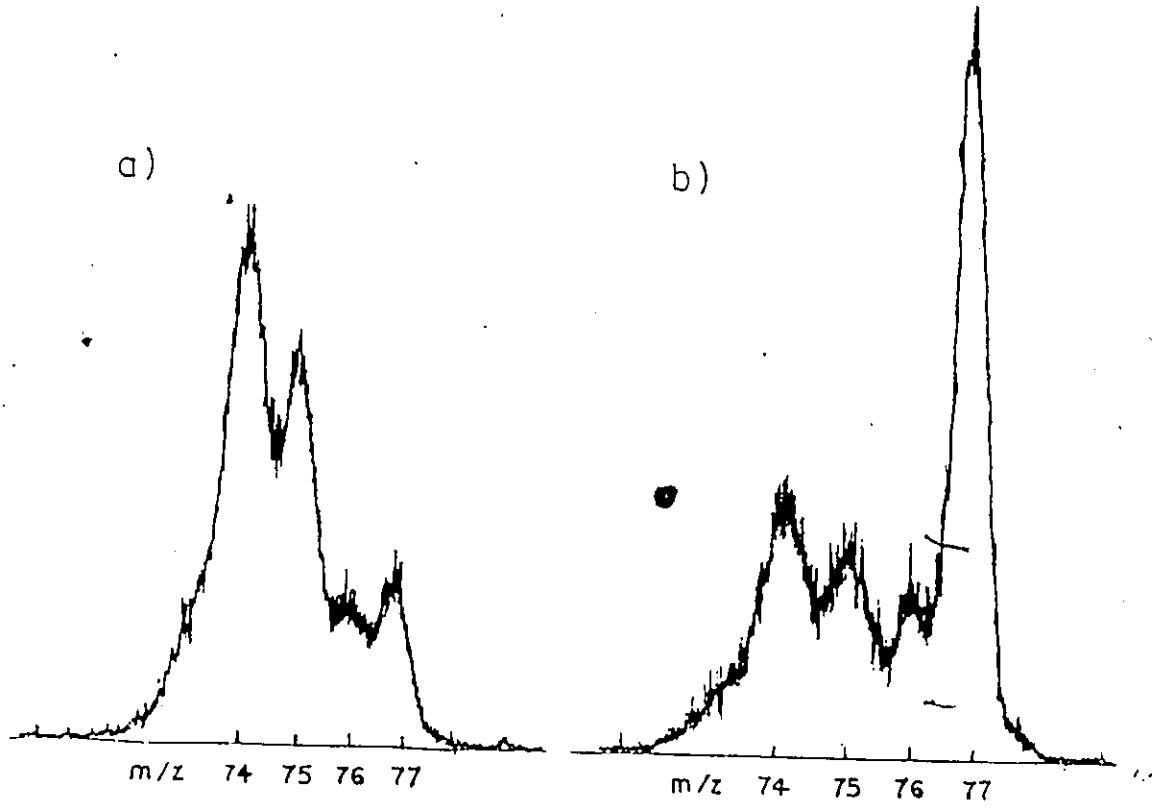

Figure 3.3: The m/z 74–77 region of the CA mass spectrum for (a) pure tropylium ions and (b) pure benzyl ions. Accelerating voltage = 8 keV.

Precursor	m/z 77/74	% Benzyl	% Tropylium
Benzyl iodide	1.67	47	53
Propylbenzene	1.61	45	55
Benzyl bromide	1.59	44	56
Bibenzyl	1.49	41	59
Benzyl chloride	1.44	39	61
Pentylbenzene	1.42	39	61
n-Butylbenzene	1.35	36	64
Ethylbenzene	1.34	35	65
Toluene	0.89	19	81
i-Butylbenzene	0.84	18	82
Allylbenzene	0.83	17	83
2,5-Norbornadiene	0.81	16	84
Cycloheptatriene	0.76	15	85
Benzyl fluoride	0.71	13	87
1,6-Heptadiyne	0.70	12	88
Bitropenyl	0.68	12	88

Table 3.1: **Isomer composition of source-generated m/z 91 ions.** Reproducibilty is ± 5%. Operating conditions: 70 eV ionising electron energy, 8 keV ion translational energy.

at the α position: $[C_6H_5CH_2-X]^{+\cdot}$. A synergystic effect may be that large, bulky substituents impede the rearrangement process in the molecular ion prior to $[C_7H_7]^+$ ion formation. However, benzyl ions formed with high internal energies (40-95 kcal/mole)[75,84] are believed to equilibrate rapidly between the tropylium and benzyl isomers thus reducing the probability of forming pure benzyl ions with 70 eV ionising electron energy. It is evident from the results of Table 3.1 that such an interconversion favours formation of the tropylium ion—the more stable of the two isomers.

A comparison of the results of the present work with literature results is presented in Table 3.2. The agreement between the present work and the previous CA study at the same ion translational energy[72] is very good, except in those cases where sample purity may have been a problem in the earlier study.[7] As can be seen from Figure 3.4, a small change in the m/z 77/74 ratio for pure tropylium ions does not appreciably affect the mixture analysis; the greatest differences between the two studies should occur for the ions which have high tropylium ion contents. The 70 eV CA results remain irreconcilable with the results obtained by IQR, which all show much higher benzyl ion concentrations.

3.3 Low ionising electron energy results

A comparison between the $[C_7H_7]^+$ ion mixtures produced at low electron ionising energies in this work with the results of the previous CA work[72]

[7]Commercially synthesized cycloheptatriene, used in previous CA studies[71,72] contains up to 10% toluene. Toluene free cycloheptatriene was synthesized for this work—see Experimental.

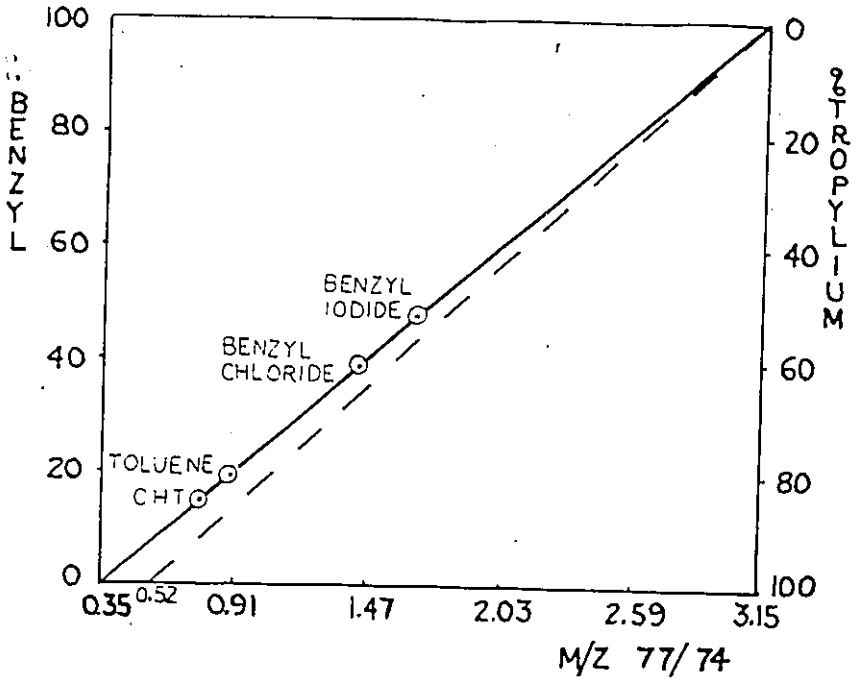

Figure 3.4: **The effect of changing the m/z 77/74 ratio for tropylium ions on the isomer mixture analysis of $[C_7H_7]^+$ ions.** Although the value of 0.35 found in the present study is lower than the value used for tropylium ions in past CA studies[72,94], only a small change in the isomer analysis is found. Solid line indicates analysis of this study, broken line indicates analysis for tropylium ion ratio = 0.52. CHT—Cycloheptatriene. All values with 70 eV ionising electron energy, 8 keV ion translational energy.

Precursor	% Benzyl		
	This work (±5%)	Previous CA (±5%)	ICR (±10%)
Benzyl bromide	44	43	94
Bibenzyl	41	45	95
Benzyl chloride	39	40	91
Ethylbenzene	35	-	90
Toluene	19	20	62
Norbornadiene	16	-	32
Cycloheptatriene	15	19	-
Benzyl fluoride	13	34	-

Table 3.2: **Comparison of 70 eV ionising electron energy $[C_7H_7]^+$ ion population analysis from this work with literature results.** Previous CA results reference [72], ion cyclotron resonance (ICR) results references [80,82].

is presented in Table 3.3. With the exception of the toluene and cycloheptatriene results of this work, there is generally good agreement among the three sources for the isomer abundances in the $[C_7H_7]^+$ ion population. This suggests that the disagreement between ICR and CA results at 70 eV ionising electron energy may be due, in part, to different extents of isomerisation between the benzyl and tropylium isomers at higher internal energies.

3.4 The threshold $[C_7H_7]^+$ ion from toluene and cycloheptatriene

Despite the excellent concurrence between the two CA studies for most precursors, there remains serious disagreement with respect to the relative abundances of the $[C_7H_7]^+$ ion isomers formed from toluene and cycloheptatriene at, or close to, threshold ionising electron energies. In a previ-

Precursor	% Benzyl		
	This Work	Previous CA[72]	ICR[80]
Benzyl bromide	100	100	97
Bibenzyl	100	100	-
Benzyl fluoride	88	-	-
Benzyl iodide	88	-	-
Benzyl chloride	80	85	93
Ethylbenzene	80	-	85[a]
Propylbenzene	80	-	-
Toluene	73	20	23
Allylbenzene	70	-	-
Cycloheptatriene	50	27	-
i-Butylbenzene	41	-	-
Bitropenyl	27	-	-

Table 3.3: **Analysis of $[C_7H_7]^+$ ion mixtures at low ionising electron energies.** Values of the present study are for source-generated ions produced with ionising electron energies lowered until m/z 91 main beam intensities were reduced by a factor of at least 250 below the energy required to produce m/z 65 metastably (*ca.* 16 eV). Reproducibility is ±8% for all results except the toluene value which is ±10%. Reference [72] values corrected as suggested in reference [40], [a]reference [82].

ous CA study[72], an increasing benzyl ion content was observed when the ionising electron energy was lowered from 70 eV to about 14.5 eV. However, at a nominal 14.5 eV, the benzyl ion content began sharply to decrease so that at the lowest ionising electron energies the $[C_7H_7]^+$ ions were thought to have mainly the tropylium structure when generated from both toluene and cycloheptatriene precursor molecules.

Experiments using toluene and cycloheptatriene precursors with the Ottawa mass spectrometer were able to repeat the *increase* in benzyl ion content at medium electron energies, but not the fall-off of benzyl at the lowest ionising energies. A recently acquired computer programmed data acquisition system[100] was employed to examine the CA spectra with improved signal-to-noise ratio at the lowest ionising energies. These experiments revealed some interesting results.

3.4.1 Toluene studies

Source-generated $[C_7H_7]^+$ ions

As the ionising electron energy approaches the threshold for formation of $[C_7H_7]^+$ ions from toluene, the m/z 74–77 region begins to be clearly contaminated with artefacts. These artefacts have two sources:

1. The major portion of the artefacts originates from the metastable decomposition, $92^{+\cdot} \rightarrow 91^+$, of toluene molecular ions in the magnetic sector. [101] The nascent m/z 91 ions manage to traverse the magnet and enter the second field-free region with a kinetic energy of 7914 eV. At 70 eV ionising electron energy,

this process causes the low intensity continuum found between m/z 92 and m/z 90 in the normal mass spectrum of toluene, as shown in Figure 3.5.

2. A small contribution ($\leq 5\%$)[8] to the artefacts comes from the m/z 93 ion, ($[^{13}CC_6H_8]^{+\cdot}$), which undergoes *metastable* and some *collision-induced decomposition* to form m/z 92 ($[^{13}CC_6H_7]^{+}$) by H loss in the first field-free region of the mass spectrometer. This m/z 92 ion also has a translational energy of 7914 eV and will traverse the magnet at a magnet setting equal to m/z 91.01.

Normally, these ions do not present a problem because their fluxes are very small, but at low ionising electron energies the *relative* proportions of these interfering ions becomes significant.[9] Both of these interfering processes result in ions which traverse the magnet and undergo collisional activation in the second field-free region. They yield fragment ions analogous to the source-generated m/z 74, 75, 76, and 77 ions, but with translational energies slightly less than those derived from the source-generated m/z 91 ion. The extraneous ions thus overlap the daughter ions derived from the source-generated m/z 91 ions. This overlap only slightly affects the normal m/z 77 ion abundance, but greatly affects the m/z 74 abundance as shown in

[8]The contribution varies with the ion source pressure. This is indicative of a collision-induced component, for as the ion source pressure increases, the amount of neutral gas that leaks into the first field-free region also increases. A minimum amount of this artefact was obtained at the indicated source pressures of $\leq 2 \times 10{-}7$ torr.

[9]Lowering the ionising electron energy reduces the internal energy deposited in the molecular ion. Fragmentation to form daughter ions in the ion source becomes less and less favorable. For toluene, the 70 eV m/z 92/91 ratio is 0.8, at low ionising energy conditions m/z 92/91 $\succ$ 100/1; hence, the m/z 93 ^{13}C molecular ion has a relative intensity $\succ$ 8 times that of the 91 source-generated ion.

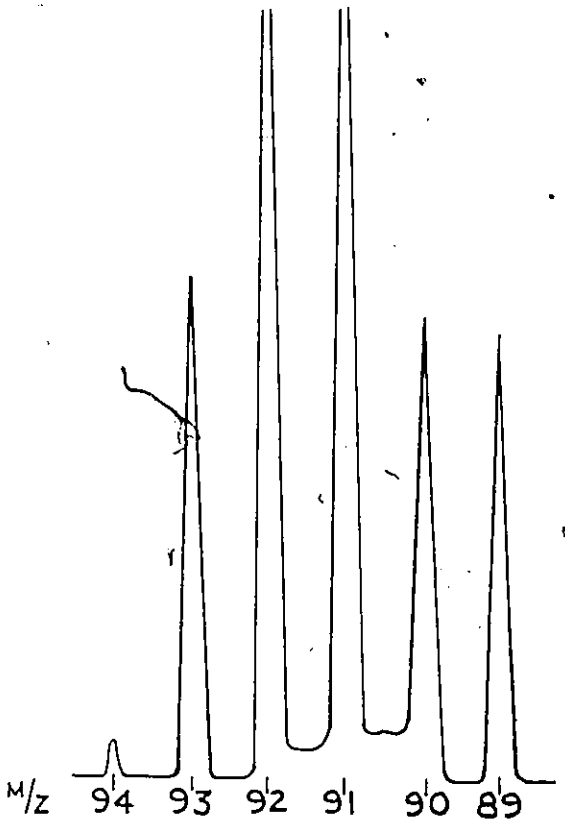

Figure 3.5: Part of the mass spectrum of toluene which shows the continuum extending from m/z 92 to m/z 90 due to the metastable decomposition $92^{+\cdot} \rightarrow 91^{+}$ in the magnetic sector.

Relative m/z 91 signal intensity	Estimated electron energy (eV)	m/z 77/74	% Benzyl (±5%)
5000	70	0.89	19
1000	16	1.21	31
50	12.4	1.81	52
20	12.2	1.89	55
10	12.1	2.05	59
7	12.05	2.0	59[a]
5	12.0	2.0	59[a]
3	11.95	2.1	63[a]
2	11.9	2.2	66[a]
1	11.8	2.4	73[a]

Table 3.4: **Benzyl ion content at different ionising electron energies to form $[C_7H_7]^+$ ions from toluene.** Values of ionising electron energy estimated by comparison of m/z 91 signal intensity fall-off from the point at which m/z 65 signal disappears (about 16 eV) with energy-selected electron measurements.[105] Indicated ion source pressure 2×10^{-7} torr. [a]Deconvoluted spectra, reproducibility $\leq \pm 10\%$.

Figure 3.6. Similar experiments with poor signal-to-noise ratios would not be able to resolve these peaks, and an analysis of such spectra could have easily been misinterpreted as due to an increasing tropylium ion content.

Since the origin and shapes of the interfering peaks are known,[10] it is possible to deconvolute the extraneous peaks from the source-generated ion spectra. The results of these deconvolutions are given in Table 3.4. The results show that the threshold source-generated $[C_7H_7]^+$ ions sampled by CA mass spectrometry are a mixture of benzyl and tropylium ion structures, and that the relative abundance of benzyl is greater than tropylium for these ions.

[10]The CA mass spectrum of the first field-free region metastable m/z 91 ions, which are transmitted through the magnetic sector at an apparent m/z of 90, should be very similar to the CA mass spectra that are given by the interfering ions.

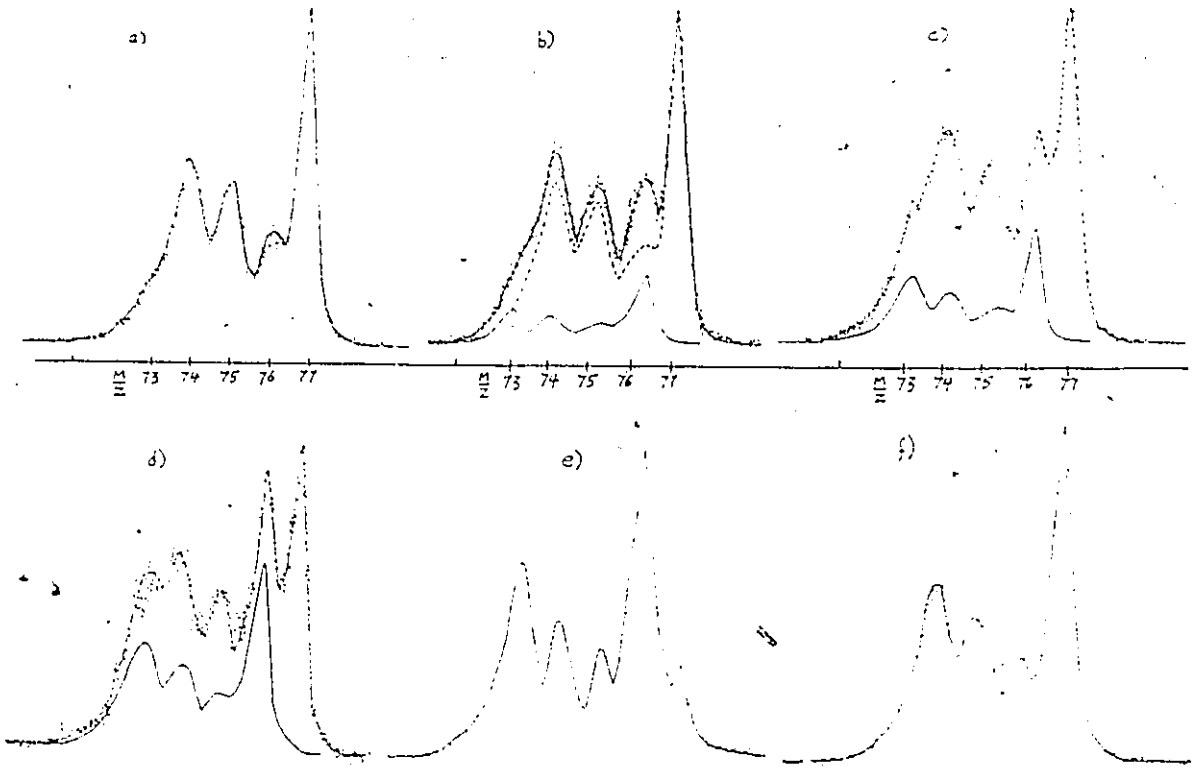

Figure 3.6: **Interference peaks in the low ionising electron energy CA spectrum of toluene.** This figure shows the growth of interference peaks as the ionising electron energy is lowered, which occur at masses corresponding to m/z 73, 74, 75, and 76: Diagrams show the interference spectrum, if present, which must be removed from the source-generated signals. (a) about 12.3 eV, (b) about 12.0 eV (dotted line shows the true source-generated signal), (c) about 11.9 eV and (d) about 11.8 eV. Diagram (e) is the spectrum obtained when the magnet is off-tuned so as to transmit m/z 91 ions generated mainly in the magnetic sector. Diagram (f) shows the CA spectrum of the first field-free region metastably-generated $[C_7H_7]^+$ ions which traverse the magnetic sector at a setting corresponding to m/z 90.

Metastably-generated $[C_7H_7]^+$ ions from toluene

For $[C_7H_7]^+$ ions generated from toluene, it is possible to compare the CA mass spectra of metastably-generated ions with those of source-generated ions, because the m/z 77/74 ratios for the metastable ions are not affected by the very small change in ion translational energy (8000 eV for source-generated ions, 7914 eV for metastably-generated ions). Since $[C_7H_7]^+$ ions generated in the first field-free region traverse the magnet at a setting equal to m/z 90, the CA mass spectra of metastably-generated ions do not have the artefact problem that occurs for source-generated ions.

The internal energy content of toluene molecular ions which fragment in the first field-free region is lower than the internal energy content of those molecular ions with sufficient internal energies to fragment in the ion source.[11] Fragment ions produced by these decompositions have correspondingly different internal energy contents; thus $[C_7H_7]^+$ ions generated in the first field-free region have lower internal energies than those generated in the ion source. The internal energies of source-generated ions produced with the lowest ionising electron energies approach the internal energies of metastably-generated ions.

An examination of metastably-generated $[C_7H_7]^+$ ions will therefore give the relative isomer abundance of ions with the lowest internal energies accessible with the present apparatus. Furthermore, decreasing the ionising

[11] This assumes that the only reacting $[C_7H_8]^{+\cdot}$ isomers are the toluene and cycloheptatriene molecular ions. Theoretically, some $[C_7H_8]^{+\cdot}$ with a high heat of formation may exist to produce $[C_7H_7]^+$ ions metastably which would have relatively high internal energies.

Relative m/z 91 signal intensity[a]	Estimated ionising energy (eV)	m/z 77/74	% Benzyl (±8%)
50	12.4	2.0	59
25	12.3	1.9	55
10	12.1	1.8	52
5	12.0	1.9	55
2.5	11.9	1.8	52
1	11.8	1.7	48

Table 3.5: **Percent benzyl in the metastably-generated $[C_7H_7]^+$ ion population as a function of the ionising electron energy.** Indicated ion source pressure 2×10^{-7} torr. [a]Relative intensity of the source-generated m/z 91 ion signal comparable to the signal intensities given in Table 3.4.

electron energy will also change the distribution of (metastable) ion internal energies. Table 3.5 gives the results of these experiments. In comparison with the results of the study of source-generated ions from toluene, the benzyl ion content appears to have gone through a small maximum as the metastably-generated ions contain less benzyl ion than that found for the lowest internal energy source-generated ions. Furthermore, when the ionising electron energy is lowered, the metastably-generated $[C_7H_7]^+$ ion isomer content becomes even slightly richer in tropylium.

Discussion

The changing isomer abundances with ionising electron energy for source and metastably-generated ions may be interpreted in a manner consistent with the known thermochemistry (see Figure 3.7). Initially, 70 eV ionisation produces toluene molecular ions with generally high internal energies. Studies indicate[62] that loss of a H atom in the source occurs mainly by

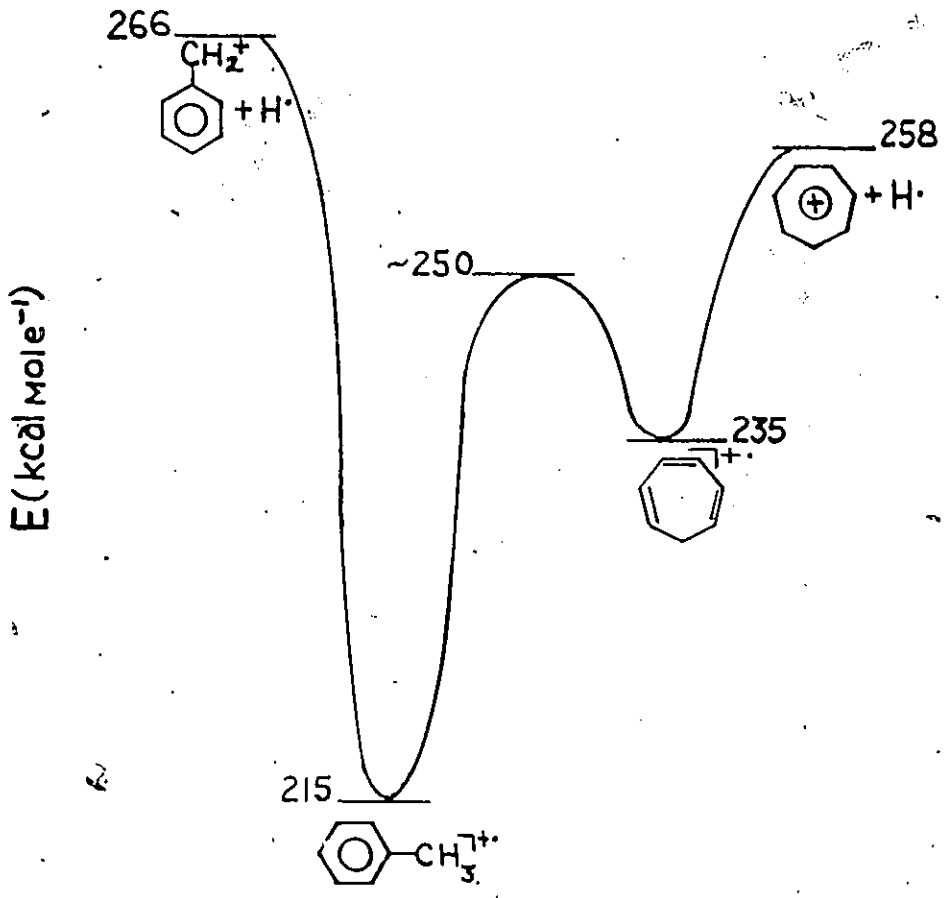

Figure 3.7: Potential energy diagram for the rearrangement of, and H atom loss from, ionised cycloheptatriene and toluene.

direct bond cleavage for high internal energy toluene molecular ions. These 70 eV, source-generated benzyl ions have sufficient internal energies to rearrange to tropylium. Lowering the ionising electron energy decreases the amount of $[C_7H_7]^+$ ions that are able to undergo this rearrangement. An increasing benzyl ion content is thus observed. Toluene molecular ions that fragment in the first field-free region have the longest lifetimes and the lowest internal energies. These factors make rearrangement to the cycloheptatriene molecular ion and subsequent H atom loss to form tropylium a more favourable reaction pathway for metastably-generated $[C_7H_7]^+$ ions than for the source-generated ions. This is consistent with the observation of greater amounts of tropylium for the metastably-generated ions than for the source-generated ions. Finally, at the lowest electron ionising energies used to generate the metastable ions, an almost equal mixture of benzyl and tropylium ions is produced. One must therefore conclude that at the lowest $[C_7H_7]^+$ ion internal energies sampled in this study, the ion population is a *mixture of the benzyl and tropylium isomers.* No support can be given to the previous conclusion based on CA mass spectrometry[72] experiments that nearly pure tropylium ions are produced by metastable decomposition of toluene molecular ions.

3.4.2 $[C_7H_7]^+$ appearance energy measurements from toluene

Further investigation of the threshold $[C_7H_7]^+$ ion from toluene was carried out with appearance energy measurements performed on two separate instruments for which the time-scales and the limiting threshold rate con-

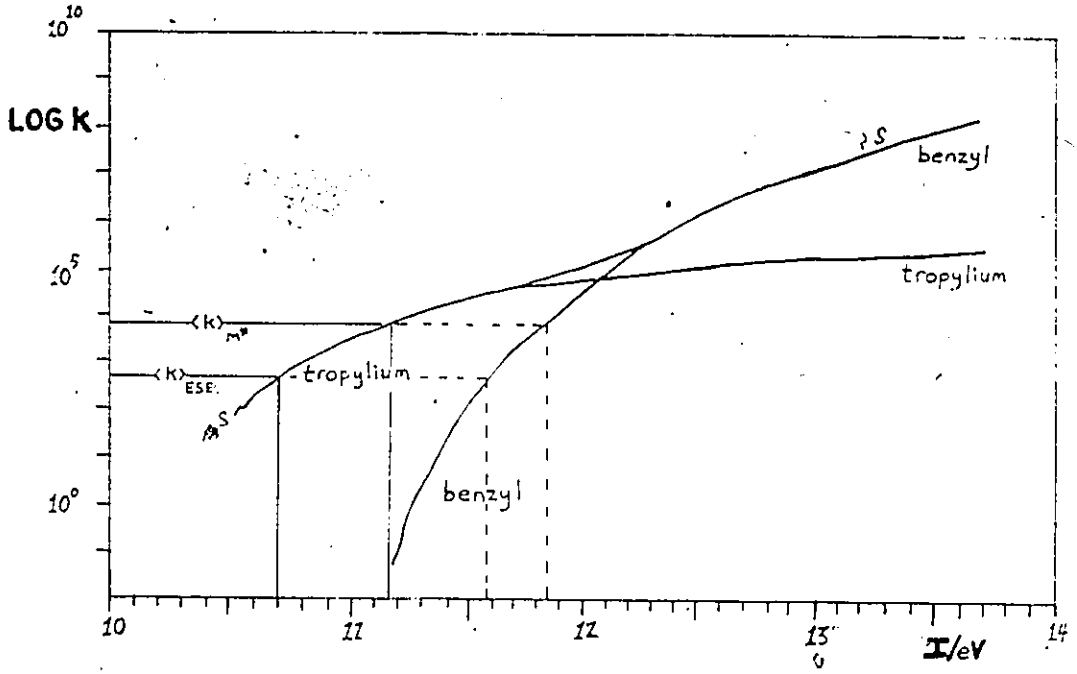

Figure 3.8: **The rate-energy function (t) for $[C_7H_7]^+$ formation and the individual rate-energy functions for tropylium and benzyl ion formation.** Also shown are the limiting threshold rate constants for appearance energy measurements with the metastable peak (m^*) and energy-selected electron (ESE) techniques. Rate-energy function curve from reference [84].

stants corresponding to these measurements have been determined[102]. These results are useful because they can be compared directly with a photoion-photoelectron coincidence (PIPECO) study of $[C_7H_7]^+$ ions generated from toluene. The PIPECO results are summarized in the rate-energy curve shown in Figure 3.8 to which has been added lines indicating the limiting threshold rate constants sampled by the metastable appearance energy technique[102] and the energy-selected electron appearance energy technique[105]. Table 3.6 gives the comparison of the experimentally determined values with those predicted from the total sum curve for $[C_7H_7]^+$ formation derived by the PIPECO technique. Although such a comparison has proven to be reliable with other ionic systems[102], the agreement of

Result	Energy-selected electrons (eV)	Metastable peak (eV)
Experimental	$11.46 \pm .05$	$11.9 \pm .2$
Sum curve prediction	10.7	11.2
Benzyl curve prediction	11.6	11.8

Table 3.6: **Comparison of experimentally obtained appearance energy results with those predicted from PIPECO rate energy sum curve for the formation of $[C_7H_7]^+$ ions.** See Figure 3.8.

the appearance energy measurements with the values predicted from the PIPECO rate-energy curve is not very good. However, it is interesting to note that the agreement of the experimental results with those values which are predicted if only the benzyl rate curve is used is excellent.

The PIPECO study was analysed by using the results of a high sensitivity photoionisation (PI) study[103]. The PI curve for the appearance of $[C_7H_7]^+$ ions is shown in Figure 3.9. This curve has a very long tail at the baseline in the energy region 10.7 to 11.2 eV and a sharply rising onset from there on. Either this tail section corresponds to ions with a low probability of formation, or this tail section corresponds to ions generated by other processes. The CA mass spectrometry studies on toluene have revealed two possible interfering processes:

1. A small amount of ^{13}C toluene molecular ion undergoes decomposition in the first field-free region. This amount increases disproportionately with increasing ion source pressure, therefore collision-induced decomposition of the ^{13}C toluene molecular ion occurs to generate an ion which traverses a magnetic sector, such

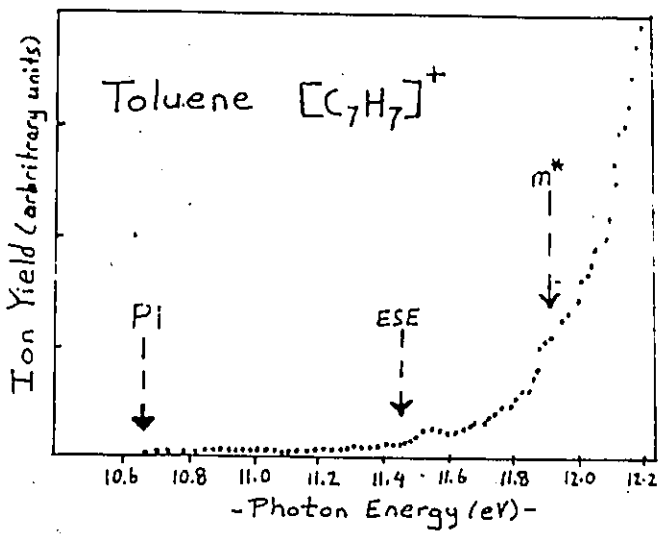

Figure 3.9: **Photoionisation efficiency curve for the production of m/z 91 from toluene.** The arrows point out the appearance energy values obtained by the energy-selected electron (ESE), metastable peak (m^*) and photoionisation (PI) techniques. Figure adapted from reference [103].

as that used in the PI study, at m/z 91. The thermochemical onset for this process is less than the appearance energy for $[C_7H_7]^+$ formation from toluene.

2. The PI study used a commercial sample of toluene without further purification[103]. The 'spectrograde' toluene obtained for the present study needed to be purified of a very small ($\prec 1\%$) m/z 106 impurity (probably a xylene or ethylbenzene). Such an impurity would produce a very small amount of m/z 91 at ionising electron energies lower than those required to form m/z 91 from toluene. The high sensitivity of the PI experiment would make that study prone to interference signal from such an impurity.

Either or both of these factors may have caused an incorrect onset to the PI

Relative m/z 91 signal intensity	m/z 77/74	% Benzyl (±5%)
10,000 (70 eV)	0.78	15
100	1.28	33
40	1.51	41
20	1.57	44
15	1.54	42
10	1.57	44
4	1.54	42
2	1.7	48[a]
1	1.8	52[a]

Table 3.7: **Analysis of the isomer content of source-generated $[C_7H_7]^+$ ions from cycloheptatriene as a function of the ionising electron energy.** Indicated source pressure 2×10^{-7} torr. [a]Reproducibilty ±8%.

curve. Extrapolation of these results into the PIPECO analysis may be the reason why the slowly-rising, almost horizontal curve that has been ascribed to tropylium ion formation does not fit the theshold measurements of the present study. If this is the case, the true $[C_7H_7]^+$ ion onset corresponds more closely to the benzyl curve which fits so well the appearance energy results of this study.

3.4.3 Cycloheptatriene threshold studies

The threshold $[C_7H_7]^+$ ion formed from cycloheptatriene has been studied using CA mass spectrometry of source-generated and metastably-generated ions at low ionising electron energies. The results of these studies are presented in Tables 3.7 and 3.8.

It was initially thought that the same interfering processes which were found in the source-generated toluene experiments would be present in the

Relative m/z 91 signal intensity[a]	m/z 77/74	% Benzyl (± 8%)
20	2.0	59
15	2.0	59
10	1.7	48
4	1.7	48

Table 3.8: **Analysis of the isomer content of metastably-generated $[C_7H_7]^+$ from cycloheptatriene as a function of the ionising electron energy.** Indicated source pressure 2×10^{-7} torr. [a]Relative signal intensities of the source-generated m/z 91 ion at the ionising electron energy used to generate the metastable ion.

CA mass spectra of source-generated $[C_7H_7]^+$ ions from cycloheptatriene. However, decreasing the ionising electron energy to the lowest possible levels did not produce any significant artefact peaks. Examination of the metastably-generated $[C_7H_7]^+$ ions revealed that the yield of metastable ions from cycloheptatriene is about 1/3 of that from toluene. Thus, fewer cycloheptatriene molecular ions undergo the transition $92^{+\cdot} \rightarrow 91^+$ in the magnetic sector, and no observable artefacts are produced.[12]

The low energy electron impact results for source and metastably-generated $[C_7H_7]^+$ ions are consistent with the known thermochemistry. At 70 eV ionising energy, H atom loss may occur directly from the cycloheptatriene molecular ion or following rearrangement to the toluene molecular ion. Many benzyl ions formed by rearrangement and subsequent H atom loss have sufficient internal energies to rearrange to the tropylium ion. Lowering the electron energy decreases the amount of benzyl ions that rearrange to tropylium. This causes the initial increase in the benzyl ion content.

[12]Higher source pressures than the that used (2×10^{-7} torr) for these studies may indeed introduce artefacts to the source-generated CA spectra.

The metastably-generated $[C_7H_7]^+$ ions from cycloheptatriene give results similar to the metastably-generated ions generated from toluene. This is not unexpected, for if the molecular ion 'equilibration' between ionised cycloheptatriene and toluene is indeed fast (compared to H atom loss) at these ionising electron energies, the two products of approximately equal heats of formations (ΔH_f(benzyl)-ΔH_f(tropylium) $\simeq$ 8 kcal/mole) should have similar relative abundances irrespective of the precursor ion.[13]

The slight decrease in the benzyl ion content at the lowest internal energy (metastable) ions may mean that truly the threshold has been reached for some molecular ions and the differences in the heats of formation of the two products come into play; i. e. an increasing number of cycloheptatriene molecular ions have sufficient internal energy to rearrange to toluene molecular ions but insufficient internal energy to undergo H atom loss, whereas H atom loss from cycloheptatriene molecular ions may still occur. However, the facile rearrangement to the toluene molecular ion ensures that a portion of the $[C_7H_7]^+$ ion population will have the benzyl structure, since the spread of internal energies of ions prepared by electron impact in conventional mass spectrometers is large enough that the two processes can not be differentiated.

[13]It has been suggested[71] that the rates of $[C_7H_7]^+$ ion formation from low internal energy toluene and cycloheptatriene molecular ions should be similar, because the lower activation energy for H atom loss from the cycloheptatriene molecular ion offsets the fact that the concentration of toluene molecular ions is greater than that of cycloheptatriene molecular ions.

3.4.4 Summary

The results of the CA mass spectrometry experiments on the production of $[C_7H_7]^+$ ions from ionised toluene and cycloheptatriene show that the benzyl-tropylium isomer content depends on the following three molecular ion internal energy ranges:

1. At the lowest ion internal energies (i. e. metastably-generated ions), fast equilibration between the toluene and cycloheptatriene molecular ions occurs prior to H atom loss. On the time-scale of such experimental observations nearly equal proportions of tropylium and benzyl ions are produced.

2. At slightly higher ion internal energies (i. e. the lowest internal energy source-generated ions), direct bond cleavage begins to be favoured. For ions derived from toluene molecular ions, this results in a *increase* in the benzyl ion content. However, for ions generated from cycloheptatriene molecular ions, this results in a *decrease* in the benzyl ion content.

3. A further increase in the molecular ion internal energy results in the production of $[C_7H_7]^+$ ions now having sufficient internal energy to interconvert between the benzyl and tropylium structures on the experimental time-scale. Since this equilibration favours the more stable tropylium ion, the benzyl isomer content of $[C_7H_7]^+$ ions from toluene decreases appreciably, while that from cycloheptatriene gradually levels off. At 70 eV ionising electron energy, $[C_7H_7]^+$ ions from

toluene and cycloheptatriene precursor molecules have similar isomer contents.

3.5 Ion translational energy effects

3.5.1 Benzyl and tropylium ions

The three previous CA studies[71,72,40] have been carried out using different ion accelerating voltages and therefore each study examined $[C_7H_7]^+$ ions with different translational energies. Published CA mass spectra of m/z 91 ions from toluene with a range of translational energies show markedly different m/z 77/74 ratios at different ion kinetic energies[85]. However, no mention was made whether these changing ratios reflect differing $[C_7H_7]^+$ isomer populations.

To answer this question, CA mass spectrometry studies were carried out at different accelerating voltages on pure benzyl and tropylium ions, and with a number of precursor molecules that give $[C_7H_7]^+$ ion mixtures. As shown in Figure 3.10, the tropylium ion m/z 77/74 ratio plotted against different accelerating voltages results in a curve that is nearly parallel to the x-axis, whereas the same plot for benzyl ions results in a sharply negative 'sloped' curve. Since decreasing the translational energies lowers the average amount of energy deposited in the $[C_7H_7]^+$ ion upon collision, the higher energy process, m/z 74, is more sensitive to changes in ion translational energy. This is consistent with the observed increase in the m/z 77/74 ratio at lower ion translational energies.

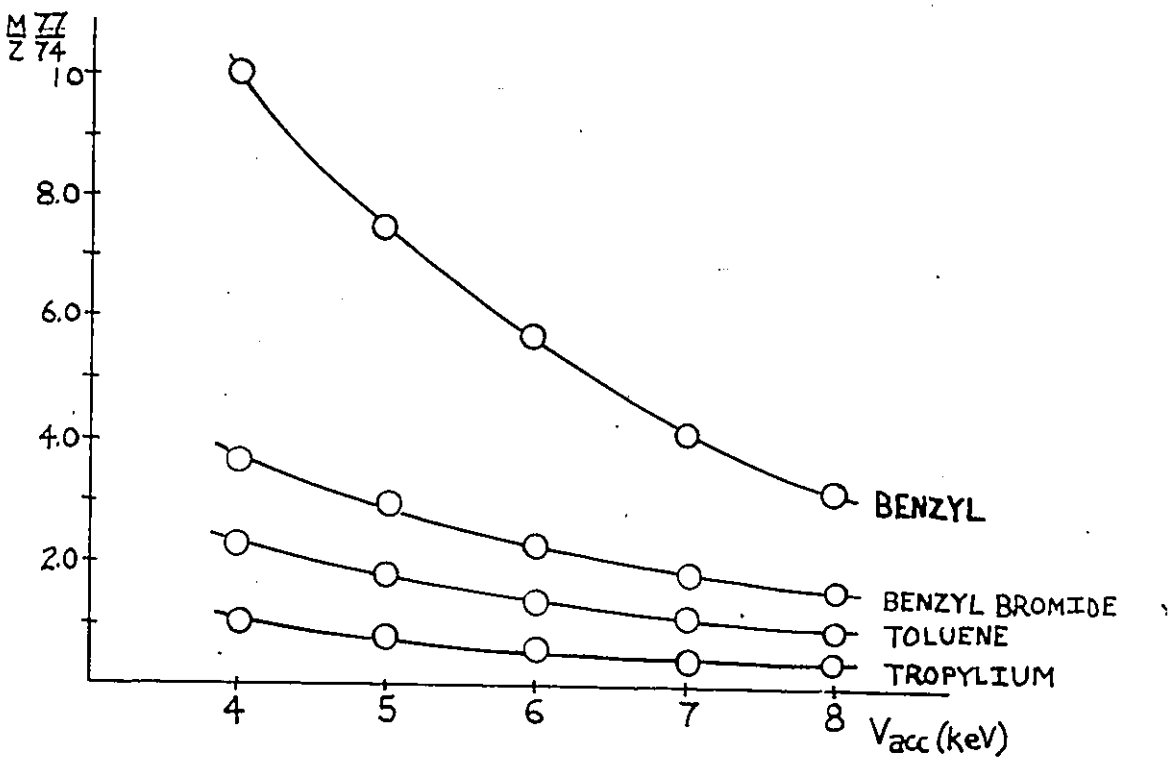

Figure 3.10: The effect of ion translational energy on the m/z 77/74 CA ratios of some precursor molecules.

Precursor/V_{acc}	% Benzyl				
	8 keV	7 keV	6 keV	5 keV	4 keV
Benzyl bromide	44	38	35	34	30
Bibenzyl	41	37	33	30	30
n-Pentylbenzene	38	36	33	32	30
n-Butylbenzene	34	31	28	26	25
Toluene	19	18	15	15	14
2,5-Norbornadiene	16	13	11	10	9

Table 3.9: **Percentage of benzyl at various accelerating voltages.** Reproducibility is best for 8 keV results (± 5%) and worst for 4 keV results (about ± 15%), as the instrumental resolution diminishes when the accelerating voltage is reduced from 8 keV.

3.5.2 $[C_7H_7]^+$ ion mixtures

The m/z 77/74 ratios from the 70 eV CA mass spectra of toluene and bibenzyl at different accelerating voltages are shown in Figure 3.10 to demonstrate the effect of ion translational energy/ion lifetime on $[C_7H_7]^+$ ion mixtures. These spectra can be analysed by taking the tropylium and benzyl lines as limits. The $[C_7H_7]^+$ ion isomer mixtures for toluene and bibenzyl are given in Table 3.9 along with those for other precursor compounds. The results clearly show a trend toward an increasing tropylium ion population at longer ion lifetimes. This is remarkable considering the change in ion lifetime is quite short (from 13 to 18 μs[28]) when changing the accelerating voltage from 8 to 4 keV.

The changing ion population with ion lifetime, if real, indicates that the benzyl-tropylium interconversion is still not equilibrated on the time-scale of these experiments. An increasing tropylium ion content at longer ion lifetimes is consistent with equilibration favouring the more stable tropylium

Precursor	This Work		Previous CA	
	8 keV	4 keV	8 keV[71]	4 keV[72]
Benzyl bromide	44	30	43	50
Bibenzyl	41	30	45	65
Benzyl chloride	39	-	40	45
n-Butylbenzene	34	25	45	-
Toluene	19	14	20	25

Table 3.10: **A comparison between the isomer content analyses for m/z 91 ions with different ion translational energies of the present CA study and past CA studies.** 8 keV data ± 5%, 4 keV data ± 15%.

ion.

This study shows that in all CA experiments care should be taken when interpreting results obtained at different ion translational energies. One cannot rule out the possibility that a change in an ion isomer population might occur, as in the case of the $[C_7H_7]^+$ ions. It is interesting to compare the results of this work at different acceleration energies with those found in the literature (Table 3.10). The literature results do not show the same trend with ion lifetime found in this study. Rather, a trend toward increasing benzyl ion content is observed. However, since different instrumentation and different reference spectra were used for the two previous CA studies[71,72], it is not surprising that the results of Table 3.9 do not concur.[14]

[14] In a recent publication[40], the authors indicated that the differences between their two previous sets of results were consistent with the experimental error. However, if a trend toward an increasing tropylium ion content with increasing ion lifetime does exist, it serves to further diminish the agreement between these previous CA results.

3.6 Metastably-generated $[C_7H_7]^+$ ions

One of the reasons for establishing the limits of benzyl and tropylium ion ratios at different accelerating voltages is to make possible analysis of $[C_7H_7]^+$ ions generated metastably. Ions generated metastably in the first field-free region have longer molecular ion lifetimes than source-generated $[C_7H_7]^+$ ions and correspond to ions of low internal energy. Differences between the isomer content of source-generated ions and metastably-generated ions may be due to (increased) isomerisation of the molecular ions. Because of their low internal energy, it is unlikely that $[C_7H_7]^+$ ions generated metastably undergo significant isomerisation between the benzyl and tropylium isomers. This permits direct comparison of the metastably-generated ion m/z 77/74 ratios with the ratios for benzyl and tropylium ions at the *same* ion translational energy as that possessed by the metastably-generated $[C_7H_7]^+$ ion.

Table 3.11 lists the results of the study of metastably-generated $[C_7H_7]^+$ ions, while a comparison with previous CA determinations[72] is given in Table 3.12. It is not understood why the agreement with the literature results is so poor considering the good agreement of the source-generated results with the same research.

Precursor	Reaction	Ion Kinetic Energy	% Benzyl
Bibenzyl	$182^{+\cdot} \rightarrow 91^{+}$	4000	95 ± 10
Benzyl bromide	$170^{+\cdot} \rightarrow 91^{+}$	4280	78 ± 10
Ethylbenzene	$106^{+\cdot} \rightarrow 91^{+}$	6870	72 ± 5
		6010[a]	59 ± 7
Propylbenzene	$120^{+\cdot} \rightarrow 91^{+}$	6070	68 ± 5
		5310[a]	70 ± 5
Toluene	$92^{+\cdot} \rightarrow 91^{+}$	7910	48 ± 5
Cycloheptatriene	$92^{+\cdot} \rightarrow 91^{+}$	7910	48 ± 5

Table 3.11: **Isomer composition of $[C_7H_7]^+$ ions generated metastably in the first field-free region.** [a]Main beam accelerating voltage 7 keV, all others 8 keV.

Precursor	This Work	Previous CA[72]
	% Benzyl	% Benzyl
Bibenzyl	95 ± 10	~ 25
Benzyl bromide	78 ± 10	~ 50
Toluene	48 ± 5	~ 0
Cycloheptatriene	48 ± 5	~ 5

Table 3.12: **Comparison between the metastably-generated $[C_7H_7]^+$ ion isomer content analysis of the present study and results obtained from the literature.**

Experimental

The CA mass spectrometry measurements were carried out on the Vacuum-Generators ZAB-2F instrument described in Chapter 1. Unless otherwise stated, the ion accelerating voltage was 8 keV, the ionising electron energy was 70 eV, the source temperature 423 K, and helium was used as the CA gas at pressures sufficient to cause no more than a 10% reduction in the $[C_7H_7]^+$ ion beam. Low ionising electron energy measurements were performed with a low ion repeller setting ($\leq$ 5 volts)—after initial focussing the only ion source control varied thereafter was the electron energy itself.

The metastable peak appearance energies of $[C_7H_7]^+$ ion from toluene was carried out on a Kratos-AEI MS902S mass spectrometer as described elsewhere[104]. The energy-selected electron appearance energies were measured with an apparatus comprising an electrostatic monochromator together with a quadrapole mass analyser and mini-computer data system[105].

The compounds used were commercial samples unless otherwise noted. Compound purity, when suspect, was checked by GC-MS. Toluene was purified from a small m/z 106 impurity by preparative gas chromatography. 1,3,5-Cycloheptatriene was prepared free of toluene by treatment of tropylium tetrafluoroborate with sodium borohydride[106]. Tropylium tetrafluoroborate was prepared by the method of Conrow[107] and showed no impurities in its proton NMR (D_2O). Tropylium bromide was prepared by a modification of the procedure of Doering and Knox[108] in which the crude material was triturated under dry diethyl ether, the ether decanted and the resulting greenish-yellow cake sublimed under vacuum ($\sim$ 1 torr)

at 345 K. The bright-yellow sublimate was deliquescent in the atmosphere and of variable purity, as the proton NMR ($d_6 - DMSO/D_2O$) of different batches revealed different relative amounts of tropylium bromide δ 9.2(s) and multiply-brominated cycloheptatrienes. Tropylium iodide was synthesized from tropylium bromide by the method of Doering and Knox[108].

Appendix

The scavenging of benzyl ions in the ion source

In the previous CA work[72,40], the reference tropylium ion CA ratio was generated by electron impact of toluene at chemical ionisation source pressures (about 0.1 torr in conventional mass spectrometers), since ICR studies[80] have shown that benzyl ions react with toluene, as in (3.1), while tropylium does not.

$$[benzyl]^+ + C_7H_8 \longrightarrow [C_8H_9]^+ + C_6H_6 \qquad (3.1)$$

The bimolecular rate constant for this reaction is reported to be 4×10^{-10} cm^3/molecule sec[68]. Assuming ideal gas behaviour, $1cm^3$ of toluene at 0.1 torr pressure and the reported[72] source temperature of 423 K contains 2.3×10^{15} molecules. This large excess of toluene will react will benzyl at a pseudo first-order rate constant, k', of about $913200s^{-1}$. Since $d[benzyl]/dt = -k'[benzyl]$, the reaction half life, $t_{1/2}$, can be obtained,

$$k't_{1/2} = -\ln(1/2[benzyl]_0/[benzyl]_0) = \ln 2$$

thus,

$$t_{1/2} = \ln 2/k' = \sim .75\mu s$$

Assuming a ion source residence time of $2\mu s$, about 12.5% of benzyl ions would remain unreacted. It appears that benzyl scavenging is not complete in a conventional mass spectrometer under the above conditions.

Isomer analysis calculation

Analysis of the benzyl and tropylium ion content using CA mass spectrometry is based on the structure characteristic m/z 77/74 peak intensity ratios for the pure flux of each isomer. The benzyl ratio has been measured as 3.15, and the tropylium ratio has been found to be 0.35. Analysis of a $[C_7H_7]^+$ ion population that is a mixture of the two isomers can be carried out by assuming a linear superposition of the two reference spectra. For example, the m/z 77/74 peak intensity ratio in the CA mass spectrum of $[C_7H_7]^+$ ions generated by 70 eV ionisation of toluene precursor molecules is 0.89. The benzyl and tropylium ion content is calculated in the following way:

$$3.15F_{Bz} + 0.35F_{Tr} = 0.89$$

where F_{Bz} and F_{Tr} are the fractions of benzyl and tropylium, and,

$$F_{Bz} + F_{Tr} = 1$$

Combining these two equations and solving for F_{Bz} gives,

$$F_{Bz} = \frac{0.89 - 0.35}{3.15 - 0.35} = 0.19$$

Thus, toluene generates 19% benzyl and 81% tropylium.

Chapter 4

The Analysis of Tolyl Ions

4.1 Reference tolyl CA mass spectra

The CA mass spectra of source-generated $[C_7H_7]^+$ ions (8 keV ion translational energy, 70 eV ionising electron energy) from the nitro and halotoluenes are similar in appearance to the spectra generated by benzyl and tropylium ions. The region m/z 74, 75, 76, and 77 that is structure characteristic for the benzyl and tropylium ions has also been used to characterize the tolyl ions. It has been found (refer to Table 4.1) that the abundance of the m/z 74 ion relative to the m/z 91 ion flux is greater for $[C_7H_7]^+$ ions with (presumably) the tolyl ion structure(s) than the m/z 74/91 ratio observed for the benzyl and tropylium ions. This observation is consistent with a different $[C_7H_7]^+$ ion structure, since other reaction pathways give m/z 74 from tolyl ions than those reactions which give m/z 74 from benzyl and tropylium ions. Tolyl ions of high purity give high yields of m/z 74. It was found that low electron energy ionisation of m and p-nitrotoluene, and chemical ionisation (CH_4 reagent gas) of p-fluorotoluene yield high purity tolyl ions, which agree with the findings of Harrison and co-workers[95],

and the CA mass spectrometry studies of McLafferty and Winkler[71] and McLafferty and Bockoff[94]. The m/z 74-77 region of the CA mass spectrum of $[C_7H_7]^+$ ions from m-nitrotoluene, which has the highest m/z 74/91 ratio, was used as the reference spectrum for the tolyl ions and is illustrated in Figure 4.1. No evidence was found in the course of this study to suggest that the tolyl ions exist in three distinct and non-interconverting structures corresponding to ortho, meta and para-tolyl cations.

4.2 Quantitative analysis of tolyl, benzyl, and tropylium ion mixtures

Analysis of the $[C_7H_7]^+$ ion populations that give tolyl, benzyl and tropylium ion mixtures compared the m/z 74/91 and m/z 77/91 ion peak intensity ratios from the mixture spectra with the ratios obtained from the tolyl, benzyl and tropylium reference CA mass spectra. The m/z 74/91 values were used to determine the tolyl versus the non-tolyl ion content, since benzyl and tropylium give the same m/z 74/91 values while the tolyl value is very different. Once the amount of tolyl ion was determined, the m/z 77/91 value (minus the tolyl ion contribution) was used to evaluate the relative amount of benzyl and tropylium in the remaining $[C_7H_7]^+$ ion population. Note that the relatively large m/z 77/91 value for benzyl ions compared to those for tolyl and tropylium ions gives a clear indication of which halotoluene molecules generate benzyl ions, as even a small amount of benzyl will appreciably affect the m/z 77 yield.

The results of the isomer analysis are given in Table 4.1. It is evident

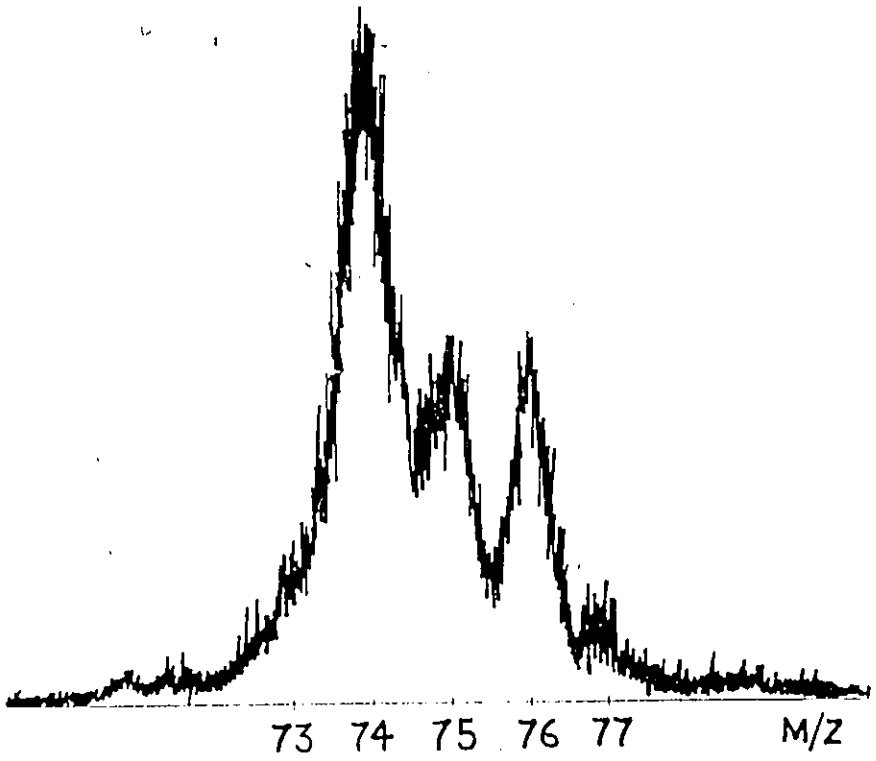

Figure 4.1: The structure characteristic region of the CA mass spectra of pure tolyl ions. Operating conditions: 8 keV ion translational energy, He collision gas pressure sufficient for not more than 10% m/z 91 ion beam reduction.

Precursor	Ionisation	%74$^+$/91$^+$	%77$^+$/91$^+$	%Tolyl	%Bz	%Tr
m-NitroT	Low EE	0.050	0.0062	100	0	0
BzBr	Low EE	0.012	0.038	0	100	0
$TrBF_4$	70 eV	0.013	0.0046	0	0	100
o-NitroT	70 eV	0.024	0.0070	30	6	64
	Low EE	0.029	0.010	43	14	43
o-FluoroT	CI	0.039	0.0044[a]	70	0	30
o-IodoT	70 eV	0.027	0.010	38	16	46
	Low EE	0.037	0.016	66	31	3
o-ChloroT	70 eV	0.014	0.018	3	39	58
o-BromoT	70 eV	0.014	0.013	3	24	73
m-NitroT	70 eV	0.034	0.0047	57	0	43
	Low EE	0.050	0.0062	100	0	0
m-FluoroT	CI	0.040	0.012[a]	73	18	9
m-IodoT	70 eV	0.028	0.0047	40	0	60
	Low EE	0.042	0.0063	78	0	22
m-ChloroT	70 eV	0.022	0.0072	24	57	19
m-Bromo	70 eV	0.016	0.012	8	22	70
p-NitroT	70 eV	0.039	0.0063	70	2	28
	Low EE	0.049	0.0069	97	3	0
p-FluoroT	CI	0.048	0.0090[a]	95	5	0
p-IodoT	70 eV	0.022	0.0072	24	7	69
	Low EE	0.019	0.015	16	30	54
p-ChloroT	70 eV	0.014	0.012	3	39	58
p-BromoT	70 eV	0.014	0.012	3	21	76

Table 4.1: **Analysis of tolyl, benzyl, and tropylium ion mixtures for source-generated $[C_7H_7]^+$ ions.** Operating conditions: 8 keV accelerating voltage, He collision gas pressure sufficient to cause no more than 10% m/z 91 ion beam reduction. Note that 74$^+$/91$^+$, 77$^+$/91$^+$ values quoted in the table are expressed as the ratios of the peak heights × 100%. The experimental reproducibility for m/z 74/91 ratios is about ±8%, that for m/z 77/91 ratios about ±12%. The resulting error in the isomer analysis is about ±7%. Low EE refers to low ionising electron energy. Chemical ionisation (CI) using methane reagent gas. Tr=tropylium, Bz=benzyl. [a]Peak heights may be affected by artefacts.

from these results that the tropylium ion is prevalent in the $[C_7H_7]^+$ ion populations generated with 70 eV ionising electron energy from most halotoluene precursor molecules. This is consistent with the results of Chapter 3 which showed that 70 eV ionisation of most precursor molecules, including the benzyl halides, produces large relative amounts of the tropylium ion.

Table 4.2 compares the results of the present study with the results obtained from a previous CA mass spectrometry study[94] of the tolyl ions. Although there is agreement with respect to some precursor molecules that give high tolyl content $[C_7H_7]^+$ ion populations, the general agreement is poor between the two sets of results. The previous CA study was not able to distinguish between benzyl and tropylium ions in the presence of tolyl isomers, and thus assumed that all non-tolyl ions were benzyl in order to simplify the analysis. The results of this study show that non-tolyl ions are mainly tropylium for the majority of precursors.

Another problem which hampered the data interpretation of this earlier CA study is that the m/z 74 yield with respect to the m/z 91 abundance for benzyl ions was different from that for tropylium ions. This error was corrected in a later paper[40], but no mention was made at that regarding how the error affected the tolyl analysis. Clearly, the previous CA study underestimated the tropylium ion content of $[C_7H_7]^+$ ion populations generated from halotoluene precursor molecules.

		This Work			Previous CA
Precursor	**Ionisation**	**%Tolyl**	**%Bz**	**%Tr**	**%Tolyl**
o-Fluoro	CI	70	0	30	100
o-Nitro	70 eV	30	6	64	85
	Low EE	43	14	43	75
o-Iodo	70 eV	38	16	46	80
	Low EE	66	31	3	75
m-Nitro	70 eV	57	0	43	95
	Low EE	100	0	0	100
m-Fluoro	CI	73	18	12	100
m-Iodo	70 eV	40	0	60	95
	Low EE	78	0	22	95
m-Bromo	70 eV	8	22	70	50
p-Nitro	70 eV	70	2	28	95
	Low EE	97	3	0	100
p-Fluoro	CI	95	5	0	100
p-Iodo	70 eV	24	7	69	75
	Low EE	16	30	54	60

Table 4.2: **Comparision of $[C_7H_7]^+$ ion mixture results of this study and the previous CA study[94].** Low EE-low ionising electron energy results.CI–chemical ionisation, methane reagent gas. Previous CA data 7.8 keV ion translational energy, this work 8.0 keV ion translational energy. Previous CA study assumed all non-tolyl $[C_7H_7]^+$ ions were benzyl, although labeling data from the same study indicated 70 eV o-iodotoluene to generate $\sim$ 66% tolyl, 17 % benzyl, and $\sim$ 17% tropylium.

4.2.1 Metastably-generated $[C_7H_7]^+$ ions

Metastable ion studies[90,91] have suggested that tolyl ions may result from slowly-decomposing halotoluenes, especially the iodotoluenes. Kinetic energy release data are given in Table 4.3 for the metastable reactions $[C_7H_7X]^{+\cdot} \rightarrow [C_7H_7]^+ + X^{\cdot}$ of the halo and nitrotoluene precursors, as measured with the ZAB-2F mass spectrometer using the mass-analysed ion kinetic energy spectrometry (MIKES) technique. The individual isomers of the bromotoluenes display very different kinetic energy releases, and the iodotoluenes give the composite metastable peaks shown in Figure 4.2. The narrow components of the three composite peaks have $T_{0.5}$ values of about 20 meV, while the broad components have $T_{0.5}$ values of roughly 360, 400 and 325 meV for the o, m, and p-iodotoluene metastable peaks, respectively. These $T_{0.5}$ values suggest that the transition states for the reactions that produce the narrow metastable peak components are similar for the three iodotoluene molecular ions, but that the three molecular ions may react *via* different transition states to produce the broad metastable peak components.

Table 4.4 provides the results of collisional activation of $[C_7H_7]^+$ ions generated metastably in the first field-free region of the mass spectrometer. Pure tolyl ions are generated metastably from meta-nitrotoluene precursor molecules. Direct bond cleavage of the NO_2 substituent to produce pure tolyl ions is in line with the small kinetic energy release accompanying this reaction. The iodotoluenes generate different amounts of the three $[C_7H_7]^+$ isomers, in general agreement with the various amounts of broad

and narrow components observed for the composite metastable peaks.[1]

As shown in Figure 4.2, it is possible to tune the magnet so as to inspect mainly the $[C_7H_7]^+$ ions generated from the reaction(s) that give a large kinetic energy release. Such experiments with the iodotoluenes have shown in a qualitative way that the large kinetic energy release component is due to reactions that generate benzyl and/or tropylium ions. The small kinetic energy release component must therefore be due to tolyl ion formation. These observations are not surprising, for a small kinetic energy release is consistent with direct bond cleavage while rearrangement reactions often produce large kinetic energy releases, especially when a more stable daughter ions is generated.

4.2.2 Discussion

Figure 4.3 summarises the reactions that have been previously postulated[71,94] to account for the reactions of the parent $[C_7H_7X]^{+\cdot}$ and their daughter $[C_7H_7]^+$ ions. The molecular ions may rearrange to a $C_6H_5CH_2X^{+\cdot}$ structure *via* methylenecyclohexadiene (MCH)-type intermediates (which may also lose halogen directly), whereas rearrangement to a halocycloheptatriene radical cation may well be sterically hindered[94]. Direct bond cleavage of the halotoluene molecular ion produces tolyl, while halogen loss from a rearranged molecular ion may give benzyl or perhaps tropylium.

The activation energy for the rearrangement to benzyl has been calculated[76]

[1] Agreement between the CA results and the amounts of tolyl and non-tolyl that would be expected by comparing the amounts of narrow and broad components is hindered, because the magnet selection for the CA experiments discriminates against the broad metastable peak components.

Precursor	Reaction	$T_{0.5}$ (meV)
o-iodotoluene	$218^{+\cdot} \rightarrow 91^{+}$	38
m-iodotoluene	$218^{+\cdot} \rightarrow 91^{+}$	30
p-iodotoluene	$218^{+\cdot} \rightarrow 91^{+}$	215
o-bromotoluene	$172^{+\cdot} \rightarrow 91^{+}$	105
	$170^{+\cdot} \rightarrow 91^{+}$	107
m-bromotoluene	$172^{+\cdot} \rightarrow 91^{+}$	285
	$170^{+\cdot} \rightarrow 91^{+}$	290
p-bromotoluene	$172^{+\cdot} \rightarrow 91^{+}$	164
	$170^{+\cdot} \rightarrow 91^{+}$	160
o-chlorotoluene	$128^{+\cdot} \rightarrow 91^{+}$	66
	$126^{+\cdot} \rightarrow 91^{+}$	65
m-chlorotoluene	$128^{+\cdot} \rightarrow 91^{+}$	48
	$126^{+\cdot} \rightarrow 91^{+}$	48
p-chlorotoluene	$128^{+\cdot} \rightarrow 91^{+}$	43
	$126^{+\cdot} \rightarrow 91^{+}$	41
o-nitrotoluene	$137^{+\cdot} \rightarrow 91^{+}$	a
m-nitrotoluene	$137^{+\cdot} \rightarrow 91^{+}$	22
p-nitrotoluene	$137^{+\cdot} \rightarrow 91^{+}$	38

Table 4.3: **Kinetic energy release, $T_{0.5}$, values for second field-free region metastable halo and nitrotoluene molecular ions.** The iodotoluenes give composite daughter ion peaks. [a]Signal intensity too small to record an energy-resolved signal.

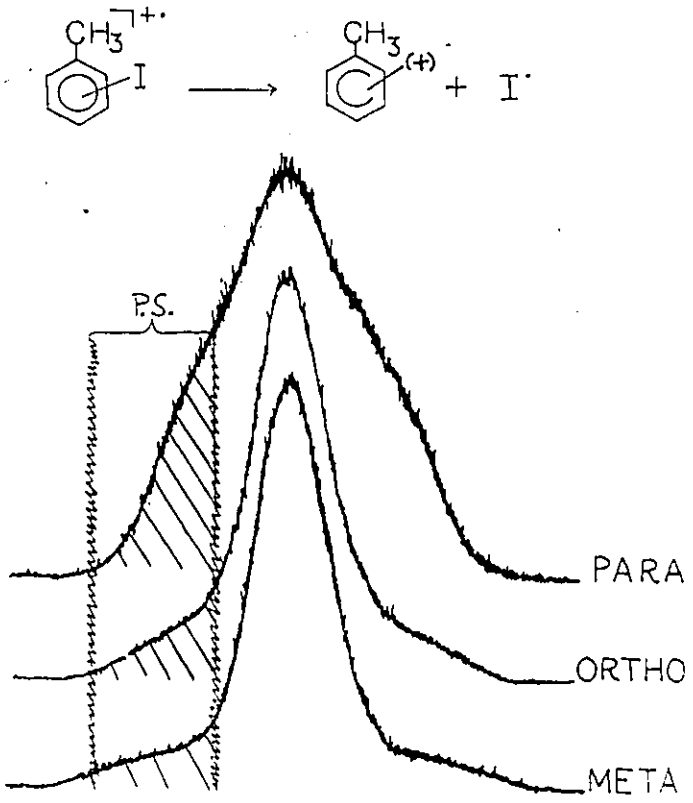

Figure 4.2: **Observed peak shapes for second field-free region iodine atom loss from the three iodotoluenes.** Shaded region indicates approximate magnet selection by 'peak slicing' of first field-free region metastable peak.

Precursor	m/z 74/91 (×2000)	m/z 77/91 (×2000)	%Tolyl (±10%)	%Bz (±10%)	%Tr (±10%)
Bibenzyl	0.004	0.040	0	100	0
Tropylium[a]	0.004	0.004	0	0	100
m-Nitrotoluene	0.029	0.009	100	0	0
o-Iodotoluene	0.012	0.011	32	15	53
m-Iodotoluene	0.027	0.007	92	0	8
p-Iodotoluene	0.009	0.016	20	30	50

Table 4.4: **Analysis of metastably-generated $[C_7H_7]^+$ ion isomer content.** Accelerating voltage varied so that all $[C_7H_7]^+$ ions have about 3340 keV ion-translational energy. The m/z 74, 77 peak intensities are relative to the *areas* of the metastable $[C_7H_7]^+$ ion signal. [a]Since no metastable reaction generates pure tropylium ions, tropylium values have been assigned by assuming m/z 74 yield ≈ m/z 74 yield for benzyl ions (true for source-generated ions); the m/z 77 yield assigned from source-generated 4 keV m/z 74/77 ratio for pure tropylium ions.

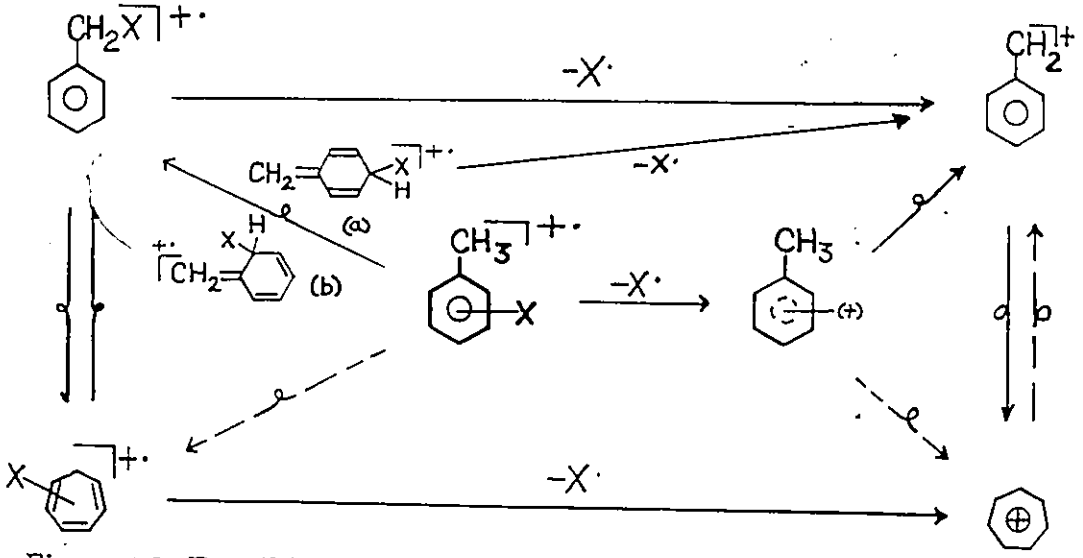

Figure 4.3: **Possible reactions of halotoluene parent molecular ions and their daughter $[C_7H_7]^+$ ions.** Structures (a) and (b) are postulated intermediates for rearrangement of halotoluene molecular ions to the benzyl halides. Halogen loss may also occur directly from (a) or (b) to give the benzyl ion.

to be about 25 kcal/mole above the tolyl heat of formation (~ 250 kcal/mole)[92]. Tolyl ions that do rearrange to benzyl most likely continue to the tropylium structure, since these ions should have sufficient internal energies to surmount the activation energy of about 33 kcal/mole[74] for the benzyl→tropylium rearrangement. The results of Chapter 3 have shown that the large majority of ions with sufficient internal energy to undergo this rearrangement remain as tropylium ions. Therefore, benzyl ions without enough internal energy to rearrange to tropylium are more likely to be derived from nitro or halotoluene molecular ions that have undergone rearrangement prior to nitro or halogen loss.

This is supported by the CA results of Table 4.1, which show that m-nitro and iodotoluene give only tolyl and tropylium ions upon 70 eV ionisation. Furthermore, lowering the electron ionising energy does not result in the production of benzyl ions. This would certainly be the case if fragmentation occurred *via* a rearranged molecular ion to generate benzyl directly, since all the molecules examined in Chapter 3 generated increased amounts of benzyl ions when the ionising electron energy was lowered from 70 eV. However, lowering the ionising electron energy does result in increased amounts of benzyl ions from the ortho and para nitro- and iodotoluenes. This is consistent with the reaction scheme presented in Figure 4.3, in which molecular ion rearrangement occurs to, or *via*, MCH-type radical cations. Such intermediates would not be as easily formed from the meta-nitro and halotoluenes as from the ortho and para-isomers. This accounts for the generally higher yields of tolyl ions from the meta-nitro

and halotoluenes than the corresponding ortho and para-compounds, since predissociative rearrangement is less favourable for the meta-isomers and more of these molecular ions undergo direct bond cleavage.

The 70 eV ionisation results of Table 4.1 show that the greatest amounts of benzyl ions are produced from the chlorotoluenes. Predissociative rearrangement of the molecular ion should be more favourable for the chlorotoluenes than the bromo, iodo and nitrotoluenes, because the lighter chlorine atom may be more mobile. Cleavage of the strong C-Cl bond results in $[C_7H_7]^+$ ions with lower excess internal energies than the other halotoluenes for a given ionising electron energy. A larger portion of the $[C_7H_7]^+$ ions generated from the chlorotoluenes has insufficient internal energy to rearrange to tropylium, which therefore results in a relatively large benzyl ion population.

It is also interesting to note from Table 4.1 that 70 eV ionisation of the o and p-chlorotoluenes generates 39% benzyl—the same amount produced from benzyl chloride under the same conditions (see Table 3.1). This observation provides further support that rearrangement of o and p-chlorotoluenes to the benzyl chloride radical cation occurs favourably. Loss of chlorine from the benzyl chloride radical cation generates benzyl directly, consistent with the relatively small kinetic energy release accompanying chlorine atom loss from the ionised chlorotoluenes.

The CA results are also consistent with predissociative rearrangement occuring favourably for the bromotoluene precursor molecules, since low numbers of tolyl ions are generated from these precursor molecules. How-

ever, the kinetic energy releases accompanying bromine atom loss from the $[C_7H_7Br]^{+\cdot}$ ions are much larger than those observed for chlorine atom loss from ionised chlorotoluenes. Furthermore, the percentage of benzyl ions generated from the bromotoluenes is much less than the 44% produced from benzyl bromide precursor molecules. In this case, it is possible that the bromotoluene molecular ions do not rearrange fully to the benzyl bromide radical cation, but react from MCH-type radical cation structures. Cleavage of the C-Br bond produces $[C_7H_7]^+$ ions with greater average internal energy than the chlorotoluenes. This results in a larger tropylium ion population than observed from the chlorotoluenes, because more $[C_7H_7]^+$ ions generated from the rearranged bromotoluene molecular ions have sufficient internal energy to undergo the benzyl→tropylium rearrangement.

Rearrangement of the iodo and nitrotoluene molecular ions to the corresponding $C_6H_5CH_2X^{+\cdot}$ is also not favourable, as the bulky iodo and nitro groups should not be very mobile. The broad kinetic energy release components of the peaks observed from iodine loss are consistent with reactions from the MCH-type radical cations, since a structure different than that of the benzyl ion is required to support a barrier for the reverse reaction. The nitro and iodotoluene molecular ions generate $[C_7H_7]^+$ ions with the highest average internal energy for 70 eV ionisation,[2] therefore rearrangement to tropylium should be most favourable for these ions.

$[C_7H_7]^+$ ions generated metastably in the first field-free region of the

[2]The C-I, C-NO_2 bond strengths are weaker than the C-Br and C-Cl bonds in the bromo and chlorotoluene molecular ions. Data in the available literature [96] give AE-IE values of about 2.4 eV for the iodo and nitrotoluenes, while the values are about 2.5 eV for the bromotoluenes and 2.8 eV for the chlorotoluenes.

mass spectrometer provide another source with which to probe the relative tendencies for molecular ion rearrangement of ionised iodotoluenes. The long-lived, low internal energy molecular ions should be more likely to undergo rearrangement prior to iodine loss than the molecular ions which fragment in the ion source chamber. Since nearly pure tolyl ions[3] are generated upon metastable loss of iodine from m-iodotoluene molecular ions, tolyl ions generated metastably from the iodotoluenes must undergo little rearrangement to benzyl or tropylium on the microsecond timescale.[4] Therefore, the non-tolyl ion content is derived mainly from molecular ions that have undergone predissociative rearrangement.

A comparison of the metastable ion results of Table 4.4 with the low ionising electron energy results of Table 4.1 shows similar isomer analyses for m and p-iodotoluene precursor molecules, but the o-iodotoluene results show a significant decrease in tolyl ion content for the metastably-generated ions. The difference between the amounts of tolyl ions observed for the o-iodotoluenes may stem from increased predissociative isomerisation on the longer, first field-free region timescale. This would suggest that molecular ion rearrangement is a rate-determining step for iodine loss for $[C_7H_7I]^{+\cdot}$ ions from o-iodotoluene, but not for those from p-iodotoluene, which give similar $[C_7H_7]^+$ populations for source and metastably-generated ions. The *decrease* in tolyl ion content, observed for source-generated $[C_7H_7]^+$ ions

[3]The CA result probably overestimates the tolyl ion content in the entire metastable ion population, because the magnet selects most of the narrow (tolyl) component and only part of the broad (non-tolyl) component.

[4]If the tolyl ions actually exist as ortho, meta and para isomers, different rates for rearrangement may exist.

from p-iodotoluene when the ionising electron energy is lowered from 70 eV, also indicates that molecular ion rearrangement is not rate-determining, as rearrangement becomes more competitive at lower ion internal energies. The difference in rates for rearrangement of o and p-iodotoluene molecular ions signifies a lower overall barrier for rearrangement and iodine loss for p-iodotoluene molecular ions. A lower barrier is consistent with the slightly smaller $T_{0.5}$ value for the broad component of the composite metastable peak accompanying iodine loss from ionised p-iodotoluene, compared to the broad component $T_{0.5}$ values for the other iodotoluene isomers. A faster rate for molecular ion rearrangement is also in line with the considerably large proportion of broad component in the composite metastable peak accompanying halogen loss from p-iodotoluene molecular ions.

Finally, chemical ionisation of the fluorotoluenes was previously thought to give pure tolyl ions[94,95]. The results of this study indicate that the ortho and meta-fluorotoluenes also generate some benzyl and/or tropylium ion, but nearly pure tolyl ions can be generated from chemical ionisation of para-fluorotoluene. Very recent theoretical and experimental work[109,110] indicates that the electron-rich aromatic ring competes with the fluorine substituent for the proton. Ring protons appear to weakly bound. Evidently, the chemistry of protonated fluorotoluenes is quite involved; HF loss may not always yield tolyl ions.

Summary

Although tolyl ions appear to be energetically capable of isomerising to either benzyl or tropylium ions, they do so relatively slowly on the millisecond time-scale since high purity tolyl ions can be detected. Therefore, it is evident that the structures of non-tolyl $[C_7H_7]^+$ ions generated from the halotoluenes depend to a considerable extent on rearrangement(s) of the molecular ion preceding halogen loss. The 70 eV ionisation results of this study are consistent with the chloro and bromotoluene molecular ions largely rearranging prior to halogen loss, while direct bond cleavage and predissociative rearrangement are competitive for the nitro and iodotoluene molecular ions. The meta-halotoluenes generally produce higher amounts of tolyl ions than their ortho and para-isomers, because rearrangement *via* MCH-type intermediates is less likely to occur.

Experimental

The CA and MIKE mass spectrometry measurements were carried out on the Vacuum-Generators ZAB-2f mass spectrometer described in Chapter 1. The ion accelerating voltage was varied from 4-8 keV, the source temperature was 423 K, and the helium collision gas pressures were sufficient to cause no more than 10% main beam reduction. Measurements with low ionising electron energies were performed at the minimum energies sufficient to give a usable precursor ion signal. The ion repeller setting was no more than 5 volts for these measurements.

The compounds used were commercial samples with stated purities of better than 98%. No impurities were observed in their normal mass spectra. It was suspected that meta-iodotoluene decomposed thermally in the septum inlet system and so all nitro and iodotoluenes were admitted *via* the cold Granville-Phillips inlet system. The bromo and chlorotoluenes were admitted *via* the septum inlet but with the septum temperatures kept low ($\leq 100^{o}C$). These compounds remained stable.

For source-generated $[C_7H_7]^+$ ions, the experiments were done in the following manner. The main beam m/z 91 ion flux was measured without collision gas in the second field-free region (indicated cell pressure $\prec 1 \times 10^{-8}$ torr). Helium was then admitted to the collision cell to a reading corresponding to 1.2×10^{-7} torr. The CA mass spectrum was recorded on the pen recorder by shunting only the sensitivity of the recorder itself. The collision gas was then pumped from the cell and the measurement was repeated at least three times. The reference spectra were repeated on

several different days. For source-generated ions, the peak heights of m/z 74 and 77 were compared to the peak height of the main beam. For metastably-generated $[C_7H_7]^+$ ions, the peak heights of the fragment ions m/z 74 and 77 were compared to the areas of the main beam ion signal. This is because the relatively wide beam of metastably-generated $[C_7H_7]^+$ ions is energy resolved by the slits of the mass spectrometer. In this case, the true flux of ions is given by the area of the observed peak.

Claims to original research

- CA mass spectrometry of $[C_7H_7]^+$ ions generated from various tropylium salts has resulted in a new value for the m/z 77/74 peak intensity ratio for pure tropylium ions.

- Examination of the CA mass spectra of $[C_7H_7]^+$ ions generated from threshold ionisation of toluene has revealed that artefact signals, derived from molecular ions fragmenting in the magnetic sector, contribute to and distort the m/z 77/74 peak intensity ratios. Deconvolution of the extraneous signal from the source-generated one results in a m/z 77/74 ratio that indicates a mixture of benzyl and tropylium isomers are generated at threshold, and not solely the tropylium ion as it had been previously thought[72].

- Analysis of benzyl and tropylium ion mixtures as a function of the ion translational energy/ion lifetime suggests that equilibration between the two isomers is not complete on the microsecond time-scale. An increasing tropylium ion content is found with longer ion lifetime-lower ion translational energy.

- The *relative* m/z 74/91 yields have been established for tropylium,

benzyl, and tolyl ions with 8 keV translational energy.

- The isomer content of metastably-generated $[C_7H_7]^+$ ions from the ionised iodotoluenes has been analysed, and have been found to generate different amounts of tolyl, benzyl and tropylium ions. Inspection of the iodotoluene composite metastable peaks has indicated that benzyl, and perhaps tropylium, are those ions associated with a large kinetic energy release. Tolyl ions appear to be associated with relatively small amounts of kinetic energy release.

Bibliography

[1] R. C. Dunbar, in *Ionic Processes in the Gas Phase*, ed. by M. A. Ferreira, Reidel Publ., New York (1984).

[2] *Gas Phase Ion Chemistry*, vol. 1, ed. by M. T. Bowers, Academic Press, New York (1979).

[3] E. E. Ferguson, F. C. Fehnsenfeld, and D. L. Albritton, in *Gas Phase Ion Chemistry*, vol. 1, ed. by M. T. Bowers, Chapt. 5, Academic Press, New York (1979).

[4] R. C. Woods, *J. Mol. Stuct.* **97**, 97 (1983).

[5] C. J. Porter, J. H. Beynon, and T. Ast, *Org. Mass Spectrom.* **16**, 101 (1981).

[6] K. V. Wood, S. A. McLuckey and R. G. Cooks, *Org. Mass Spectrom.* **21**, 11 (1986).

[7] R. G. Cooks, R. M. Caprioli, G. R. Lester and J. H. Beynon, *Metastable Ions*, Elsevier, Amsterdam (1973).

[8] M. M. Rosenstock, M. B. Wallenstein, H. Eyring, and A. L. Wahrhaftig, *Proc. Natl. Acad. Sci. (U. S.)* **38**, 667 (1952).

[9] K. Levsen and H. Schwarz *Angew. Chem. Int. Ed. Eng.* **9**, 509 (1976).

[10] J. H. Beynon and J. R. Gilbert, in *Gas Phase Ion Chemistry*, vol. 2, ed. by M. T. Bowers, Chapt. 13, Academic Press, New York (1979).

[11] J. L. Holmes and J. K. Terlouw, *Org. Mass Spectrom.* **15**, 383 (1980).

[12] G. Holzmann, J. K. Terlouw, C. A. C. E. Hop, and P. C. Burgers, *Org. Mass. Spectrom.* **21**, 105 (1986).

[13] J. K. Terlouw, W. Heerma, J. L. Holmes, and P. C. Burgers, *Org. Mass Spectrom.* **15**, 582 (1980).

[14] J. L. Holmes and J. K. Terlouw, *Can. J. Chem.* **53**, 2076 (1975).

[15] J. K. Terlouw, J. Wezenberg, P. C. Burgers and J. L. Holmes, *J. Chem. Soc. Chem. Commun.*, 1121 (1983).

[16] C. E. C. A. Hop, J. K. Terlouw, and J. L. Holmes, *Org. Mass Spectrom.* **21**, 776 (1986).

[17] J. L. Holmes, M. Fingas, and F. P. Lossing, *Can. J. Chem.* **59**, 80 (1981).

[18] J. L. Holmes, in M. T. P. *International Review of Science, Physical Chemistry Series Two*, Vol. 5: *Mass Spectrometry*, ed. by A. Maccoll, Chapt. 6, Butterworths, London (1975).

[19] J. C. Traeger and R. G. McLoughlin, *Int. J. Mass Spectrom. Ion Phys.* **27**, 319 (1978).

[20] F. P. Lossing and J. C. Traeger, *Int. J. Mass Spectrom. Ion Phys.* **19**, 9 (1978).

[21] J. B. Pedley and J. Rylance, *Sussex-NPL. Computer Analysed Thermochemical Data: Organic and Organometallic Compounds*, University of Sussex (1977).

[22] F. P. Lossing, *Can. J. Chem.* **49**, 357 (1971).

[23] F. W. McLafferty, T. Wachs, C. Lifshitz, G. Innorta, and P. Irving, *J. Am. Chem. Soc.* **92**, 6867 (1970).

[24] J. R. Gilbert and A. J. Stace, *Int. J. Mass Spectrom. Ion Phys.* **15**, 311 (1974).

[25] P. C. Burgers, J. L. Holmes, J. K. Terlouw and B. van Baar, *Org. Mass Spectrom.* **20**, 202 (1985).

[26] W. J. Bouma, R. H. Nobes and L. Radom, *J. Am. Chem. Soc.* **105**, 1743 (1983).

[27] R. Postma, P. J. A. Ruttink, B. van Baar, J. K. Terlouw, J. L. Holmes, and P. C. Burgers, *Chem. Phys. Lett.* **123**, 409 (1986).

[28] J. L. Holmes, *Org. Mass Spectrom.* **20**, 169 (1985).

[29] K. R. Jennings, *Int. J. Mass Spectrom. Ion Phys.* **1**, 227 (1968).

[30] F. W. McLafferty, *J. Am. Chem. Soc.* **95**, 2120 (1973).

[31] F. W. McLafferty, *J. Am. Chem. Soc.* **95**, 3886 (1973).

[32] J. H. Beynon, R. G. Cooks, and T. Ast, *J. Am. Chem. Soc.* **94**, 1004 (1972).

[33] J. Durup, in *Recent Developments in Mass Spectrometry*, ed. by K. Ogata and T. Hayakawa, University Park Press, Baltimore (1969).

[34] J. L. Holmes, A. A. Mommers, J. K. Terlouw and C. A. C. E. Hop,*Int. J. Mass Spectrom. Ion Processes* **68**, 249 (1986).

[35] H. Yamaoka, P. Dông, and J. Durup, *J. Chem. Phys.* **51**, 3465 (1969).

[36] M. S. Kim and F. W. McLafferty, *J. Am. Chem. Soc.* **100**, 3279 (1978).

[37] P. C. Burgers, J. L. Holmes, A. A. Mommers and J. E. Szulejko, *Org. Mass Spectrom.* **18**, 596 (1983).

[38] I. W. Griffiths, E. S. Mukhtar, R. E. March, F. M. Harris and J. H. Beynon, *Int. J. Mass Spectrom. Ion Phys.* **37**, 159 (1981).

[39] A. A. Mommers, *Ph. D Thesis*, University of Utrecht, Utrecht, The Netherlands (1985).

[40] F. W. McLafferty and C. J. Proctor, *Org. Mass Spectrom.* **18**, 193 (1983).

[41] P. N. Rylander, S. Meyerson, and H. M. Grubb, *J. Am. Chem. Soc.* **79**, 842 (1957).

[42] W. von E. Doering and L. H. Knox, *J. Am. Chem. Soc.* **76**, 3202 (1954).

[43] D. O. Schissler and D. P. Stevenson, *J. Chem. Phys.* **22**, 151 (1954).

[44] J. B. Farmer, F. P. Lossing, D. G. H. Marsden and C. A. McDowell, *J. Chem. Phys.* **24**, 52 (1956).

[45] H. M. Grubb and S. Meyerson in *Mass Spectrometry of Organic Ions*, ed. by F. W. McLafferty, Academic Press, New York, N.Y., 493 (1963).

[46] S. Meyerson, *Rec. Chem. Progr.* **26**, 257 (1965).

[47] V. Hanuš and Z. Dolejšek, *Collec. Czech. Commun.* **28**, 652 (1963).

[48] J. T. Bursey, M. M. Burscy and D. G. I. Kingston, *Chem. Rev.* **73**, 213 (1973), and references therein.

[49] A. S. Siegel, *J. Am. Chem. Soc.* **92**, 5277 (1970).

[50] R. A. Davidson and P. S. Skell, *J. Am. Chem. Soc.* **95**, 6843 (1973).

[51] K. L. Rhinehart, Jr., A. C. Buchholz, C. E. van Lear, and H. L. Cantrill, *J. Am. Chem. Soc.* **90**, 2983 (1968).

[52] F. W. McLafferty and H. D. R. Schuddemage, *J. Am. Chem. Soc.* **91**, 1866 (1969).

[53] I. Howe and F. W. McLafferty, *J. Am. Chem. Soc.* **92**, 3937 (1970).

[54] M. K. Hoffman and M. M. Bursey, *Tetrahedron Lett.* 2539 (1971).

[55] M. K. Hoffman, *Z. Naturforsch.* **29a**, 1077 (1974).

[56] J. A. Berson, *Acc. Chem. Res.* **1**, 152 (1968).

[57] K. Levsen, F. W. McLafferty, and D. M. Jerina, *J. Am. Chem. Soc.* **95**, 6332 (1973).

[58] M. J. S. Dewar and D. Landman, *J. Am. Chem. Soc.* **99**, 2446 (1977).

[59] L. Andrews and B. W. Keelan, *J. Am. Chem. Soc.* **102**, 5732 (1980).

[60] J. Bartmess, *J. Am. Chem. Soc.* **104**, 335 (1982).

[61] P. C. Burgers, J. K. Terlouw, and K. Levsen, *Org. Mass Spectrom.* **17**, 295 (1982).

[62] M. A. Baldwin, F. W. McLafferty and D. M. Jerina, *J. Am. Chem. Soc.* **97**, 6169 (1975).

[63] I. Howe and F. W. McLafferty, *J. Am. Chem. Soc.* **93**, 99 (1971).

[64] R. G. Cooks, J. H. Beynon, M. Bertrand and M. K. Hoffman, *Org. Mass Spectrom.* **7**, 1303 (1973).

[65] S. Wexler and R. Clow, *J. Am. Chem. Soc.* **90**, 3940 (1968).

[66] Y. Yamamoto, S. Tukamuka, and H. Sakurai, *J. Am. Chem. Soc.* **94**, 661 (1972).

[67] R. C. Dunbar, *J. Am. Chem. Soc.* **95**, 472 (1973).

[68] R. C. Dunbar, *J. Am. Chem. Soc.* **97**, 1382 (1975).

[69] J. Shen, R. C. Dunbar, and G. A. Olah, *J. Am. Chem. Soc.* **96**, 6228 (1974).

[70] J. Winkler and F. W. McLafferty, *J. Am. Chem. Soc.* **95**, 7533 (1973).

[71] F. W. McLafferty and J. Winkler, *J. Am. Chem. Soc.* **96**, 5182 (1974).

[72] F. W. McLafferty and F. M. Bockhoff, *J. Am. Chem. Soc.* **101**, 1783 (1979).

[73] F. A. Houle and J. L. Beauchamp, *J. Am. Chem. Soc.* **100**, 3290 (1978).

[74] C. Cone, M. J. S. Dewar, and D. Landman, *J. Am. Chem. Soc.* **99**, 372 (1977).

[75] L. Andrews and B. W. Keelan, *J. Am. Chem. Soc.* **103**, 99 (1981).

[76] M. J. S. Dewar and D. Landman, *J. Am. Chem. Soc.* **99**, 7439 (1977).

[77] K. M. Harmon in *Carbonium Ions.* Vol. IV, ed. by G. A. Olah and P. von R. Schleyer, Wiley Interscience, New York, N. Y., 1973.

[78] B. S. Freiser, *Ann. Rev. Phys. Chem.* **22**, 527 (1971).

[79] R. C. Dunbar, *J. Am. Chem. Soc.* **92**, 4354 (1971).

[80] J. -A. Jackson, S. G. Lias, and P. Ausloos, *J. Am. Chem. Soc.* **99**, 7515 (1977).

[81] D. K. Sen Sharma and P. Kebarle, *Can. J. Chem.* **59**, 1592 (1981).

[82] P. Ausloos, J. -A. Jackson, and S. G. Lias, *Int. J. Mass Spectrom. Ion Phys.* **33**, 269 (1980).

[83] P. Ausloos, *J. Am. Chem. Soc.* **104**, 5258 (1982).

[84] R. Bombach, J. Dannacher and J. -P. Stadelmann, *J. Am. Chem. Soc.* **105**, 4205 (1982).

[85] F. W. McLafferty in *Tandem Mass Spectrometry*, ed. by F. W. McLafferty, John Wiley and Sons, New York, N. Y., 282 (1983).

[86] J. M. Abboud, W. J. Hehre, and R. W. Taft, *J. Am. Chem. Soc.* **98**, 6072 (1976).

[87] E. W. Fu, P. P. Dymerski, and R. C. Dunbar, *J. Am. Chem. Soc.* **98**, 337 (1976).

[88] P. Brown, *J. Am. Chem. Soc.* **90**, 4461 (1968).

[89] P. Brown, *Org. Mass Spectrom.* **3**, 639 (1970).

[90] J. L. Holmes, A. S. Blair, G. M. Weese, A. D. Osborne, and J. K. Terlouw, *Adv. Mass Spectrom.* **7**, 1227 (1978).

[91] B. J. Stapleton, R. D. Bowen, and D. H. Williams, *J. C. S. Perkin II*, 1219 (1979).

[92] A. N. H. Yeo and D. H. Williams, *J. Chem. Soc. Chem. Commun.*, 886 (1970).

[93] S. Tajima, Y. Niwa, M. Nakajima, and T. Tsuchiya, *Bull. Chem. Soc. Jap.* **44**, 2343 (1971).

[94] F. W. McLafferty and F. M. Bockhoff, *Org. Mass Spectrom.* **14**, 181 (1979).

[95] H. -W. Leung, H. Ichikawa, Y. -H. Li, and A. G. Harrison, *J. Am. Chem. Soc.* **100**, 2479 (1978).

[96] H. M. Rosenstock, K. Draxl, B. W. Steiner, and J. T. Herron, *J. Phys. Chem. Ref. Data Suppl. 1* **6** (1977).

[97] G. Hvistendahl, K. Undheim and P. Gyōrōsi, *Org. Mass Spectrom.* **7**, 903 (1973).

[98] J. Tamas, J. Hegedūs-Vajda and A. Messmer, *Acta Chimica Academiae Scientarium Hungaricae Tomus* **99**, 193 (1979).

[99] R. J. Gardner, *Org. Mass Spectrom.* **5**, 83 (1971).

[100] A. A. Mommers and J. C. Traeger, *Org. Mass Spectrom.* **22**, No. 8 (1987).

[101] R. G. Cooks, J. H. Beynon, R. M. Caprioli, and G. R. Lester, *Metastable Ions*, Elsevier Scientific Publishing Company, Amsterdam (1973). pp. 50-57.

[102] P. C. Burgers and J. L. Holmes, *Int. J. Mass Spectrom. Ion Proc.* **58**, 15 (1984).

[103] J. C. Traeger and R. G. McLoughlin, *Int. J. Mass Spectrom. Ion. Phys.* **27**, 319 (1978).

[104] P. C. Burgers and J. L. Holmes, *Org. Mass Spectrom* **17**, 123 (1982).

[105] F. P. Lossing and J. C. Traeger, *Int. J. Mass Spectrom. Ion Phys.* **19**, 9 (1976).

[106] *Reagents for Organic Synthesis, Vol. 1*, ed. by L. F. Fieser and M. Fieser, John Wiley and Sons, New York, N. Y., (1967) p. 177.

[107] K. Conrow in *Organic Synthesis* **43**, 101 (1963).

[108] W. von E. Doering and L. H. Knox, *J. Am. Chem. Soc.* **79**, 352 (1957).

[109] R. S. Mason, M. T. Fernandez and K. R. Jennings, *J. Chem. Soc. , Faraday Trans. II* p.89 (1987).

[110] M. T. Fernandez, K. R. Jennings and R. S. Mason, *J. Chem. Soc. , Faraday Trans. II* p.159 (1987).